

**Scale and ecological and historical determinants of a
species' geographic range: The plant parasite
Phoradendron californicum Nutt. (Viscaceae)**

By

Andrés Lira Noriega

Submitted to the graduate degree program in Ecology and Evolutionary Biology and the
Graduate Faculty of the University of Kansas in partial fulfillment of the requirements
for the degree of Doctor of Philosophy.

Chairperson Jorge Soberón

Chairperson A. Townsend Peterson

Mark E. Mort

Craig E. Martin

Stephen L. Egbert

Date Defended: April 8, 2014

The Dissertation Committee for Andrés Lira Noriega
certifies that this is the approved version of the following dissertation:

**Scale and ecological and historical determinants of a
species' geographic range: The plant parasite
Phoradendron californicum Nutt. (Viscaceae)**

Chairperson Jorge Soberón

Chairperson A. Townsend Peterson

Date approved: April 8, 2014

Abstract

Geographic ranges of species are fundamental units of study in ecology and evolutionary biology, since they summarize views of how species' populations and individuals are organized in space and time. Here, I assess how abiotic and biotic factors limit and constrain species' geographic range, structure its distributions, and change in importance at multiple spatial and temporal scales. I approach this challenge using models and testable hypothesis frameworks in the context of ecological, geographic, and historical conditions. Concentrating on a single species, the desert mistletoe, *Phoradendron californicum*, I assess the relative importance of factors associated with dispersal, host-parasite-vector niche overlap, and phylogeographic patterns for cpDNA within a 6 mya timeframe and at local-to-regional geographic extents. Results from a comparison of correlative and process-based modeling approaches at resolutions 1-50 km show that dispersal-related parameters are more relevant at finer resolutions (1–5 km), but that importance of extinction-related parameters did not change with scale. Here, a clearer and more comprehensive mechanistic understanding was derived from the process-based algorithm than can be obtained from correlative approaches. In a range-wide analysis, niche comparisons among parasite, hosts, and dispersers supported the parasite niche hypothesis, but not alternative hypotheses, suggesting that mistletoe infections occur in non-random environmental subsets of host and disperser ecological niches, but that different hosts get infected under similar climatic conditions, basically where their distributions overlap that of the mistletoe. In a study of

40 species, including insects, plants, birds, mammals, and worms distributed across the globe, genetic diversity showed a negative relationship with distance to environmental niche centroid, but no consistent relationship with distance to geographic range center. Finally, *P. californicum*'s cpDNA phylogenetic/phylogeographic relationships were most probable under a model of geologic events related to formation of the Baja California Peninsula and seaways across it in the Pliocene and the Pleistocene; however, fossil record, niche projections to the LGM, and haplotype distribution suggested shifting distributions of host-mistletoe interactions and evidence of host races, which may explain some of the genealogical history of the cpDNA. In sum, the chapters presented here provide robust examples and methodologies applied to estimating the importance and scale at which different sets of abiotic and biotic factors act to structure a species' geographic range.

Acknowledgements

I wish to express my deepest gratitude to all of those who helped me throughout this learning experience. I am indebted to my advisors Jorge Soberón and A. Townsend Peterson for their unconditional support and friendship. From them I learned not only how to think about science but about life.

I am grateful to my coauthors, committee members, and collaborators, and for the scientific knowledge gained in working with them. Specifically, I wish to thank: Jorge Soberón, Curtis P. Miller, A. Townsend Peterson, Joe Manthey, Oscar Toro, Jamie Oaks, and Mark Mort. The support of my committee members throughout work on this dissertation as well as other academic activities at KU was invaluable. This includes guidance on remote sensing from Steve Egbert, on ecophysiology from Craig Martin, on molecular work from Mark Mort. I feel privileged to count myself among the collaborative team that developed from the Ecological Niche Modeling seminar. This working group has been one of the most significant components of my academic exercises at KU. From this group I thank Yoshinori Nakazawa, Alberto Jiménez-Valverde, Sean Maher, Narayani Barve, Vijay Barve, Mona Papeş, Erin Saupe, Cori Myers, Hannah Owens, and Peter Hosner. I also want to give special thanks to my friends and colleagues Victor Baruch, Lindsay Campbell, Jesse Grismer, Carl Oliveros, Cam Siler, Charles Linkem, and Fabricio Villalobos.

For their contributions to the fieldwork research presented in chapter 1, I am grateful to Luis A. Sánchez-González, Gerardo Cendejas, Fran Recinas, and Rebecca

Crosthwait. I wish to thank the personnel from several institutions and herbaria where we stored specimens: Socorro González (Centro Interdisciplinario de Investigaciones para el Desarrollo Integral Regional, Durango), Hilda Flores (Instituto de Biología, UNAM), José Delgadillo (Universidad Autónoma de Baja California, Ensenada), and Jon Rebman (San Diego Natural History Museum). I thank the curators and staff of the following herbaria for providing access to their digital data: ARIZ, ASC, ASU, BCMEX, BNHM, CANB, COCHISE, DES, GBIF, GCNP, IZTA, KANU, LL, MABA, MO, NMBCC, NY, RM, SNM, TEX, UCR, UNM, USON, UTC, UVSC, XAL. I thank Luis Eguiarte and Mark Olson for help with logistics, and the families of Gela and Alberto Búrquez, Sharon Herzka and Juan Pablo Lazo, Socorro González, Gerardo Cendejas, and Rebecca Crosthwait for their warm hospitality. Initial discussions about this work with Carlos Martínez del Río and statistical guidance from Exequiel Ezcurra were crucial. I also thank A. Townsend Peterson for insightful comments on this work and Narayani Barve for help with weather values interpolation. Conversations with Richard Felger and Mark Robbins were important to clarify points on climatic limiting factors and dispersal of the species.

For the work related to chapter 2 I thank Sean Maher for guidance on niche overlap estimates, Mark Robbins for advice on potential mistletoe bird dispersers, Richard Felger for help with species identifications and valuable comments on background areas, and Ben Wilder for valuable comments on the manuscript.

For their comments on chapter 3, I thank John K. Kelly, Jorge Soberón, A. Townsend Peterson, Lindsay P. Campbell, Jose Alexandre F. Diniz-Filho and three anonymous reviewers who helped us to improve previous versions of this manuscript.

For their contributions to chapter 4 I thank Ben Wilder for obtaining samples from Isla del Tiburón and Isla Ángel de la Guarda; Richard Felger and Pedro Peña for help with regionalization of the Sonoran Desert; and Jenny Archibald and Farzana Ahmed for help with lab work and DNA extractions. Comments from A. Townsend Peterson, Richard Glor, and Emily McTavish helped to improve previous version of the manuscript. I thank curators from ASU for permission to sample loaned specimens as well as Craig Freeman and Caleb Morse from KANU for supporting this project.

Scholarship support from Consejo Nacional de Ciencia y Tecnología, Mexico (189216) enabled me to finance the first four years of studies at KU. Collecting trips were possible thanks to financial support from a University of Kansas Biodiversity Institute Panorama small grant award (Bunker Fund), a Tinker Award from the University of Kansas Center of Latin American Studies, a Young Researchers Award from the Global Biodiversity Information Facility (GBIF). Living expenses were also provided by a scholarship from Secretaría de Educación Pública, Mexico, a Summer Research grant in 2013 from the KU Department of Ecology & Evolutionary Biology, and grants from JRS Biodiversity Foundation and the Instituto de Ecología, Xalapa, México (SAGARPA-IICA-INECOL 2013). An Interdisciplinary Seed Grant from The Commons gave me the opportunity to participate in one of the most enriching experiences—a multidisciplinary research project with Ford Ballantyne IV, Donald Worster and Jorge Soberón. Participation in conferences was possible thanks to financial support from the KU Department of Ecology and Evolutionary Biology, the KU Office of Graduate Studies, the KU Biodiversity Institute, the National Science Foundation's IGERT Program at KU,

and the Next Generation Sonoran Desert Researchers. A Marcia Brady Tucker Student Travel Award funded travel to present research at the 127th AOU Meeting.

KU offered the best possible environment for this dissertation.

Special thanks to my friends Quica and Esteban Lerner, Monica Papeş and Arpi Nyari, the Lira-Noriega foundation, the Campbell, Soberón and Peterson families, and Emily Ryan for their support.

Table of Contents

| | |
|---|-----|
| Abstract..... | iii |
| Acknowledgements..... | v |
| Introduction | 1 |
| Process-based and correlative modeling of desert mistletoe distribution: A multiscalar approach | 8 |
| Abstract | 9 |
| Introduction..... | 10 |
| Conceptual framework..... | 13 |
| Methods | 16 |
| Distribution of species presences and landscape characteristics | 16 |
| Host tree mapping..... | 18 |
| Climate, host, and disperser summaries | 19 |
| Process-based model..... | 21 |
| Correlative models | 23 |
| Model evaluations and comparisons | 24 |
| Results | 26 |
| Discussion | 35 |
| Acknowledgments | 42 |
| Range-wide ecological niche comparisons of parasite, hosts and dispersers in a vector-borne plant parasite system | 44 |
| Abstract | 45 |
| Introduction..... | 46 |
| Materials and Methods | 50 |
| Input data | 50 |
| Niche modelling..... | 52 |
| Niche similarity estimates | 54 |
| Results | 56 |
| Overall host and mistletoe-infected niche comparisons..... | 56 |
| Disperser niche comparisons | 59 |
| Discussion | 62 |
| Acknowledgements | 67 |
| Relationship of genetic diversity and niche centrality: A survey and analysis | 68 |

| | |
|---|-----|
| Abstract | 69 |
| Introduction..... | 69 |
| Methods | 74 |
| Species' occurrences and genetic diversity..... | 74 |
| Niche characterization and distances to niche and geographic centroids..... | 76 |
| Results | 81 |
| Discussion | 89 |
| Acknowledgements..... | 92 |
| The roles of history and ecology in chloroplast phylogeographic patterns of the vector- borne plant parasite <i>Phoradendron californicum</i> Nutt. (Viscaceae) in the Sonoran Desert | 93 |
| Abstract | 94 |
| Introduction..... | 95 |
| Materials and Methods | 97 |
| Sampling | 97 |
| DNA extraction, amplification, and sequencing..... | 99 |
| Alignment and phylogenetic analyses..... | 100 |
| Hypothesis testing in a phylogenetic context | 102 |
| Ecological niche modeling | 105 |
| Host and mistletoe macrofossils | 107 |
| Results | 107 |
| DNA sequences..... | 107 |
| Gene tree reconstruction | 108 |
| Parsimony network | 109 |
| Gene tree topology and ecological versus historical hypothesis testing | 109 |
| Present-Last Glacial Maximum suitability | 112 |
| Host and mistletoe macrofossils | 114 |
| Discussion | 116 |
| Mistletoe phylogeny and phylogeographic patterns | 116 |
| Historical and ecological hypotheses | 118 |
| Present and past distributions | 121 |
| Acknowledgments | 123 |
| References | 124 |
| Appendices..... | 143 |
| Appendix 1.1 Derivation of the formulas for the process-based model..... | 143 |

| | |
|--|-----|
| Table S1.1. Summary of model performance..... | 146 |
| Figure S1.1 Example binary maps for different models and sets of environmental..... | 147 |
| Figure S1.2 Example of map comparison with fuzzy Kappa statistic. | 148 |
| Appendix 2.1 Model evaluation. | 149 |
| Appendix 3.1 Genetic diversity measures and estimates of distances to geographic range center and niche centroid. | 150 |
| Appendix 4.1 Information on individuals and localities sampled in this study. Partitioning of individuals into populations according to each hypothesis (see Table 4.1) and DNA sequences GenBank accession numbers..... | 151 |
| Appendix 4.2. Methods to obtain the layers on the historical, ecological, and geographic conditions used for population partitioning in the Bayesian coalescent analysis. | 161 |
| Appendix 4.3 Packrat midden localities from western North America with hosts and mistletoe macrofossil information. | 164 |
| Appendix 4.4 Model evaluation. | 165 |
| Table S4.1 Results from delimitation of lineages using the ML GMYC method..... | 166 |
| Table S4.2 Marginal likelihood and Bayes factor of the hypotheses used to test the phylogenetic relationships of the gene tree without population 225 (see Table 4.1)..... | 167 |
| Table S4.3 Levels of nucleotide variability per sequenced chloroplast region. | 168 |
| Figure S4.1 <i>Phoradendron californicum</i> haplotype network and potential distribution for mistletoe (inset) and hosts distributions during the LGM (21 kya) according to the CCSM climate scenario. | 169 |
| Figure S4.2 Haplotype network configuration on concatenated data sets including two cpDNA regions..... | 170 |

Introduction

The ways in which species are formed, the changes of their geographic ranges through time and the role of environmental conditions on those ranges are issues that have always been central to the study of biodiversity. Since the publication of the works by Darwin (1859) and Wallace (1858), and later with studies on species ecological niches, evolution and interactions (Elton 1927, Grinnell 1917, Hutchinson 1957), it has become clear that species distributions are affected by a variety of physical and biological factors, and that this mosaic of conditions is constantly changing and influencing species behavior, abundance and evolution (Darwin 1859, Andrewartha and Birch 1954, Udvardy 1969, Darlington 1957, MacArthur 1972, Mayr 1963). These factors include the geographic configuration and change of continents, islands and oceans, since they may act as barriers or conduits for dispersal; their climates, soils, and habitats; and the fluctuations in the abundance of those species that interact in a positive or negative way with a given species.

Geographic ranges of species are fundamental units of study in ecology and evolutionary biology since they summarize how species' populations and individuals are organized in space and time (Gaston 2003). Historically, this led scientists to ask questions about: (1) the conditions that allow populations to maintain a positive growth rate, and (2) the impacts that individuals from such populations have on their environment (Hutchinson 1957, 1978, Chase and Leibold 2000). The study of geographic ranges is formed by multiple research programs. Many of these are characterized by the search for

general patterns of species distributions and associations looking at statistical relationships to explain the distribution of biodiversity at large scales, based on the idea that small-scale local processes alone were not able to fully explain the abundance and distribution of species. Examples of such approaches include the field of 'areography,' interested in the description of the structure and position of the ranges (Rapoport 1982), and that of 'macroecology,' which focuses on large-scale description of patterns of abundances across and on the associations of species incorporating their physiological requirements in relation to body size (Brown and Maurer 1989). These approaches, however, usually lack a mechanistic explanation for the patterns and can only generalize on the distributional patterns based on correlative approaches, although this situation is currently changing (Keith et al. 2012).

These 'non-experimental' approaches are informed by a plethora of observations and field experiments, in many ways similar to the keen observations of distributional patterns and of the effect of changes in scale we find in Darwin's work. Despite so much accumulated research, estimating a species' geographic distribution and its limiting factors in space and time is still a challenge, and a priority, given the need to estimate biodiversity under current and future conditions and understanding the processes that generate it.

The estimation of the distribution of species from the perspective of which environmental conditions permit their existence (niches, or Grinnellian niches, when conditions are restricted to certain classes of variables) has been extremely fruitful. When studying species' distributions and niches, it is useful to distinguish interacting variables

(bionomic variables) from those that are dynamically uncoupled from the presence or abundance of the species in question (scenopoetic variables; Hutchinson 1989, Soberón 2007). These variables may have contrasting effects at fine versus coarse spatial resolutions (Wiens 1989, Levin 1992). The many ways in which scenopoetic variables operate at different extents and resolutions can be used to explain distributions of the species and propose scale-dependent hypotheses regarding factors most relevant at different scales (Pulliam 2000, Gaston 2003, Soberón and Peterson 2005, Soberón 2007, 2010, Peterson et al. 2011).

In the chapters presented here, I use information on the natural history of a small set of interacting species to hypothesize how different configurations among the causal factors underlying geographic distributions of species, in the heuristic device called BAM diagram (Soberón and Peterson 2005, Peterson et al. 2011), act at different spatial scales. The BAM diagram displays relationships between abiotic or uncoupled (A) and coupled biotic factors (B), and the movement or dispersal capacities of the species (M). This framework can be used to make explicit the possible arrangements of factors that determine distributions of species, and gives the opportunity to generate hypothetical scenarios, depending on the degree and geometry of their overlap (see Fig. 1.2). Specifically, with this framework, we can analyze interactions of factors at fine and coarse spatial resolutions (Peterson et al. 2011). As a complement to this framework, I conduct analysis and comparisons with methods used in ecology and systematics. Such a multidisciplinary approach allowed me to understand the patterns and processes underlying the distribution and maintenance of species populations at multiple scales.

Here I explore how factors that limit a species' range are structured at multiple spatial and temporal scales. In particular, I ask how biotic and abiotic factors change in importance depending on the spatial and temporal scale at which they are measured. To do this, I build models and testable frameworks for hypotheses in the context of ecological, geographic, and historical conditions limiting and structuring a species range and its genetic diversity and relationships.

For most of the dissertation (chapters 1, 2, and 4), I concentrate primarily on a single species, the desert mistletoe, *Phoradendron californicum* Nutt. (Viscaceae). This allowed me to optimize data acquisition and modelling across a species' geographic range. In particular, I take advantage of the vector-borne parasitic nature of the species to understand the relative importance of scenopoetic variables and dispersal, and the overall role of hosts and dispersers in limiting the species geographic range. This research builds upon previously published work, most of it collected at local scales (a few hectares; e.g., Overton 1997, Aukema 2001), and generalizes the influence of scenopoetic variables, interaction with hosts and dispersal on the expansion and contraction of the species range since 6 mya. A fourth chapter (chapter 3) uses published information on genetic diversity for 40 species which include plants, insects, birds, mammals, and worms, to test the relationship of the abundant-center hypothesis in terms of niche centrality and geographic centrality.

In chapter 1 I explore how dispersal and scenopoetic factors act synergistically to explain the distribution of *P. californicum*, at five spatial resolutions (1, 5, 10, 20, 50 km). I compare correlative niche modeling methods (GARP, Maxent, GAM) with a process-based

model derived from a metapopulation-dynamic framework coupling rates of colonization and extinction. I hypothesize that, as resolution coarsens, variables associated with abiotic factors (climate) will become more important, but that the opposite will apply for biotic variables (dispersal). I developed analyses within the distributional area of the disperser species. Results show that correlative models improved when layers associated with hosts and disperser were used as predictors, in comparison with models based on climate only; however, they tended to overfit to data as more layers were added. Dispersal-related parameters were more relevant at finer resolutions (1–5 km), but the importance of extinction-related parameters did not change with scale. I observed greater coincidence between correlative and process-based models when based only on dimensions of the abiotic niche (climate), but a clearer and more comprehensive mechanistic understanding was derived from the process-based algorithm.

In chapter 2 I test whether the distribution of the mistletoe *P. californicum* is mediated by host distributions (host niche hypothesis, HNH), or by factors such as the mistletoe's autecology (parasite niche hypothesis, PNH) or that of its vectors (vector niche hypothesis, VNH). The null hypothesis is that the ecological niche of the mistletoe will not be distinct from that of its hosts or vectors; alternatively, mistletoe infections might appear in hosts only in regions where host distributions overlap suitable conditions for the parasite. To do this I used ecological niche modelling approaches to summarize suitable environmental conditions for hosts infected and uninfected with mistletoes, as well as for avian dispersers during winter and throughout the year. I compared ecological niches among pairs of species using background similarity tests in relation to the climatic

conditions available and accessible to each species. Niche comparisons supported all PNH expectations but none of the predictions of HNH or VNH. This suggests that hosts and dispersers of mistletoes generally have distinct ecological niches, that mistletoe infections occur in non-random environmental subsets of host and disperser ecological niches, but that mistletoe infections in different hosts, occur under similar climatic conditions. Thus, in this system, the parasite has a rather strictly circumscribed ecological niche, and host species become infected with mistletoe only where they overlap its suitable areas.

In chapter 3 I tested whether the abundant-center hypothesis for ecological niches (Martinez-Meyer et al. 2013) would hold for genetic diversity. One hypothesis predicts that natural populations at geographic range margins will have lower genetic diversity relative to those located centrally in species' distributions due to a link between geographic and environmental marginality; alternatively, genetic variation may be unrelated with geographic marginality via decoupling of geographic and environmental marginality. I investigate the predictivity of geographic patterns of genetic variation based on geographic and environmental marginality using published genetic diversity data for 40 species (insects, plants, birds, mammals, worms). Results showed that only about half of species showed positive relationships between geographic and environmental marginality. Three analyses (sign test, multiple linear regression, and meta-analysis of correlation effect sizes) showed a negative relationship between genetic diversity and distance to environmental niche centroid but no consistent relationship of genetic diversity with distance to geographic range center.

In chapter 4 I tested how different ecological and historical (vicariant) factors shape distributions of individuals and genes in *P. californicum*. I first describe the phylogeographic patterns based on three non-coding chloroplast DNA regions and assess the marginal probability of 16 *a priori* hypotheses related to geologic events and ecological factors in order to predict the cpDNA variation across the geographic range of the species within a Bayesian phylogenetic framework. Complementarily, I use macrofossil record from packrat middens and niche model projections on Last Glacial Maximum climatic conditions for hosts, mistletoe, and a bird specialist to interpret phylogeographic patterns. Results show that patterns of variation in cpDNA haplotypes are most probable under a model reflecting a series of geologic events related to formation of the Baja California Peninsula and seaways across it in the Pliocene and the Pleistocene. Alternatively, fossil record, niche projections, and haplotype distribution suggested shifting distributions of host-mistletoe interactions and evidence of host races, which might explain some of the genealogical history of the cpDNA; however, these hypotheses were not favored by the Bayesian statistical tests. Depending on molecular rate, age estimates for well-supported nodes were compatible with geologic events or climatic oscillations. Our findings suggest that variation of cpDNA across the species range results from the interplay of vicariant events, past climatic oscillations, and more dynamic factors related to ecological processes at finer scales.

Chapter 1

Process-based and correlative modeling of desert mistletoe distribution: A multiscale approach¹

¹ Lira-Noriega A, Soberón J, Miller CP (2013) Process-based and correlative modeling of desert mistletoe distribution: A multiscale approach. *Ecosphere* **4**, art99.

Abstract

Because factors affecting distributional areas of species change as scale (extent and grain) changes, different environmental and biological factors must be integrated across geographic ranges at different resolutions, to understand fully the patterns and processes underlying species' ranges. We expected climate factors to be more important at coarse resolutions and biotic factors at finer resolutions. We used data on occurrence of a parasitic plant (*Phoradendron californicum*), restricted to parts of the Sonoran and Mojave deserts, to analyze how climate and mobility factors explain its distributional area. We developed analyses at five spatial resolutions (1, 5, 10, 20, 50 km) within the distributional area of the disperser species, and compared ecological niche models from three commonly used correlative methods with a process-based model that estimates colonization and extinction rates in a metapopulation framework. Correlative models improved when layers associated with hosts and disperser were used as predictors, in comparison with models based on climate only; however, they tended to overfit to data as more layers were added. Dispersal-related parameters were more relevant at finer resolutions (1-5 km), but importance of extinction-related parameters did not change with scale. We observed greater coincidence between correlative and process-based models when based only on dimensions of the abiotic niche (i.e., climate), but a clearer and more comprehensive mechanistic understanding was derived from the process-based algorithm.

Introduction

The relative roles of biotic and abiotic factors in determining distributions of species at specific spatial scales are a central organizing theme in ecology (Levin 1992).

Understanding how patterns at one scale are manifestations of or influence processes operating at other scales is a particular challenge (Levin and Pacala 1997, Pearson and Dawson 2003, Hastings et al. 2010). The core of this challenge lies in disentangling how changes in scale affect the importance of different factors in shaping species' distributional patterns and processes.

When studying species' distributions, it is useful to distinguish interacting variables from those that are dynamically uncoupled from the presence or abundance of the species in question (scenopoetic variables; Hutchinson 1978). These variables may have contrasting effects at fine versus coarse spatial resolutions (Wiens 1989). The many ways in which scenopoetic variables operate at different extents and resolutions can be used to explain distributions of the species and propose scale-dependent hypotheses regarding factors most relevant at different scales (Pulliam 2000, Gaston 2003, Soberón and Peterson 2005, Soberón 2007, 2010, Peterson et al. 2011).

Using data available documenting species' occurrence and climatic variation, researchers have been able to estimate environmental requirements of many species across broad regions (Guisan and Zimmermann 2000, Elith et al. 2006). Factors manifested at finer resolutions are less well studied at the scope of broad geographic ranges, leaving a gap in understanding as to how effects of these factors vary spatially and temporally. Also, knowledge of species' distributions at local scales may be sparse or

biased spatially across geographic ranges, which makes analyzing the relative importance of variables even more difficult (MacArthur 1972, Levin 1992). These considerations explain why studies of spatial distributions of species that combine broad-scale and fine-scale views remain uncommon (e.g., Mackey and Lindenmayer 2001, Gaston et al. 2004, Heikkinen et al. 2007, Cunningham et al. 2009).

Correlative and process-based modeling are two approaches for exploring factors important in determining distributions of species at different spatial scales (Robertson et al. 2003, Kearney et al. 2010). The main difference between these approaches is that correlative methods simply seek associations between environments and occurrences from across broad geographic ranges, whereas process-based methods incorporate explicit hypotheses about biological processes (Robertson et al. 2003, Kearney and Porter 2009, Monahan 2009, Morin and Thuiller 2009, Cabral and Schurr 2010, Kearney et al. 2010). In particular, a set of factors that is emerging as crucial in process-based modeling studies is dispersal: incorporating dispersal factors improves model performance markedly (Allouche et al. 2008, Cabral and Schurr 2011, Brotons et al. 2012).

In this paper, we explore how dispersal and scenopoetic factors act synergistically to explain the distribution of the Desert Mistletoe, *Phoradendron californicum*, at varying spatial resolutions. *P. californicum* is a hemi-parasitic plant associated with legume hosts in the Sonoran and Mojave deserts, and it is dispersed in largest part by the bird species *Phainopepla nitens* (Walsberg 1975, Kuijt 2003). This parasite-host-disperser system offers two advantages for understanding how scaling of biological processes govern distributions (Overton 1996, Aukema and Martínez del Rio 2002, Aukema 2003, 2004): (1)

hosts are known, and their distributions can be studied at high spatial resolution using aerial photographs; and (2) dispersal is determined chiefly by a single disperser. We modeled the portion of the distribution of *P. californicum* in the U.S., where detailed data on *Phainopepla nitens* are available (almost 900,000 km²; Fig. 1.1), encompassing approximately half of the parasite species' range. We compare commonly-used correlative niche modeling methods (GARP, Maxent, GAM) with a process-based model derived from a metapopulation-dynamic framework coupling rates of colonization and extinction. Following Pearson and Dawson (2003) and others, we hypothesize that, as resolution coarsens, variables associated with abiotic factors (e.g., climate) will become more important, but that the opposite will apply for biotic variables (e.g., dispersal).

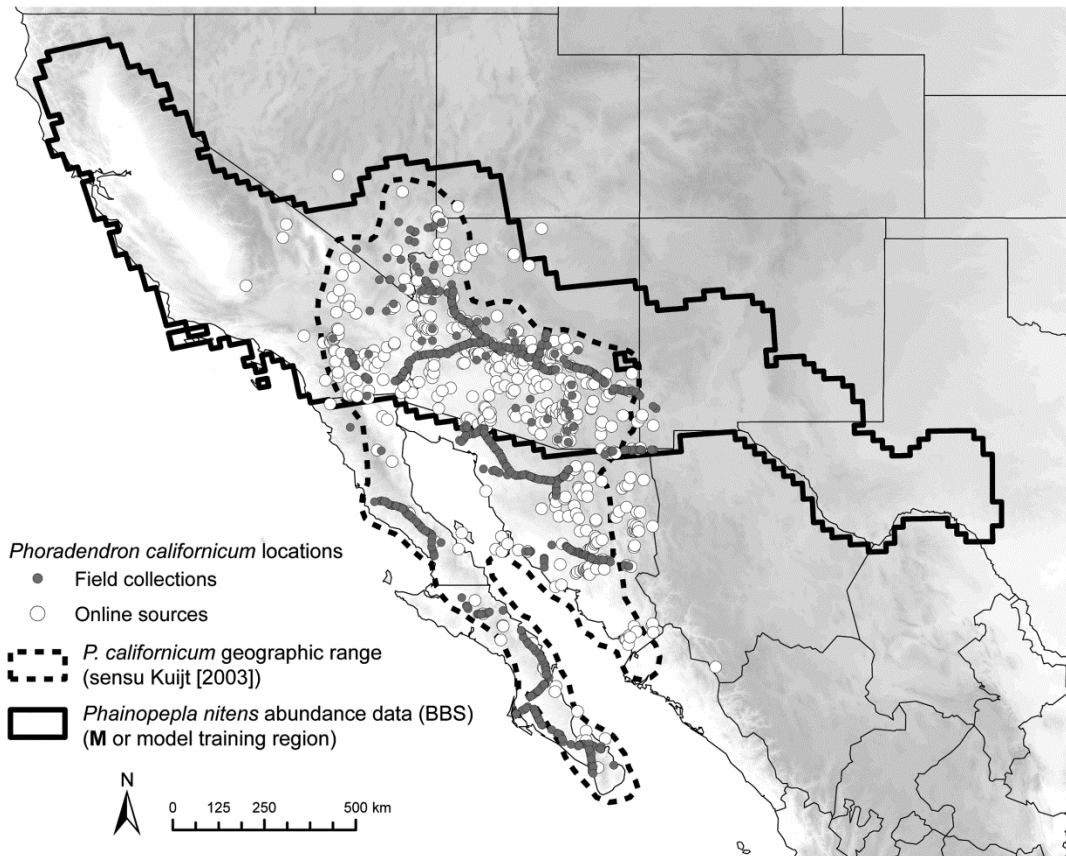


Figure 1.1. Author-collected (A.L.-N.) and Internet-located occurrences of *P. californicum* and extent of study area. The study area corresponds to the distributional area of the principal disperser, assumed to represent accessible areas for the mistletoe (**M**), for which abundance data are available (thickest black line). Notice there are areas where the disperser or hosts can be present but not the mistletoe; these areas are relevant to understand the interaction of factors that limit the distribution of the species as well as challenging areas in which to test the models.

Conceptual framework

To help understand causal factors underlying geographic distributions of species, a heuristic device called the BAM diagram is useful (Soberón and Peterson 2005, Peterson et al. 2011). The BAM diagram displays relationships between abiotic or uncoupled (**A**) and coupled biotic factors (**B**), and the movement or dispersal capacities of the species (**M**). This framework can be used to make explicit the possible arrangements of factors that determine distributions of species, and gives the opportunity to generate

hypothetical scenarios, depending on the degree and geometry of their overlap (Fig. 1.2). Specifically, with this framework, we can analyze interactions of factors at fine and coarse spatial resolutions.

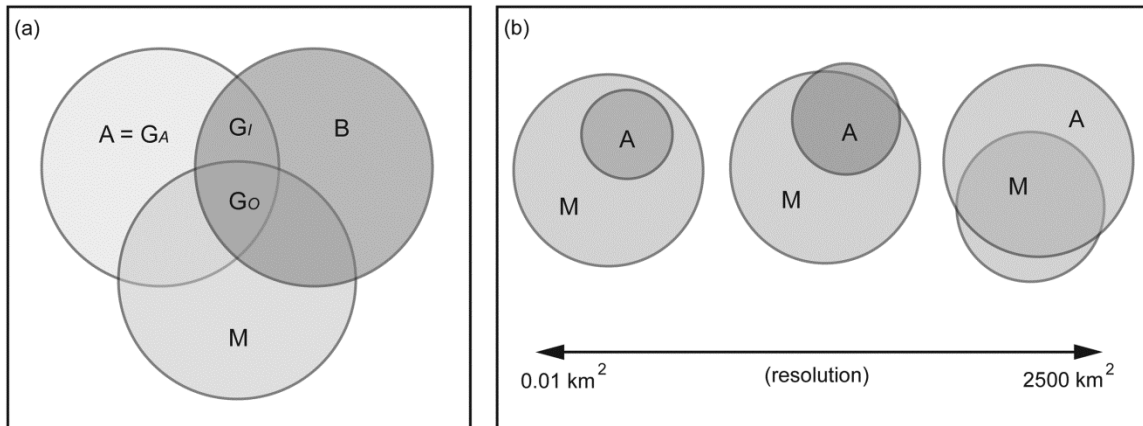


Figure 1.2. Conceptual framework showing (a) the relationship between biotic-abiotic-mobility (BAM) conditions for a species to be present. (b) Interpretation of the BAM diagram in this modeling exercise restricts to the use of abiotic conditions (**A**) and accessible areas (**M**), assuming that the interaction between host and parasite is uncoupled, and that the positive interaction between disperser and parasite makes biotic conditions (**B**) and accessible area (**M**) coincident. As scale changes, limiting factors in **A** and **M** will also change. At higher resolutions, almost the entire area is accessible, and climate is not so limiting, whereas at coarser resolutions dispersal becomes more difficult and climate is more constant.

In the mistletoe-host-disperser system, the BAM diagram can be simplified significantly by making some reasonable assumptions. The conditions manifested across **A** (Soberón and Peterson 2005, Soberón 2007) represent those under which the species can have a positive growth rate (Hutchinson 1978); therefore, conditions in **A** are linked intimately to the environmental dimensions on which mechanisms of establishment and survivorship depend (Wiens 2000). Factors in **M** are related to movement: what happens across **M** determines how populations will be structured, demographically and

genetically, although testing this particular idea will be accomplished in a later phase of this project (Lira-Noriega et al. in prep).

We hypothesize that, to a first degree of approximation, the interaction with the host can be regarded as uncoupled, since hosts have expected lifetimes at least 10-fold longer than those of parasites (Overton 1996, 1997) and therefore their population dynamics can be regarded as approximately static relative to the faster demography of the parasites. The simplifying assumption of uncoupled dynamics of the total host population is often made in epidemiological studies (Anderson, 1981). This means that we regard climate and presence of hosts as part of the **A** circle. Second, we did not include the effect of competitors, which are not known to be present, nor of herbivores or pollinators, because information about them at the spatial extent of our study is simply unavailable.

Finally, in the mistletoe system, one major biotic factor, birds, act directly as dispersers. From a certain point of view the dispersers may be considered as part of **B**, but their effect is clearly felt in the dispersal circle, making **B** and **M** coincident. In consequence, we can simplify our system to a two-factor diagram: the abiotic climatic factors (**A**) and the hosts substrate, that determine overall potential distributions, and the movement or dispersal capacity of the species (**M**), driven mainly by the bird that disperses seeds among trees. **M** represents a hypothesis of the regions that have been accessible for the species over relevant time periods; as such, **M** is the area across which models should be calibrated (Barve et al. 2011; see also Acevedo et al. 2012). Following this reasoning, we designated an **M** as the area of distribution of the mistletoe's main

disperser, *P. nitens*, for which we have detailed abundance information (Fig. 1.1).

Although other potential dispersers of the mistletoe species in question are known, none is as closely associated as this species (Walsberg 1975); adding the densities of other bird species to the model would not have changed our results, given that they overlap broadly in their distribution and behavior with that of *P. nitens*. This assumption can be relaxed in future studies, but for the present simplifies the process-based modeling exercise considerably.

Methods

We designed a comparison of a process-based model with correlative models from three algorithms to understand the distribution of *P. californicum* at five spatial resolutions (1, 5, 10, 20, 50 km). We first describe the series of steps we followed in order to obtain data on the distribution of the parasite followed by the assemblage of three sets of environmental variables: spatial variation in disperser density, spatial variation in numbers of hosts, and climatic factors across the study area. We then describe the design and implementation of each model type and finally the comparisons among them.

Distribution of species presences and landscape characteristics

To estimate proportions of mistletoe-infected trees, we recorded geographic locations of infected host trees along roads. One of us (A.L.-N.) sampled occurrences of host trees infected by *P. californicum* across the southwestern United States and northwestern Mexico (Fig. 1.1). We used roads as sampling transects as an efficient means of surveying the species' range limits, allowing us to gather information regarding the broader set of

climatic situations where the species occurs. We used a GPS unit to record geographic coordinates for each infected host tree located within 100 m of the road. In total, we sampled 16,000 km (4153 km within the modeling extent) of roads, and collected 17,371 unique geographic coordinates of infected trees (Fig. 1.1), 12,578 of which fell within the modeling extent (see below).

Sampling along roads may potentially bias the data, since roads are usually areas of higher water accumulation, thus impacting quality of the hosts (Norton and Smith 1999). However, given that we are generalizing prevalence of the species from host trees at several spatial resolutions (cells of 1, 5, 10, 20 and 50 km by side), we assume that the effect of roads is constant and will not influence our general understanding of mistletoe distributions. Identification of host and mistletoe species was achieved via collection of herbarium specimens at sites every ~50 km across the study area or every time changes in host species composition were suspected. We used a second GPS unit to record landmarks by which to annotate general descriptions of species composition and vegetation physiognomy and landscape characteristics along the road; this information was used in processing aerial photographs (see below). All voucher specimens are deposited at the Ronald L. McGregor Herbarium, University of Kansas; copies of the collection were deposited at different herbaria in Mexico and the United States (see Acknowledgements). The two GPS units were Garmin 60CSx, with antennas to improve precision of coordinate estimates.

Host tree mapping

To derive proportions of infected trees for the process-based model, we extracted geographic coordinates of tree canopies along roads sampled. This step was achieved using National Agriculture Imagery Program (NAIP) aerial photographs, ideal for tree mapping because of their high spatial and spectral resolution (1 m and four bands—red, green, blue, and near infrared). We carried out object-oriented classification of these photographs with the software eCognition 3.0 (Baatz et al. 2003). We first identified all 3.75' x 3.75' aerial photographs that intersected the roads sampled. We further reduced the set of aerial photographs to those including the land use cover types in which mistletoe infections were found via comparisons with the 2001 National Land Cover Database (30 m resolution; Homer et al. 2004); land cover types considered were barren land, cultivated land, deciduous forest, development low density, development medium intensity, development open space, emergent herbaceous wetlands, hay/pasture, herbaceous, open water, shrub/scrub, and woody wetlands. We selected at random 10% (67) of the aerial photographs for the states of Arizona (25; from 2007), New Mexico (6; 2009), California (13; 2009), and Nevada (23; 2006). Because of significant computational demands in the classification process, each 3.75' x 3.75' image was split into four equal portions for processing, generating a total of 268 images to classify.

In eCognition, we first segmented each image into two levels, with the following parameters: level 1 (scale = 10, color = 0.8, shape = 0.2, smoothness and compactness = 0.5) and level 2 (scale = 3, color = 0.8, shape = 0.2, smoothness and compactness = 0.5). Then, to classify trees, we selected polygons manually from the level 2 objects to be used

as canopy samples, and classified each image using the standard nearest neighbor with the mean of each of the four bands (R, G, B, and NIR), the mean difference from neighbors, and the mean difference between the level 2 objects nested within the level 1 super-object. These procedures have been used in previous studies that have analyzed mesquite distributions in similar landscapes and regions (e.g., Laliberte et al. 2004). Using ArcGIS 9.3, we dissolved the raw polygon output from eCognition to obtain single-tree polygons. This step was necessary because the output sometimes contained multiple polygons subdividing single tree crowns. Although this procedure sometimes reduced numbers of trees estimated, it was not a common problem overall, and estimates of trees were close to true numbers of trees in each image ($R^2 = 0.617$, $P < 0.001$). This step allowed us to extract 5,786,586 polygons corresponding to tree crowns, and count actual numbers of trees within the 200 m strip along roads, to estimate proportions of trees infected (via the GPS coordinates of mistletoes described above).

Climate, host, and disperser summaries

These datasets were each derived at five spatial resolutions, as follows. Climatic layers used were annual mean temperature and annual precipitation, obtained from the WorldClim database (Hijmans et al. 2005), using the 30", 2.5', 5', and 10' resolution products to match 1 km, 5 km, 10 km, and 20 km resolutions, respectively; for the 50 km resolution, we scaled the values up with the mean of the 10' raster layers using a bilinear interpolation from nearest neighbor cells. Because other climatic factors, particularly freezing temperatures and sunny days, can be important limiting factors for the mistletoe, we tested models with two other variables estimated directly from weather-

station data (Easterling et al. 1999) for a 20-yr period (number of continuous days of freezing temperatures and number of continuous rainless days). Because models resulting showed similar or lower performance scores, these variables were not included in our final analyses.

The raster data layer summarizing abundances of *Phainopepla nitens* was obtained from the Breeding Bird Survey database (v.12.07.2011 [Sauer et al. 2011]), which comes as a vector-format data layer with cells at a resolution of 25 km, the product of interpolating point abundance information across the bird species' distribution in the United States. In contrast to the rest of the layers used for modeling, this data layer was used statically at its native resolution (i.e., not scale-dependent) for the first four resolutions of our analyses.

To estimate numbers of host trees across the region, we developed models to predict numbers of trees per cell at 1 km resolution using random forests (randomForest in R; Liaw and Wiener 2002). This estimate was based on 580 1-km cells sampled across the region from 85 images from the NAIP (55 images from Arizona, 7 from New Mexico, 7 from California, and 16 from Nevada) that were classified following the protocol described above. Specifically, we asked for a total of 10,000 trees developed under the random forest protocol, from which we estimated the logarithm of the number of host trees with the following statistical model: \log_{10} of host trees \sim GRS 2000 + NVG 2000 + annual mean temperature + annual precipitation + maximum temperature of the warmest month + precipitation of the wettest month + slope + elevation + aspect + latitude + longitude. The grass/scrub/woodland (GRS 2000) and barren/very sparsely

vegetated land (NVG 2000) are raster data layers obtained from the Harmonized World Soil Database v 1.1 (Fischer et al. 2008). The final estimate of the number of host trees was more explanatory (67.0% of total variation) and showed better fit between observed and predicted numbers of trees ($r = 0.91$, $P < 0.01$) and between observed and independent external data set aside from the classified images ($r = 0.60$, $P < 0.01$) than other random forests based on different combinations of variables, numbers of observations, and numbers of trees within the process. This procedure also gave better results than the two most explanatory (67.7–68.1% of total variation) generalized additive models (GAMs) of different combinations of same predictors as used in the random forest ($r = -0.22$, $P > 0.01$; $r = -0.16$, $P > 0.01$). Although the explained variances are similar, the shape of the relationship in the random forests is more regular and linear than with the GAMs.

Process-based model

To estimate probability of occurrence of *P. californicum* in grid cells via a process-based modeling approach, we developed a spatially explicit model incorporating the balancing rates of colonization and local extinction, as proposed in the theory of metapopulations (Hanski 1999, Vandermeer and Goldberg 2003, Roberts and Hamann 2012). The model was developed as follows.

After some assumptions related to using a mean-field approximation, we fit the following equation following Hanski's (1999) incidence function model:

$$\bar{p}_J = \frac{\bar{c}_J}{\bar{c}_J + \bar{e}_J},$$

where \bar{p}_J represents the proportion of hosts in a composite cell J occupied by mistletoes.

The parameter \bar{c}_J is the mean colonization rate, assumed to be a function of the density of birds and host trees in the focal cell J and neighboring cells. The parameter \bar{e}_J is the mean death rate of mistletoes, assumed to be a function of the distance between optimal climate, as estimated as the difference of average climatic conditions across known occurrence points (for each resolution) and the climate in the cell J . This model was fit for each of the five spatial resolutions using a maximum likelihood routine implemented in R. Derivations of formulas for this model are provided in Appendix 1.1.

To estimate variability in parameters, we resampled the data with replacement 115 times to obtain a distribution of colonization and extinction-related parameter values with the following number of observations in each iteration: 200 (56% of the original data matrix) at 1 km resolution, 70 (63%) at 5 km, 50 (68%) at 10 km, 30 (54%) at 20 km, and 20 (64%) at 50 km. The distributions obtained were used to assess whether parameters differed from zero, and how different they were among scales, using t -tests. Specifically, we evaluated two colonization parameters, disperser abundance and disperser cost of movement across neighboring cells; in the extinction formula, we tested the deviation from a climate optimum as defined by Mahalanobis distance to the environments in the occurrence points for each resolution (see Appendix 1.1).

Correlative models

We ran a total of 45 correlative models: three algorithms, three sets of environmental predictors, and five spatial resolutions. We used two presence-background correlative niche-modeling algorithms: DesktopGARP (best subsets version in OpenModeller v.1.1.0; de Souza Muñoz et al. 2011) and Maxent v.3.3.3 (Phillips et al. 2006), as well as the presence-absence algorithm generalized additive models (GAM; mgcv [Wood 2011]). We set parameters in GARP as follows: occurrence data for training 50%, soft omission threshold, 100 replicate runs, and best subsets option; the rest of the settings were as default. In Maxent, we set 50% of occurrence points for model calibration, and chose logistic output; the rest of settings were as default. To run models, we selected 5% ($N = 629$) of the total number of infected trees, after considering the spatial lag of spatial autocorrelations in environmental characteristics as follows. The spatial lag was estimated on the first principal component of the 19 bioclimatic variables as a surrogate for the environmental space in the study region. Principal components were calculated using a correlation matrix in R (stats; R Development Core Team 2011) and the spatial lag was estimated as the distance associated with the sill of a semivariogram in the package Spatial Analysis in Macroecology (SAM 4.0; Rangel et al. 2010). We then sampled the 5% of the occurrence points subject to the constraint that they be separated by at least that distance in space.

We explored influences of different environmental factors on the distribution of *P. californicum* in correlative models using three sets of variables: (1) annual mean temperature and annual precipitation (“climate”); (2) abundance of *Phainopepla nitens*

and numbers of host trees (“disperser + host”); and (3) a combination of all three (“climate + disperser + host”). All models were trained and projected within the extent that corresponds to the distribution of the disperser (**M**) at each spatial resolution. The importance of environmental predictors at each scale was estimated using the jackknife of regularized training gain in Maxent, recalculation of GARP accuracy using jackknife in openModeller, and the *P*-value for significance of each variable in GAMs. These procedures form part of the output of each algorithm.

Model evaluations and comparisons

All 50 models (45 correlative and 5 process-based) were evaluated using the partial AUC approaches implemented by Peterson et al. (2008), using 262 independent unique occurrence points for *P. californicum* from the Global Biodiversity Information Facility (www.gbif.org; search in September 2010). This procedure allowed us to evaluate performance of each model as compared to random expectations, as well as to compare performance across scales and modeling methods. Partial AUC approaches limit analysis to portions of the ROC curve that are relevant to the question at hand (i.e., within omission error tolerances); so one calculates the ratio between the area under the curve for observed values against the area under the line of random discrimination, AUC ratios are expected to depart upwards from one as model performance is better than random. The main advantage of this procedure is that the comparison covers only the range of values over which each algorithm predicts, thus avoiding problem caused by using equal scales of values when such is not the case in all comparisons (e.g., Maxent and GARP; Peterson et al. 2008).

To do this testing, we first multiplied grids by 1000, and converted each floating-point grid to an integer grid in ArcGIS 10. Using the modeled suitability values associated with each independent testing point, we implemented partial AUCs by running 1000 bootstrap simulations in a Visual Basic program (Barve, www.biodiversity-informatics-training.org), with 50% of points resampled with replacement in each iteration of the bootstrap, and $E = 0.05$, given that these testing occurrences were obtained from GBIF and may be subject to some georeferencing or identification error. Distributions of the randomized ratios were compared with z-tests to see if ratios were consistently larger than 1 (1 corresponds to random discrimination). The ratios that resulted from this procedure were also used to compare models in a three-way ANOVA for type of algorithm, environmental predictors, resolution, and interactions of these three factors using R (stats; R Development Core Team 2008).

The degree of spatial agreement between model predictions was calculated using a fuzzy Kappa statistic in the software Map Comparison Kit (Visser and de Nijs 2006), and Pearson and Spearman correlations were estimated between 3000 random points for resolutions 1-20 km and between the 527 pixels at the 50 km resolution following the Dutilleul method to correct for spatial autocorrelation in SAM 4.0 (Rangel et al. 2010), which corrects the number of degrees of freedom of estimated variances. Kappa statistics were calculated for models thresholded using the minimum training presence value (Liu et al. 2005, Wilson et al. 2005), given that we are confident that occurrence points used for model calibration correspond to a *P. californicum* with no error ($E = 0$). Finally, we

compared the area predicted as suitable for each model using boxplots to examine effects of model type, environmental predictors, and spatial resolution visually.

Results

All models, except for a marginally lower result in the 1 km process-based model, performed better than random expectations when tested against independent occurrence points (all $P < 0.05$; Table S1.1). Comparisons of model performance using AUC ratios indicated differences in performance of models depending on the algorithm, environmental predictors, and resolution, as well as interactions among these factors (Table 1.1). At all resolutions, the lowest AUC ratios were for models using climate only as environmental predictors; AUC ratios were in general higher for models with disperser + host and climate + disperser + host environmental predictors alone (Fig. 1.3). AUC ratios at resolutions of 1 and 5 km were highest when the environmental predictors were climate + disperser + host, followed by the AUC ratios when the environmental predictors were disperser + host, and comparatively lower AUC ratios when the environmental predictor was climate (Fig. 1.3). AUC ratios at resolutions of 10 and 20 km had lower mean ratios when the whole set of predictors were used. At the coarsest resolution (50 km), AUC ratios remained low for climate and disperser + host, but were considerably higher for climate + disperser + host (Fig. 1.3).

Table 1.1. Three-way ANOVA on partial AUC ratios using as factors the different sets of variables (“climate”, “disperser + host”, “climate + disperser + host”), algorithms (process-based, GARP, Maxent, GAM), and resolutions (1, 5, 10, 20, 50 km), including interactions among factors. All comparisons were significantly different at $P < 10^{-15}$.

| | Sum of squares | d.f. | F |
|------------------------------------|----------------|--------|----------|
| Algorithm | 184.031 | 3 | 16981.19 |
| Resolution | 11.253 | 4 | 778.75 |
| Variables | 110.021 | 2 | 15228.07 |
| Algorithm : Resolution | 55.616 | 11 | 1399.61 |
| Algorithm : Variables | 32.411 | 4 | 2243.01 |
| Resolution : Variables | 39.347 | 8 | 1361.5 |
| Algorithm : Resolution : Variables | 49.288 | 16 | 852.74 |
| Residuals | 177.01 | 49,000 | |

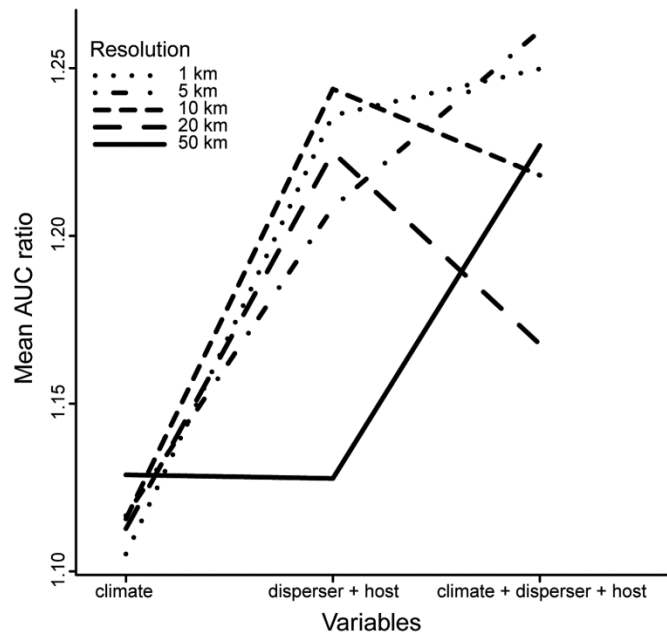


Figure 1.3. Interaction plot of AUC ratios after 1000 iterations in the partial ROC based on independent occurrences of *Phoradendron californicum*. Differences in model performances are statistically significant ($P < 0.001$). Process-based model results were included in the set of variables “climate + disperser + host.”

Coincidence among models, after converting them to binary maps, was highly variable in terms of both amount of area predicted as suitable and amount of overlap. Proportional areas identified as suitable differed depending on algorithm and environmental predictors, but not on resolution (Fig. 1.4; see also Fig. S1.1). On the other

hand, amount of overlap between models at each resolution varied considerably when compared with the fuzzy Kappa statistic (Fig. 1.5). The spatial variation in the area identified as suitable can be divided in two broad groups: contiguous areas with high geographic coincidence and more disjunct areas with lower geographic coincidence (see an example in Fig. S1.2). In general, most map comparisons fell in the more disjunct category, meaning that completely overlapping areas are unusual (Fig. 1.5). Moreover, these broad groups did not fall in the same categories when compared across scales. Correlations between models using raw output values instead of thresholded values coincided with results from fuzzy Kappa comparisons (Table 1.2).

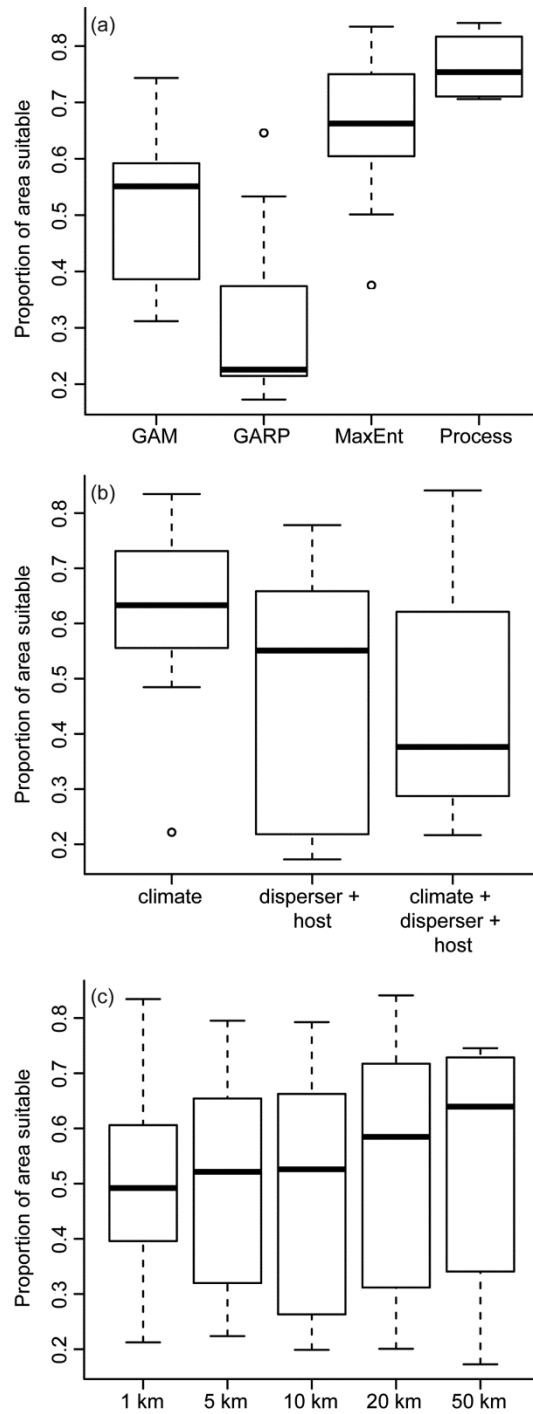


Figure 1.4. Proportion of area predicted as suitable summarized by (a) model or algorithm type, (b) predictor variables, and (c) resolution. Suitable area was considered after converting models into binary predictions using a minimum training presence threshold approach.

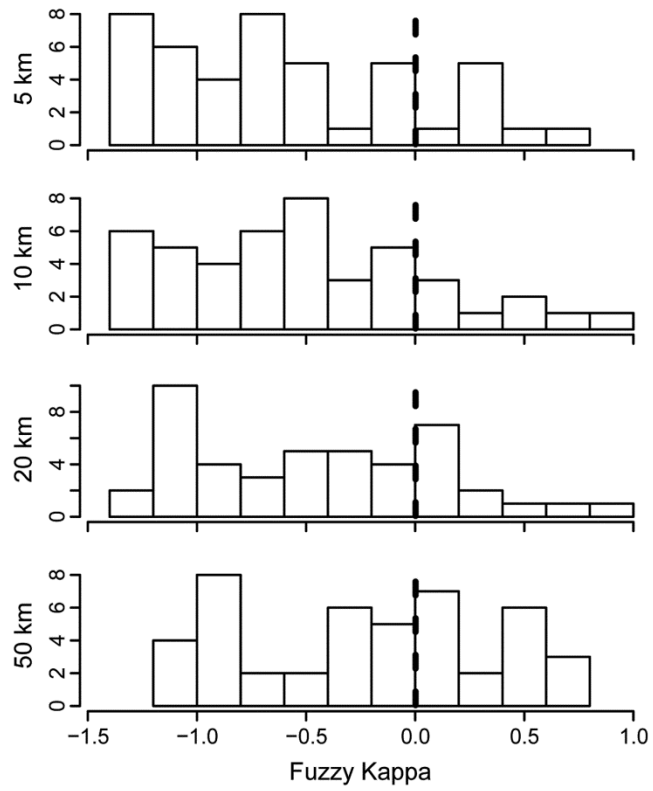


Figure 1.5. Summary of degree of coincidence or overlap between pairs of maps (45 in total) using fuzzy Kappa statistics (Hagen 2003). Fuzzy Kappa shows values greater than 0 when maps have a large coincidence between areas predicted as suitable or non-suitable, and values less than 0 (either suitable or not) when maps show less contiguous more disjoint predictions.

Table 1.2. Pairwise correlations between models after correcting for spatial autocorrelation with Dutilleul method in SAM (see Methods for details). g = GARP, gm = GAM, m = Maxent, process = metapopulation process-based model; c = climate, d = disperser, h = host.

| Comparison | | 1 km | | 5 km | | 10 km | | 20 km | | 50 km | | |
|------------|--------|--------|--------|--------|--------|-------|--------|-------|--------|-------|--------|--------|
| Mod 1 | Mod 2 | Pear. | Prob. | Pear. | Prob. | Pear. | Prob. | Pear. | Prob. | Pear. | Prob. | |
| process | g_dh | 0.38 | 0.011 | 0.31 | 0.082 | 0.31 | 0.086 | 0.18 | 0.241 | 0.24 | 0.182 | |
| | g_c | 0.28 | 0.012 | 0.66 | <0.001 | 0.66 | <0.001 | 0.74 | <0.001 | 0.66 | <0.001 | |
| | g_cdh | 0.34 | 0.017 | 0.34 | 0.052 | 0.37 | 0.04 | 0.2 | 0.188 | 0.3 | 0.112 | |
| | gm_dh | 0.41 | 0.012 | 0.37 | 0.061 | 0.37 | 0.063 | 0.2 | 0.214 | 0.32 | 0.128 | |
| | gm_c | 0.21 | 0.108 | 0.65 | <0.001 | 0.68 | <0.001 | 0.49 | <0.001 | 0.42 | 0.008 | |
| | gm_cdh | 0.37 | 0.023 | 0.42 | 0.036 | 0.44 | 0.019 | 0.26 | 0.095 | 0.31 | 0.14 | |
| | m_dh | 0.39 | 0.009 | 0.37 | 0.036 | 0.39 | 0.03 | 0.19 | 0.208 | 0.32 | 0.107 | |
| | m_c | 0.21 | 0.056 | 0.69 | <0.001 | 0.78 | <0.001 | 0.73 | <0.001 | 0.61 | <0.001 | |
| g_dh | m_cdh | 0.28 | 0.023 | 0.43 | 0.005 | 0.48 | 0.002 | 0.27 | 0.063 | 0.38 | 0.056 | |
| | g_c | 0.27 | 0.1 | 0.28 | 0.063 | 0.24 | 0.126 | 0.23 | 0.12 | 0.18 | 0.197 | |
| | g_cdh | 0.91 | <0.001 | 0.9 | <0.001 | 0.89 | <0.001 | 0.97 | <0.001 | 0.79 | <0.001 | |
| | gm_dh | 0.92 | <0.001 | 0.91 | <0.001 | 0.93 | <0.001 | 0.94 | <0.001 | 0.86 | <0.001 | |
| | gm_c | 0.37 | 0.06 | 0.39 | 0.04 | 0.38 | 0.053 | 0.4 | 0.032 | 0.39 | 0.022 | |
| | gm_cdh | 0.88 | <0.001 | 0.86 | <0.001 | 0.82 | 0.001 | 0.83 | <0.001 | 0.76 | 0.001 | |
| | m_dh | 0.91 | <0.001 | 0.91 | <0.001 | 0.94 | <0.001 | 0.91 | <0.001 | 0.9 | <0.001 | |
| | m_c | 0.26 | <0.001 | 0.31 | 0.03 | 0.35 | 0.049 | 0.35 | 0.045 | 0.34 | 0.059 | |
| g_c | m_cdh | 0.75 | <0.001 | 0.75 | <0.001 | 0.8 | <0.001 | 0.93 | <0.001 | 0.76 | 0.003 | |
| | g_cdh | 0.29 | 0.064 | 0.34 | 0.023 | 0.34 | 0.023 | 0.27 | 0.063 | 0.19 | 0.181 | |
| | gm_dh | 0.31 | 0.077 | 0.33 | 0.047 | 0.27 | 0.1 | 0.26 | 0.101 | 0.23 | 0.158 | |
| | gm_c | 0.81 | <0.001 | 0.78 | <0.001 | 0.73 | <0.001 | 0.67 | <0.001 | 0.58 | <0.001 | |
| | gm_cdh | 0.4 | 0.023 | 0.42 | 0.015 | 0.4 | 0.012 | 0.38 | 0.012 | 0.3 | 0.064 | |
| | m_dh | 0.29 | 0.072 | 0.29 | 0.057 | 0.26 | 0.085 | 0.24 | 0.101 | 0.22 | 0.158 | |
| | m_c | 0.83 | <0.001 | 0.88 | <0.001 | 0.81 | <0.001 | 0.85 | <0.001 | 0.78 | <0.001 | |
| | m_cdh | 0.44 | <0.001 | 0.46 | <0.001 | 0.47 | <0.001 | 0.34 | 0.018 | 0.32 | 0.036 | |
| g_cdh | gm_dh | 0.9 | <0.001 | 0.89 | <0.001 | 0.91 | <0.001 | 0.92 | <0.001 | 0.86 | <0.001 | |
| | gm_c | 0.34 | 0.076 | 0.43 | 0.021 | 0.42 | 0.027 | 0.4 | 0.031 | 0.41 | 0.021 | |
| | gm_cdh | 0.85 | <0.001 | 0.87 | <0.001 | 0.85 | <0.001 | 0.83 | <0.001 | 0.74 | 0.005 | |
| | m_dh | 0.9 | <0.001 | 0.91 | <0.001 | 0.92 | <0.001 | 0.9 | <0.001 | 0.87 | <0.001 | |
| | m_c | 0.28 | 0.029 | 0.37 | 0.01 | 0.4 | 0.022 | 0.36 | 0.036 | 0.36 | 0.05 | |
| | m_cdh | 0.75 | <0.001 | 0.8 | <0.001 | 0.87 | <0.001 | 0.93 | <0.001 | 0.81 | 0.002 | |
| | gm_dh | gm_c | 0.45 | 0.037 | 0.49 | 0.02 | 0.45 | 0.032 | 0.46 | 0.022 | 0.5 | 0.01 |
| | gm_cdh | 0.94 | <0.001 | 0.95 | <0.001 | 0.89 | <0.001 | 0.89 | <0.001 | 0.9 | <0.001 | |
| gm_dh | m_dh | 0.89 | <0.001 | 0.92 | <0.001 | 0.96 | <0.001 | 0.92 | <0.001 | 0.96 | <0.001 | |
| | m_c | 0.26 | 0.074 | 0.34 | 0.032 | 0.39 | 0.039 | 0.39 | 0.034 | 0.43 | 0.038 | |
| | m_cdh | 0.74 | <0.001 | 0.77 | <0.001 | 0.82 | <0.001 | 0.92 | <0.001 | 0.89 | 0.001 | |
| | gm_c | gm_cdh | 0.52 | 0.013 | 0.58 | 0.005 | 0.58 | 0.003 | 0.59 | 0.002 | 0.56 | 0.004 |
| | m_dh | 0.36 | 0.069 | 0.87 | <0.001 | 0.41 | 0.033 | 0.41 | 0.026 | 0.46 | 0.018 | |
| | m_c | 0.79 | <0.001 | 0.42 | 0.01 | 0.89 | <0.001 | 0.75 | <0.001 | 0.82 | <0.001 | |
| | m_cdh | 0.48 | 0.002 | 0.8 | <0.001 | 0.58 | <0.001 | 0.46 | 0.01 | 0.6 | <0.001 | |
| | gm_cdh | m_dh | 0.86 | <0.001 | 0.41 | 0.031 | 0.83 | 0.002 | 0.8 | 0.002 | 0.87 | <0.001 |
| m_dh | m_c | 0.33 | 0.022 | 0.83 | <0.001 | 0.52 | 0.004 | 0.48 | 0.006 | 0.51 | 0.012 | |
| | m_cdh | 0.76 | <0.001 | 0.54 | <0.001 | 0.86 | <0.001 | 0.96 | <0.001 | 0.86 | 0.002 | |
| | m_c | 0.31 | 0.02 | 0.33 | 0.019 | 0.38 | 0.026 | 0.38 | 0.025 | 0.4 | 0.048 | |
| | m_cdh | 0.81 | <0.001 | 0.78 | <0.001 | 0.86 | <0.001 | 0.96 | <0.001 | 0.89 | 0.001 | |

m_c m_cdh 0.5 <0.001 0.53 <0.001 0.56 <0.001 0.44 0.007 0.58 0.002

In the process-based model, the colonization parameter associated with disperser cost of movement across the landscape showed significant departure from zero for the 1 and 5 km resolutions, and the parameter associated with disperser abundance showed significant departure from zero at all resolutions but was significantly higher at the three finest resolutions (Table 1.3; Fig. 1.6). Comparing across resolutions, the parameter associated with disperser cost of movement was significantly higher for the scales of 1 and 5 km. Also, when comparing across resolutions, the parameter associated with disperser abundance at 1 km resolution was significantly higher than those for 20 and 50 km; the value from 5 km was higher than that of the value of 20 km; and the value from 10 km was significantly higher than the values from 20 and 50 km (Table 1.4). Parameter values associated with the extinction function of the process-based model did not differ significantly from one another across scales.

Table 1.3. Departure from zero (*t*-test) of colonization parameters for disperser movement cost across the landscape given topographic heterogeneity and disperser abundance. **P* < 0.1, ***P* < 0.05, ****P* < 0.01.

| Parameter | Observed | Mean | S.E. | <i>t</i> | Prob. |
|---------------------|----------|-------|-------|----------|----------|
| Movement cost | | | | | |
| 1 km | 1.000 | 0.995 | 0.016 | 62.295 | 0.000*** |
| 5 km | 0.135 | 0.130 | 0.008 | 16.681 | 0.000*** |
| 10 km | 0.002 | 0.006 | 0.008 | 0.266 | 0.791 |
| 20 km | 0.009 | 0.009 | 0.006 | 1.348 | 0.180 |
| 50 km | 0.003 | 0.007 | 0.007 | 0.409 | 0.683 |
| Disperser abundance | | | | | |
| 1 km | 1.649 | 1.434 | 0.514 | 3.206 | 0.002*** |
| 5 km | 0.607 | 0.582 | 0.121 | 4.999 | 0.000*** |
| 10 km | 1.649 | 0.981 | 0.382 | 4.318 | 0.000*** |
| 20 km | 0.174 | 0.150 | 0.082 | 2.109 | 0.037 |
| 50 km | 0.365 | 0.195 | 0.103 | 3.549 | 0.001 |

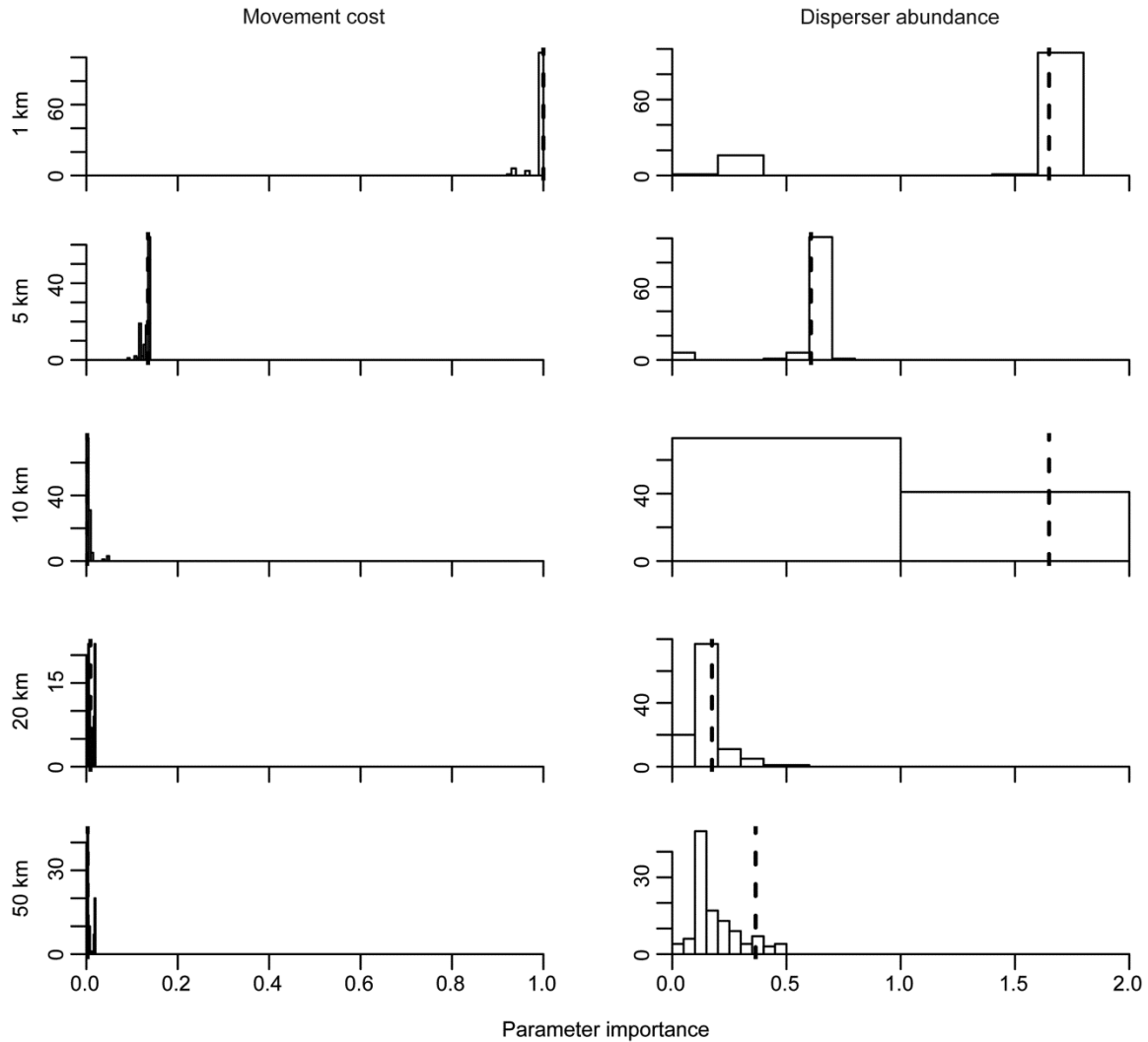


Figure 1.6. Importance of parameters from the process-based model associated with (1) cost of movement for the disperser across the landscape given by topographic heterogeneity and (2) disperser abundance.

The importance of variables within each of the correlative models was generally consistent across algorithms and resolutions (Table 1.5). For the climate model, mean annual temperature was the most important variable, except in GAM at 5 km, where precipitation was more important. When models were trained with climate + disperser + host as environmental predictors, the most important variable was the disperser, except

GARP at 20 km, where host was more important, and Maxent at 50 km, where annual mean temperature and annual precipitation were overall more relevant; GAMs also showed high importance of temperature at resolutions of 5 and 10 km, precipitation at 20 km, and host at 1 and 5 km. When trained with disperser + host as predictors, GARP showed host as most relevant, while Maxent and GAM showed disperser as most important (Table 1.5).

Table 1.5. Variable importance in correlative models calculated from jackknifing permutations in GARP and Maxent, and from significance values in GAM. * $P < 0.1$, ** $P < 0.05$, *** $P < 0.01$.

| Algorithm | Model | Variables | 1 km | 5 km | 10 km | 20 km | 50 km |
|----------------------|------------------------|----------------------|---------|---------|---------|---------|---------|
| GARP | climate | temperature | 86.09 | 90.52 | 85.84 | 98.97 | 100.00 |
| | | precipitation | 13.91 | 9.48 | 14.16 | 1.03 | 0.00 |
| | climate+disperser+host | temperature | 13.64 | 16.33 | 16.54 | 25.00 | 25.84 |
| | | precipitation | 19.70 | 23.47 | 21.05 | 21.43 | 24.72 |
| | | disperser | 45.45 | 25.51 | 41.35 | 14.29 | 35.96 |
| | disperser+host | host | 21.21 | 34.69 | 21.05 | 39.29 | 13.48 |
| | | disperser | 30.30 | 29.31 | 12.00 | 34.38 | 45.45 |
| Maxent | climate | temperature | 77.12 | 65.83 | 56.69 | 87.01 | 78.74 |
| | | precipitation | 22.88 | 34.17 | 43.31 | 12.99 | 21.26 |
| | climate+disperser+host | temperature | 17.16 | 17.11 | 28.38 | 2.65 | 57.97 |
| | | precipitation | 10.20 | 10.79 | 20.32 | 2.04 | 35.77 |
| | | disperser | 70.75 | 66.48 | 51.29 | 93.86 | 2.38 |
| | disperser+host | host | 1.88 | 5.62 | 0.00 | 1.44 | 3.88 |
| | | disperser | 94.50 | 89.88 | 93.34 | 95.47 | 100.00 |
| GAM | climate | temperature | 0.00*** | 0.29 | 0.00*** | 0.00*** | 0.00*** |
| | | precipitation | 0.67 | 0.005** | 0.22 | 0.00*** | 0.00*** |
| | (deviance explained) | 48.80% | 47.50% | 47.20% | 40.10% | 39.60% | |
| | climate+disperser+host | temperature | 0.21 | 0.002** | 0.00*** | 0.60 | 0.46 |
| | | precipitation | 0.022* | 0.65 | 0.014* | 0.006** | 0.0215* |
| | | disperser | 0.00*** | 0.00*** | 0.00*** | 0.00*** | 0.00*** |
| | disperser+host | host | 0.007** | 0.004** | 0.07 | 0.57 | 0.21 |
| | | (deviance explained) | 91.60% | 91.00% | 91.80% | 93.80% | 94.20% |
| | disperser+host | disperser | 0.00*** | 0.00*** | 0.00*** | 0.00*** | 0.00*** |
| | | host | 0.80 | 0.85 | 0.70 | 0.38 | 0.002** |
| (deviance explained) | 87.30% | 87.60% | 85.60% | 88.40% | 87.10% | | |

Discussion

The two modeling approaches that we implemented are very different in nature (Morin and Thuiller 2009). In the process-based model, we made explicit assumptions about the way that the mistletoe could be dispersed and in this way “explore” the region, and reasons behind it successfully establishing or not given the availability of hosts and abiotic climatic conditions. On the other hand, in the correlative models, mechanisms shaping the distribution are implicit in associations between occurrence of the species and environmental factors. The differences and similarities between the results of the two approaches illuminate the roles of different factors across different spatial scales (Schurr et al. 2012). We could think of process-based models as a hypothetic-deductive approach by which to test hypothesis, whereas correlative models are an inductive way to propose hypotheses; the differences in results are explained by the ways in which the two methods make use of observations.

The results from the process-based model suggest that dispersal factors are most relevant at fine resolutions, but that they become practically irrelevant at coarser resolutions, where climatic factors dominate, as expected under the Eltonian Noise Hypothesis (Soberón and Nakamura 2009, Peterson et al. 2011). This result is consistent with previous general thinking about effects of scale on the relative importance of different factors on distributional ecology (Whittaker et al. 2001, Pearson and Dawson 2003), and also with previous results on spatial aggregation patterns of *P. californicum* (Aukema 2004). This later study found mistletoe aggregation within trees and at about 1.5-2 km, and again at a distance ≥ 4 km, that was correlated with elevation. This finding

led the author to hypothesise that dispersal was key to the first two scales (within trees and ~1500 m) and abiotic factors to the > 4 km scale. Although our simulations did not include these finer resolutions, our results are consistent where comparisons were possible. Coincident aggregation patterns have also been reported in studies of the Indian mistletoe *Taxillus tomentosus* (Lemieux et al. 2011).

The fact that parameters of the extinction rate did not show significant change across resolutions is consistent with the relative stability of scenopoetic variables across a broad set of scales (Soberón 2007). Scenopoetic variables are related to the abiotic fundamental niche, an adaptive feature related to physiology (James et al. 1984, Jackson and Overpeck 2000). In this case, climate is relevant because it adjusts species' survival limits in each cell of the grid. Overall, what is apparently changing with scale are factors associated with dispersal of the species, as seen in the colonization part of this model, whereas climate is a constant determinant of the species' range across scales. These results support the hypotheses proposed with the BAM diagram in the conceptual framework (Fig. 1.2).

Process-based models, which are much more time-consuming to implement than correlative models, are nevertheless potentially very informative. After comparing the models generated in this exercise, it is evident that incorporating colonization and extinction processes within a metapopulation framework sheds light on the importance that factors related to dispersal may have at finer scales for this species (Overton 1994, 1996, Aukema 2004, Lemieux et al. 2011), and that more stable factors like climate either

remain constant across resolutions or become more important in controlling the distribution of the species as the resolution becomes coarser.

Using correlative methods, we were able to perceive differences in contributions of variables as a function of changes in resolution, as other authors have shown (e.g., Buckley et al. 2010). However, interpretation of the roles of different variables, not being linked to mechanisms, was not straightforward, and potentially would lead to interpretations very different from what we observed using the process-based model (Cabral and Schurr 2010). Araújo and Luoto (2007) used GAMs to test whether biotic interactions played a role at macroscales for the butterfly *Parnassius mnemosyne*: they found that the type of interaction (contingent on species) and methods considered played significant roles in explaining distributions of species at coarse scales. Other studies using correlative approaches have shown improvement in predictions of species' distributions when resource-related variables are incorporated (Heikkinen et al. 2007, Real et al. 2009, Wisz et al. 2012). In our exercise, when we used correlative models, we also found that biotic-related predictors play a role at coarse scales, but were most relevant at scales finer than the macroscale of Araújo and Luoto (2007). These authors worked only at a scale similar to the coarsest of our analysis (50 km); they might have detected additional patterns if their analysis had extended to finer resolutions. Their results match ours at the coarsest resolution if we consider both disperser and host layers as part of the mistletoe's biotic interactions: in our case, the disperser layer showed some explanatory power, although not very significant, whereas, in Araújo and Luoto's example, the host plant distribution of the butterfly did not improve results drastically, but rather echoed climate

signals (Figs. 1.3 and 1.4). Although these results from correlative models suggest that non-scenopoetic variables are important at coarse scales, the process-based model helped us to understand interactions among predictors, and revealed contrasting importance of factors at different resolutions.

Our analysis suggests that different combinations of environmental predictors, whether biotic or abiotic, may affect interpretation of model predictions drastically, offering a step towards understanding model overfitting. Addition of the disperser layer resulted in concentration of the mistletoe's predicted distribution in the area of highest density of the disperser. Although model overfitting is known to complicate estimates of species' ecological niches (Peterson et al. 2007), in this case, it also shows how combinations of abiotic and dispersal-related predictors restrict the area predicted as suitable. An improvement on this exploration would be to test for significance of explanatory power of other (less important) dispersers and perhaps different suites of hosts in the model.

It is interesting to notice that the different modeling approaches produced predictions with only fair to good agreement. One possible explanation for such lack of coincidence is that the climate-only predictions agree closely with the distribution of the disperser, which is the element of the process-based model that covers the entire extent moving the parasite across cells in search for suitable conditions for its establishment (**M**; Barve et al. 2011). However, in the metapopulation framework of the process-based model, the disperser is just one part of the formula, and how the mistletoe reaches its distributional limits depends on the balance between colonization and extinction.

Assuming that the disperser actually carries mistletoe seeds all across the study extent and that hosts are present, our study suggests that the mistletoe is able to reach and potentially establish in areas more distant than the known geographic range edges; however, its populations are restricted to an area smaller than its “accessible area,” suggesting that other factors (including climate) constrain its survival. In a more realistic process-based modeling approach, actual seed processing times and dispersal distances could be incorporated (e.g., Overton 1996, 1997, Liu et al. 2011).

The fact that the species is not present in the northwestern and southeastern parts of the disperser’s range suggests that the species is responding to some combination of biotic and abiotic factors that reduces suitability in those regions (Fig. 1.1; see also Fig. S1.1). The two areas are consistently predicted as climatically suitable, but densities of disperser and hosts are much lower towards these two areas, very different from the central part of the study area, where we observed highest mistletoe abundances; areas similar to these areas may be worth exploring in detail for sink population dynamics. From observations during field work, the transition between absence and presence, moving from east to west, could also be explained by a combination of biogeographic barriers for the species and dramatic environmental gradients, which represent limits to dispersal (although other generalist and specialist species are present in these other regions) and successful establishment. Our observations do not suggest interference by other species (i.e., other biotic factors, such as competition) in this part of the range; rather, it is more likely that the species has not been able to adapt to abiotic conditions there, preventing it from being more widespread.

This may explain why the species is restricted to the Sonoran Desert and parts of the Mojave Desert, and does not occur in other, adjacent desert areas in North America, such as California's Central Valley, the Chihuahuan Desert, or the Valle de Tehuacán in Mexico, that present different combinations of either hotter and wetter or colder and dryer climates, in comparison to areas where the species is present (Dimmit 2000).

Although our exercise is realistic according to what we know about the species' distribution and how biotic and abiotic factors operate across scales, it carries some significant assumptions and limitations. First, the environmental predictors we used and the way they were developed is far from ideal. We chose predictors that are likely important to the species, but generating them and matching their resolutions was not always possible. In particular, this concern applies to the disperser layer: it was originally created at a spatial resolution of 461 km² (Sauer et al. 2011), but data availability considerations prevented us from scaling it directly to other resolutions. Scaling it to high resolutions requires a larger density of survey routes than is actually available; as a consequence, we used this single resolution for the first four resolutions, and generalized it still more for the coarsest.

Other bioclimatic variables could have been chosen, such as those associated with extremes of temperature and precipitation; however, in tests using other sets of climate variables and the entire set of 19 bioclimatic variables of Hijmans et al. (2005), neither the process-based model nor the correlative approach appeared to benefit from such additional information (data not shown). To check this point more thoroughly, we tested the performance and geographic predictions of correlative models with two other

environmental layers that were calculated using daily weather stations information for a period of 20 years: number of continuous days of freezing temperatures and number of continuous rainless days. However, these models did not produce results markedly better than annual mean temperature and annual precipitation visually, nor did models increase in performance, which suggests that different trends would not result in either the model prediction or in model performance.

For the process-based model, it would be possible to create and explore other colonization and extinction functions. In particular, the extinction function used was a simple exponential of the difference between the estimated optimal niche and the environments of a given cell: clearly, more complex may prove more appropriate (Martínez-Meyer et al. 2013). However, based on extensive initial exploration and simulations (not shown), in which our basic results were supported, it is not likely that major differences and conclusions from our current findings would emerge.

Other types of information could be incorporated in new models, as well as in experiments that could analyze details of mistletoe population dynamics in different parts of the range. For example, numbers of viable seeds dispersed by *Phainopepla nitens* and other bird species may indicate regions with unfavorable niche conditions and sink population dynamics, or perhaps even other physiological mechanisms of host-parasite recognition. Other studies of such dynamics in *P. californicum* have been carried out at much finer resolutions than ours, and are very illuminating when compared with our macro-geographic approximations (e.g., Overton 1994, 1996, Aukema and Martínez del Rio 2002, Liu et al. 2011). From an ecological point of view, for example, these analyses

would allow exploring whether abundance, genetic variation, population differentiation, or gene flow vary as functions of centrality within the geographic range (Thuiller et al. 2010, Torres et al. 2012, Martínez-Meyer et al. 2013) or the ecological niche of the species, thus presenting different opportunities for local optima and associated adaptation (VanDerWal et al. 2009, Martínez-Meyer et al. 2013).

Acknowledgments

We are thankful to Luis A. Sánchez-González, Gerardo Cendejas, Fran Recinas, and Rebecca Crosthwait for invaluable support during field work. We are indebted to several institutions and herbaria where we stored specimen material: Centro Interdisciplinario de Investigaciones para el Desarrollo Integral Regional, Durango (Socorro González), Instituto de Biología, UNAM (Hilda Flores), Universidad Autónoma de Baja California, Ensenada (José Delgadillo), and San Diego Natural History Museum (Jon Rebman). We thank Luis Eguiarte and Mark Olson for help with logistics, and the warm hospitality of the families of Alberto Búrquez, Pablo Lazo, Socorro González, Gerardo Cendejas, and Rebecca Crosthwait made field work much easier. Initial discussions about this work with Carlos Martínez del Río and statistical guidance from Exequiel Ezcurra were crucial. We also thank A. Townsend Peterson for insightful comments on this work and Narayani Barve for help with weather values interpolation. Conversations with Richard Felger and Mark Robbins were important to clarify points on climatic limiting factors and dispersal of the species. We thank the curators and staff of the following herbaria for providing access to their digital data: ARIZ, ASC, ASU, BCMEX, BNHM, CANB, COCHISE, DES, GBIF, GCNP, IZTA,

KANU, LL, MABA, MO, NMBCC, NY, RM, SNM, TEX, UCR, UNM, USON, UTC, UVSC, XAL.

Comments from David M. Watson and two anonymous reviewers were highly valuable in improving the quality and clarity of the analyses. A Tinker Award from the Department of Latin American Studies and Biodiversity Institute Panorama small grant award (Bunker Fund), University of Kansas, supported part of the collecting trip. C.P.M.'s work was supported by Microsoft Research grant 47780. A.L.-N. received a graduate fellowship support from the Consejo Nacional de Ciencia y Tecnología (189216).

Chapter 2

Range-wide ecological niche comparisons of parasite, hosts and dispersers in a vector-borne plant parasite system²

² Lira-Noriega A, Peterson AT (In press) Range-wide ecological niche comparisons of parasite, hosts and dispersers in a vector-borne plant parasite system. *Journal of Biogeography*. Doi: 10.1111/jbi.12302

Abstract

We aim to test whether the distribution of the mistletoe *Phoradendron californicum* is mediated by host distributions (host niche hypothesis, HNH), or by factors such as the mistletoe's autecology (parasite niche hypothesis, PNH) or that of its vectors (vector niche hypothesis, VNH). Our null hypothesis is that the ecological niche of the mistletoe will not be distinct from that of its hosts or vectors; alternatively, mistletoe infections might appear in hosts only in regions where host distributions overlap suitable conditions for the parasite. We used ecological niche modelling approaches to summarize suitable environmental conditions for hosts infected and uninfected with mistletoes, as well as for avian dispersers during winter and throughout the year. We compared ecological niches among pairs of species using background similarity tests in relation to the climatic conditions available and accessible to each species. Results show that niche comparisons supported all PNH expectations, but none of the predictions of HNH or VNH. These findings suggest that hosts and dispersers of mistletoes generally have distinct ecological niches; mistletoe infections occur in non-random environmental subsets of host and disperser ecological niches; mistletoe infections in different hosts, however, occur under similar climatic conditions. Hence, in this system, the parasite has a rather strictly circumscribed ecological niche, and host species become infected with mistletoe only where they overlap its suitable areas.

Introduction

Parasites are abundant in the natural world. Because their life cycles often involve interactions among multiple species, parasites offer great study opportunities to understand degrees of specificity and transmission capacities in the context of species' ecological and evolutionary dynamics (Morand and Krasnov, 2010). These phenomena are important in illuminating the relationships of parasites with hosts, the ranges of hosts that parasite species can infect and mechanisms of infection. In general, two interesting questions arise: to what extent are animal and plant populations affected by parasitism and disease (Begon et al., 2006), and under what conditions do infections occur?

Recent studies of the ecology of mistletoes have opened opportunities to understand plant parasitism and species' distributions at multiple spatial scales. Mistletoes are vector-borne parasites that play dual roles in biological communities: as parasites of host plants and as mutualists with birds (Martínez del Rio et al., 1996; Aukema, 2003). Birds obtain nutrients, energy and water from mistletoes, whereas mistletoes benefit from seed dispersal to safe establishment sites (Reid, 1991). The desert mistletoe, *Phoradendron californicum* Nutt. (Viscaceae; henceforth simply 'mistletoe'), is a hemiparasitic plant distributed in parts of the Sonoran and Mojave deserts (Kuijt, 2003) that is parasitic almost exclusively on leguminous trees. Host species include *Acacia constricta* Benth., *Acacia greggii* A. Gray, *Cercidium floridum* Benth. ex A. Gray, *Cercidium microphyllum* (Torr.) Rose and I.M. Johnst., *Olneya tesota* A. Gray, *Prosopis glandulosa* Torr. and *Prosopis velutina* Wooton, and less commonly *Larrea tridentata* (Sessé and Moc. ex DC.) Coville (Zygophyllaceae), *Celtis pallida* Torr. (Cannabaceae), *Condalia*

warnockii M.C. Johnst. (Rhamnaceae) and *Tamarix ramosissima* Ledeb. (Tamaricaceae) (Haigh, 1996).

The mistletoe's distribution is shaped at least in part by the activities of avian seed-dispersers (Larson, 1996; Aukema, 2001). Differences in fruit removal and dispersal distances result from different combinations of frugivore abundances and plant aggregation, two large-scale processes that can control and structure small-scale neighbourhood patterns (Carlo and Morales, 2008). Particularly important are the roles of specialist and generalist mistletoe fruit consumers in dispersing seeds closer to existing infections or beyond them, respectively (Aukema and Martínez del Rio, 2002a; Rawsthorne et al., 2012).

Because mistletoe fruits are among the few berries available in these North American deserts during winter, they represent an important food source for birds when other food is scarce (Cowles, 1936). The most common birds feeding on *Phoradendron californicum* berries include *Phainopepla nitens* (Swainson, 1838) (Ptilonotidae), *Melanerpes uropygialis* (S.F. Baird, 1854) (Picidae), *Mimus polyglottos* (Linnaeus, 1758) (Mimidae) and *Toxostoma curvirostre* (Swainson, 1827) (Mimidae), and less commonly *Bombcilla cedrorum* (Vieillot, 1808) (Bombycillidae), *Campylorhynchus brunneicapillus* (Lafresnaye, 1835) (Troglodytidae), *Carpodacus mexicanus* (Statius Müller, 1776) (Fringillidae), *Callipepla gambelii* (Gambel, 1843) (Odontophoridae), *Myadestes townsendi* (Audubon, 1838) (Turdidae), *Sialia currucoides* (Bechstein, 1798) (Turdidae), *Sialia mexicana* (Swainson, 1832) (Turdidae), *Sialia sialis* (Linnaeus, 1758) (Turdidae), *Turdus migratorius* (Linnaeus, 1766) (Turdidae), *Oreoscoptes montanus* (J.K. Townsend,

1837) (Mimidae), *Toxostoma crissale* (Henry, 1858) (Mimidae) and *Zonotrichia leucophrys* (J.R. Forster, 1772) (Emberizidae) (Larson, 1996). Of these species, *P. nitens* is considered the primary and most efficient mistletoe seed disperser (Larson, 1996). Indeed, phainopeplas have a digestive system specialized to be able to process hundreds of mistletoe berries per day (Walsberg, 1975), and their breeding season in the desert coincides with fruiting periods of mistletoes (Chu and Walsberg, 1999).

Mistletoe distribution and prevalence have been explained more generally in terms of interactions among local and regional determinants, although the precise mechanisms and differential influences of biotic and abiotic factors remain largely unknown (Watson, 2009; Kavanagh and Burns, 2012; Lira-Noriega et al., 2013). Although most studies have focused at local scales, some recent studies have examined influences of factors at multiple spatial scales (e.g. Rist et al., 2011; Kavanagh and Burns, 2012; Lira-Noriega et al., 2013). Nonetheless, variation in host quality and specificity (Watson, 2009) and the effectiveness of seed dispersal by different vectors (Montaño-Centellas, 2013) remain important factors. To date, however, no study has examined ecological and geographical relationships among mistletoes, hosts and seed dispersers in the context of climatic conditions as range-wide determinants; such an approach would complement the current knowledge of mistletoe ecology.

In a study of range-wide determinants of plague (*Yersinia pestis*) distribution in North America, Maher et al. (2010) analysed niche overlap among infected and uninfected hosts to test whether the distribution of plague in North America is mediated by the ecological niches of mammal hosts or rather by those of the vectors or the

pathogen *per se* (Fig. 2.1). Here, we test whether the mistletoe's distribution is mediated by ecological niches of its hosts ('host niche hypothesis'), or rather by its own ecology ('parasite niche hypothesis') or that of its multiple dispersers ('vector niche hypothesis'). The null expectation is that mistletoe infections occur under environmental circumstances not distinguishable from the ecological niches of its hosts or dispersers; alternatively, mistletoe infections might appear only where host distributions overlap suitable areas for the parasite. To test these hypotheses, we used an ecological niche modelling approach to estimate ecological niches, and then compared niches of pairs of species, specifically assessing the amounts of niche overlap in relation to the overlap of environmental conditions accessible and available to each species (Warren et al., 2008).

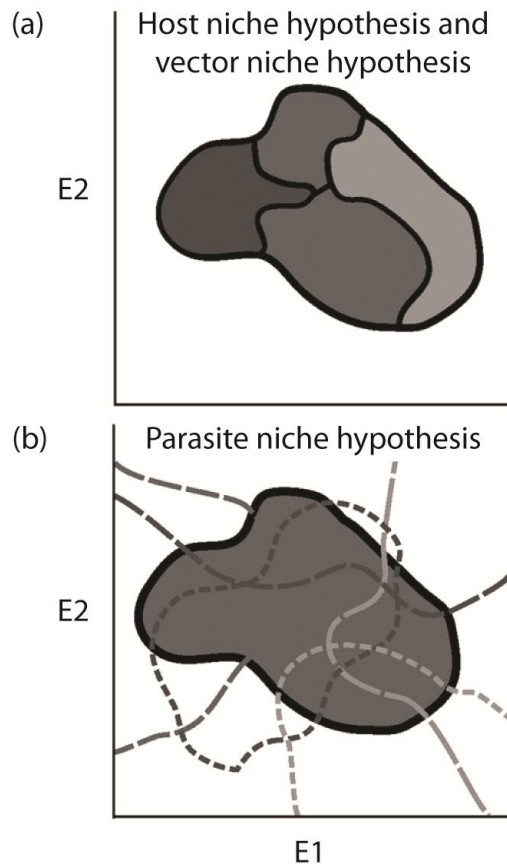


Figure 2.1 Conceptual diagram of relationships between mistletoe occurrences, host and vector occurrences, and environmental variation (a) under the host niche hypothesis (HNN) and vector niche hypothesis (VNH), and (b) under the parasite niche hypothesis (PNH). Occurrence of the parasite with respect to two dimensions of the scenopoetic fundamental niche (E1 and E2) is shown as a thick black line. Grey polygons in the upper panel show a mosaic of host or vector niches; in the lower panel, the grey polygon shows the parasite's niche and dashed outlines show the niches of hosts and/or vectors. (Figure modified from Maher *et al.*, 2010.)

Materials and Methods

Input data

We collected occurrence data based on herbarium voucher specimens for each of the eight most common mistletoe host species across their entire range from the Global Biodiversity Information Facility (<http://www.gbif.org/>) and the Southwest Environmental Information Network (<http://swbiodiversity.org/portal/index.php>). These tree species all

occur in the Sonoran Desert, some extending as far as the mid-western United States or central Mexico. The numbers of unique occurrences available for these species were: *Acacia constricta*, 326; *Acacia greggii*, 946; *Cercidium floridum*, 345; *C. microphyllum*, 694; *Larrea tridentata*, 616; *Olneya tesota*, 631; *Prosopis glandulosa*, 914; and *Prosopis velutina*, 1169. We also assembled information on mistletoe occurrences associated with each host species from the same online databases, as well as from A.L.-N.'s field collections across the geographical range of the species in 2010 and 2012 (Lira-Noriega et al., 2013). The numbers of unique occurrences of infected hosts were: *A. constricta*, 8; *A. greggii*, 131; *C. floridum*, 13; *C. microphyllum*, 23; *L. tridentata*, 8; *O. tesota*, 30; *P. glandulosa*, 37; and *P. velutina*, 45. Special attention was paid to obtaining adequate numbers of occurrences well spread across the species' range. To corroborate that the scientific names we used provided accurate numbers and distributions of records, we conducted further searches using synonyms and subspecies, but this step did not substantially alter the numbers or distributions of occurrences.

A list of 10 potential bird dispersers for this study was derived from our own field observations and those of knowledgeable ornithologists (A.L.-N.; A.T.P.; Mark Robbins, University of Kansas, pers. comm.). This list overlaps with what has been reported in the literature (Larson, 1996). Distributional data for potential bird dispersers were drawn from eBird (<http://ebird.org/content/ebird/>), and numbers of unique occurrences year-round and for winter (December–February) were *Mimus polyglottos* (year, 247,566; winter, 91,717), *Myadestes townsendi* (22,600; 7156), *Phainopepla nitens* (15,487; 5491), *Toxostoma curvirostre* (6666; 1944), *Sialia currucoides* (23,601; 5944), *S. mexicana*

(39,788; 14,036), *S. sialis* (72,734; 62,923), *Bombycilla cedrorum* (171,102; 47,225), *Melanerpes uropygialis* (11,401; 4498) and *Turdus migratorius* (300,925; 91,355).

To characterize environmental variation across the region, we used climatic summaries from the WorldClim data archive (Hijmans et al., 2005; <http://www.worldclim.org/>) at a spatial resolution of 2.5'. To avoid fitting models in environmental spaces with too many dimensions, we used principal components analysis (PCA) on standardized variables with the 'prcomp' function in R (R Development Core Team 2013) among 15 'bioclimatic' variables (annual mean temperature, mean diurnal temperature range, isothermality, temperature seasonality, maximum temperature of the warmest month, minimum temperature of the coldest month, annual temperature range, mean temperature of the warmest and coldest quarters, annual precipitation, precipitation of the wettest and driest months, precipitation seasonality and precipitation of the wettest and driest quarters). We then reduced dimensionality to the first six principal components, which accounted for > 95% of overall variance in the environmental variables. Principal components were generated for the geographical extent that encompasses all of the species' background areas, but models were calibrated across each species' individual background area (see below).

Niche modelling

Ecological niche models must be calibrated and compared across regions relevant to the species. Model calibration should thus be restricted to the accessible area: the set of sites that the species is likely to have 'sampled' over a relevant period of time (Barve et al., 2011). Here, we designed model calibration regions for each species. As a simple means

of estimating the accessible area, we assigned this region to cover the ecoregions (Olson et al., 2001) in which species' occurrence points fell, plus a 200-km buffer around them. This region is a simple hypothesis of the areas accessible to each species that was used in both model calibration and niche-overlap comparisons using background similarity tests (see below).

The occurrences used to characterize ecological niches were selected as follows. To model each host species' ecological niche, we selected sets of 100 occurrences at random, but we used all occurrences for mistletoe infections of host trees. For dispersers, we selected three sets of 100 occurrences at random per species for both year-round and winter distributions. Each host species thus had a single niche estimate, whereas each bird had six. Two additional niche estimates were included in niche similarity comparisons with potential dispersers (see below): an overall 'niche' of all host species was estimated using three sets of 100 points selected at random from the set of non-infected host occurrences, and the overall mistletoe niche was estimated using all mistletoe occurrences regardless of host.

We used MAXENT (3.3.3.e; Phillips et al., 2006) to calibrate the niche models. We used 10 bootstrap replications and a threshold of $E = 10\%$ of calibration occurrence data over the median estimate to convert the initial model outputs to binary predictions (Peterson *et al.*, 2011). The remaining parameters were given their default values. The final niche estimates for bird species corresponded to regions where all three thresholded estimates coincided, thus providing a conservative estimate of suitable environmental conditions.

The performance of the binary predictions was evaluated using a one-tailed cumulative binomial test to calculate the probability of obtaining that level of sensitivity by chance alone. We ran this test with 100 independent test points in cases in which numbers of records were sufficient to set aside 100 independent test points (29 models); for species with 14–100 records, we evaluated models by calibrating models with 50% of occurrences and applying the binomial test to the remaining 50% (6 models). The overall mistletoe niche binary prediction was assessed with 100 independent test points from *Phoradendron californicum* occurrences that were available in the databases but that did not specify a host species. Binary predictions from species with fewer than 14 occurrences (three models) were evaluated using a jack-knifing approach (Pearson et al., 2007), which requires a model to be run for each subset of $n - 1$ occurrences, and model performance to be tested over the removed coordinate; these probabilities were calculated using PVALUECOMPUTE (Pearson et al., 2007).

Niche similarity estimates

Niche similarity among species was estimated using Schoener's D and Hellinger's I indices via the 'niche.overlap' function in PHYLOCLIM (Heibl and Calenge, 2013), following the background similarity test proposed by Warren et al. (2008). This test assesses environmental differences between known occurrences of two species but – critically – considers the 'background', which we interpret as equivalent to the accessible area for each species (Barve et al., 2011). The test works by comparing observed overlap values between geographical manifestations of two niches to a distribution generated from comparing the niche models based on the observed distribution of one species to niche

models based on the background of the other; background occurrence points are drawn at random from the accessible area, in numbers matching the sample size available for the species (Warren *et al.*, 2008).

These comparisons were carried out between all combinations of mistletoe-infected and non-infected hosts, and between mistletoe distributions and those of potential bird dispersers, year-round and only in winter (also including overall host and mistletoe distributions). The first set of comparisons was made considering the background of each host species for niche models based on occurrences of infected and non-infected hosts, and also only for the area where each host's accessible area intersects the mistletoe's accessible area. This last selection of background areas created a more strict and conservative comparison. The second set of comparisons was made considering the backgrounds of each bird species, overall hosts, and the mistletoe.

Background similarity distributions were estimated using 100 replicate models calibrated and thresholded in MAXENT exactly as for the observed models, except that occurrences were collections of random points equivalent in number to those used to construct 'observed' niche models (see Warren *et al.*, 2008). All models were thresholded (see above) prior to the calculation of similarity indices, which reduces the effects of overfitting (Peterson *et al.*, 2007). We also constrained models to the same geographical extent by merging them with a zero-value raster of the same spatial resolution as the environmental layers. In comparing niche models, we sought to identify situations in which niches were significantly different, i.e. when niche overlap between a pair of species is less similar than expected at random. Hence, our null hypothesis was that the

two species were similar, which we rejected when the observed I and D values from niche models on the basis of known occurrence points fell in the lowest 5% of background similarity values.

Results

Overall host and mistletoe-infected niche comparisons

The mistletoe occurrences were all recorded in the Sonoran Desert and parts of the Mojave Desert. They were unevenly distributed across the region, showing more or less restricted patterns depending on the host species they were parasitizing (Fig. 2.2).

Considerable variation in numbers of mistletoe-positive occurrences was observed, depending on host. Hence, this system offered rich regional and environmental variation, and thereby an excellent basis for the hypothesis-testing that is the focus of this study.

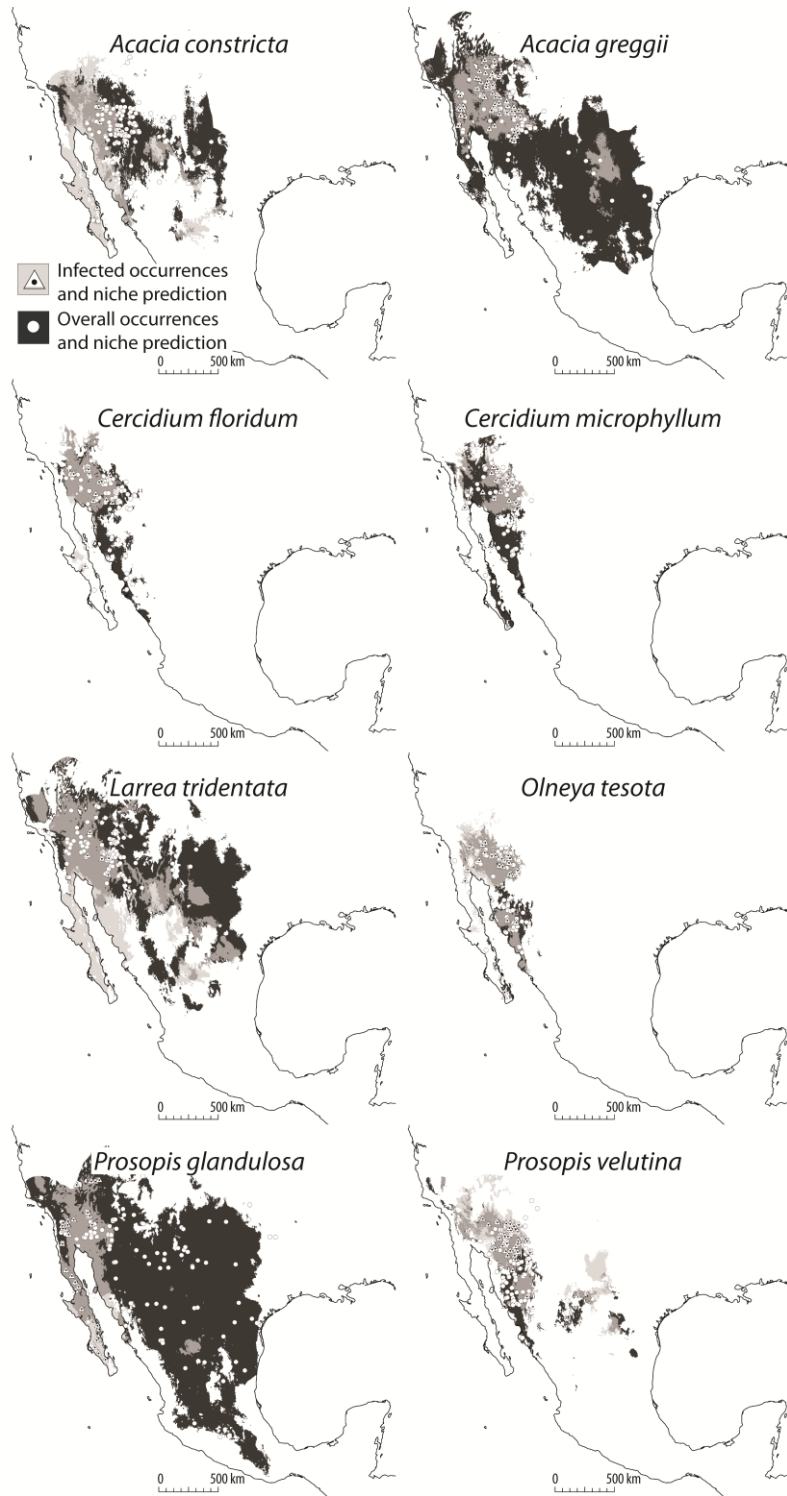


Figure 2.2 Comparison of host niche models and mistletoe-infected-host niche models. In each map, the host's overall suitable area is in black, the mistletoe-infected portion of the host's distribution in transparent light grey, host occurrence points are shown as white dots, and mistletoe-infected host occurrence points as white triangles containing black dots. North America Albers equal-area conic projection.

All niche models performed significantly better than random expectations in all model evaluation exercises ($P < 0.001$; Appendix 2.1). The modelled niches based on mistletoe-infected hosts differed markedly from those based on all host occurrences (Fig. 2.2), and none of the geographical projections of mistletoe-infected hosts covered the entirety of any of the host niche estimates (Fig. 2.2). Examples of background similarity tests between the overall mistletoe niche and dispersers are shown in Fig. 2.3.

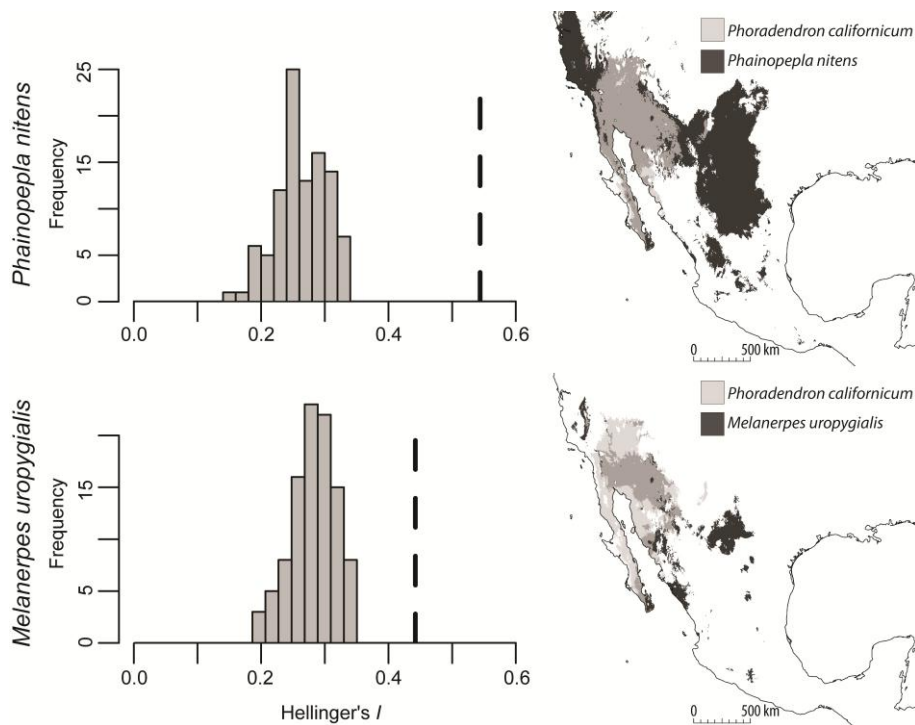


Figure 2.3 Two example background similarity tests showing amounts of niche overlap of the mistletoe overall distribution with specialist (*Phainopepla nitens*) and generalist (*Melanerpes uropygialis*) bird dispersers. The histogram shows the distribution of Hellinger's I from the 100 random-draw models; the observed overlap value of the index for each pair of species is shown as a dashed line. The maps show the two niche-model-based predictions of the mistletoe and each bird species according to winter occurrences. North America Albers equal-area conic projection.

Niche dissimilarity between host niche distributions was observed generally between host species with large geographical ranges (*Acacia greggii*, *Prosopis glandulosa* and *Larrea tridentata*) and backgrounds of more geographically restricted species

(*Cercidium floridum*, *C. microphyllum*, *Olneya tesota* and *Prosopis velutina*). This effect was observed in 13 of 56 comparisons ($P < 0.05$; Fig. 2.4). In contrast, no mistletoe-infected hosts showed dissimilarity against the background of any host species ($P < 0.05$; Fig. 2.4).

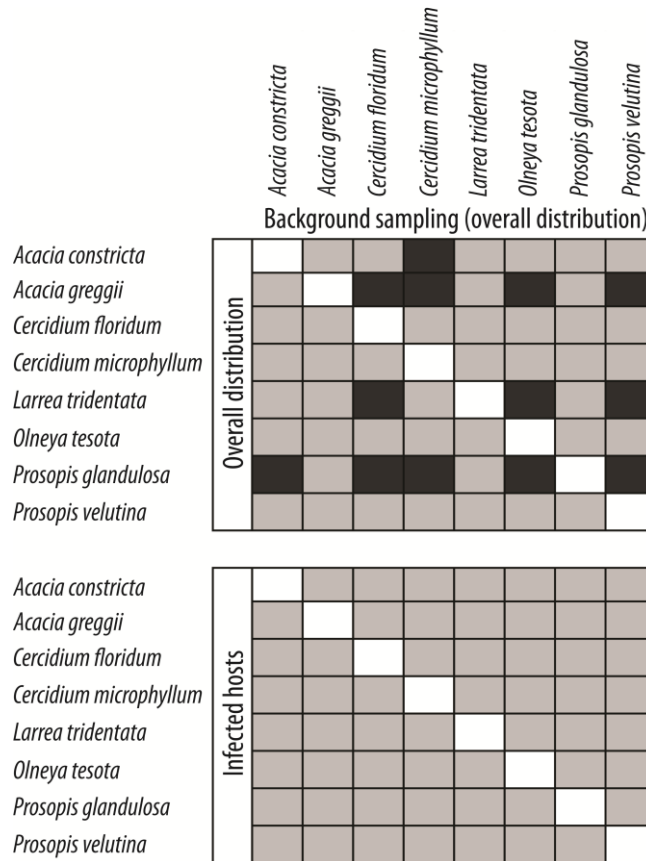


Figure 2.4 Results of background similarity tests from comparisons of host niche models and mistletoe-infected-host niche models. Rows represent point occurrence data and columns show species' background areas in the similarity test. Results based on the two similarity indices were the same. Grey indicates that similarity could not be rejected ($P > 0.05$); black indicates that similarity was rejected ($P < 0.05$).

Disperser niche comparisons

Most disperser ranges covered large areas of North America, the only exceptions being species restricted to the Sonoran Desert (e.g. *Melanerpes uropygialis* and *Phainopepla nitens*). Niche comparisons among the 10 bird species showed frequent niche

dissimilarities in tests of year-round and winter distributions ($P < 0.05$; Fig. 2.5); the similarity was less, however, when niches were based on occurrences from the entire year. Two species in particular tended towards higher niche overlap in winter compared to year-round distributions: *Sialia currucoides* and *Turdus migratorius* ($P < 0.05$; Fig. 2.5). Most cases of niche dissimilarity were observed in comparisons involving *Myadestes townsendi*, *S. sialis* and *T. migratorius*; in contrast, *Melanerpes uropygialis*, *Mimus polyglottos*, *P. nitens*, *S. mexicana* and *Toxostoma curvirostre* showed similarity with other species ($P < 0.05$; Fig. 2.5).

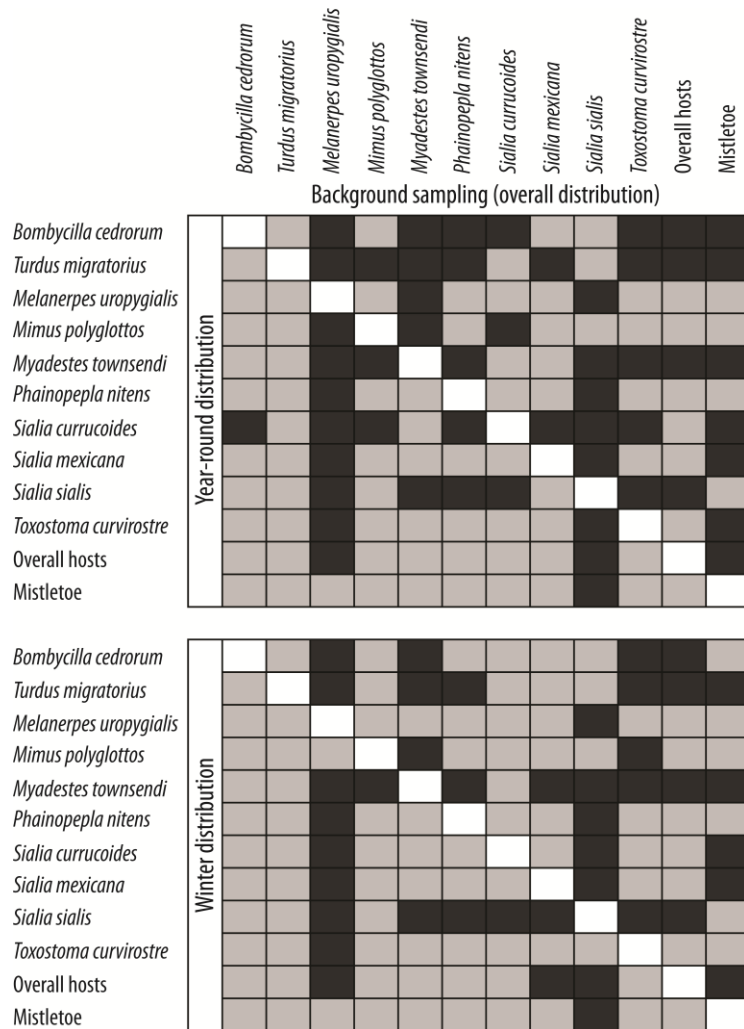


Figure 2.5 Results of background similarity tests in comparisons of bird disperser niche models for year-round and winter distributions and overall mistletoe and host niche models. Rows represent point occurrence data and columns show background areas in similarity tests. Results based on the two similarity indices were the same. Grey indicates that similarity could not be rejected ($P > 0.05$); black indicates that similarity was rejected ($P < 0.05$).

Niche comparisons between overall hosts and mistletoe against dispersers' backgrounds showed greater niche similarity than comparisons in the other direction ($P < 0.05$; Fig. 2.5). Hosts were similar overall to the year-round niches of *Bombycilla cedrorum*, *Turdus migratorius*, *M. polyglottos*, *Myadestes townsendi*, *P. nitens*, *S. currucoides*, *S. mexicana* and *Toxostoma curvirostre*, and to winter niches of the same

species (except *S. mexicana*). The mistletoe's niche was similar to year-round and winter niches of all 10 potential dispersers except *S. sialis*.

Comparing niches of dispersers to the overall host background, only *Melanerpes uropygialis*, *Mimus polyglottos*, *P. nitens*, *S. currucoides*, *S. mexicana* and *T. curvirostre* were similar for year-round and winter niche predictions. Compared to the mistletoe background, the dispersers *Melanerpes uropygialis*, *Mimus polyglottos*, *P. nitens* and *S. sialis* were similar in year-round niche predictions (see Fig. 2.3 for an example), and these same species plus *B. cedrorum* and *T. curvirostre* were similar in winter niche predictions.

Discussion

Our analyses showed that: (1) hosts and dispersers of mistletoe have distinct individual ecological niches; (2) mistletoe infections occur in non-random subsets of the niche of each host; and (3) mistletoe infections in different hosts occur under similar niche conditions. Dispersers showed different amounts of niche overlap between year-round and winter, but only generalist species and one mistletoe specialist (*P. nitens*) were consistently associated with the mistletoe's and hosts' niches. These results support the expectation of PNH, but none of the predictions of HNH or VNH. In particular, PNH anticipates significant non-similarity between hosts in general, but similarity among hosts when infected with mistletoe, leading to the conclusion that host species get infected with mistletoe only where they range into suitable and accessible areas for the mistletoe.

Another possibility is that a single host may drive the geographical distribution of mistletoe, such that ecological niche characteristics of that host would be similar to those

of mistletoe infections in other host taxa. However, of the 49 pairwise comparisons of mistletoe-infected host niche models to hosts' overall backgrounds, none rejected similarity (Fig. 2.4), suggesting that mistletoe infections are restricted to suitable portions of the mistletoe's background. This pattern thus shows a strong association of mistletoe to an important functional group of plants, but only under particular climatic conditions of these North American deserts.

In a study of spatial distribution and host use across 65 mistletoe species in Australia, Kavanagh and Burns (2012) found diversity to be unrelated to productivity, but that host ranges (i.e. number of infected host species) were broader in areas with more potential host species. From this perspective, it is plausible that the association of *Phoradendron californicum* with legumes evolved in this semi-arid region because of its high legume diversity, offering many potential hosts (Dimmitt, 2000; Garcillán and Ezcurra, 2003). According to the PNH, however, hosts would get infected only in areas climatically suitable for the parasite. Our results apparently also follow what a recent network analysis described as a non-nested and modular interaction pattern (Genini et al., 2012), in which each of four mistletoe species from the Brazilian Pantanal (*Psittacanthus cordata*, *Psittacanthus calyculatus*, *Phthirusa abdita* and *Phoradendron* sp.) interacted with a particular set of hosts, with low host specificity, but with hosts highly susceptible to mistletoe infections. That pattern is also consistent with the PNH, in which similarity among hosts appears only in sites at which the mistletoe can occur.

Attributes of hosts and dispersers, as well as other mechanisms at multiple spatial and temporal scales, are important to understanding the mistletoe's distribution. As

proposed in the 'host-quality hypothesis' (Watson, 2009), variation in host quality may account for non-random occurrence patterns of parasitic plants: parasites are expected to establish and survive on higher-quality hosts. Host quality for mistletoes often depends on tree height and architecture, bark texture, age and accessibility to water or drainage sites, and host species (Norton et al., 1997; Lei, 1999; Norton and Smith, 1999; Aukema and Martínez del Rio, 2002b; Callaway et al., 2002; Marquardt and Pennings, 2010). Examples of differential responses to host quality in *P. californicum* include birds' general preference for taller trees with larger numbers of mistletoe plants – causing concentrated intra-host infections (Aukema and Martínez del Rio, 2002a,b) – and the responses of birds to mistletoe prevalence, causing disproportionate seed deposition patterns (Overton, 1996; Aukema, 2004).

Because host races (i.e. a partly reproductively isolated population of a parasite species) and host specialization occur in *P. californicum* (Glazner et al., 1988; Overton, 1997) and other mistletoe species (Clay et al., 1985; Nickrent and Stell, 1990; Jerome and Ford, 2002), it is possible to find a non-random distribution of mistletoe depending on the mistletoe's differential affinity for different host genera. Host specialization in *P. californicum* may evolve more frequently in host-depauperate areas (Kavanagh and Burns, 2012) and in areas of high host prevalence (Overton, 1997), a pattern expected from the numbers and distribution of infections in this study. Several questions remain regarding susceptibility to mistletoe parasitism and related to immunity, abundance and changes in host quality owing to previous infection (Watson, 2009). Phylogenetic analyses may be important in defining the relationships between the densely connected (but non-

overlapping) subsets of host species within a mistletoe's network (Genini et al., 2012), and analyses of phylogeographical and genetic structure could improve the understanding of consequences of seed-dispersal patterns, population evolution and host-race formation (Amico and Nickrent, 2009; Stanton et al., 2009; Zuber and Widmer, 2009; Lira-Noriega et al., unpubl. data).

The distribution and ecology of vector species is a determinant of mistletoe distribution and aggregation patterns at multiple spatial scales (Larson, 1996; Overton, 1996; Aukema and Martínez del Rio, 2002a,b; Aukema, 2004; Rist et al., 2011; Lira-Noriega et al., 2013). In our analyses, overall host and mistletoe niches showed similarity with nine species of potential dispersers in year-round and winter distributions. However, pairwise comparisons of potential dispersers and mistletoe backgrounds showed niche similarity with only six species (Fig. 2.5). The fact that more bird species showed niche similarity against the mistletoe background in winter comparisons coincides with the fact that these species concentrate in this desert region when the mistletoe is a food resource. Genini *et al.* (2012) hypothesized that the modularity of infection in four mistletoe species from the Brazilian Pantanal derives from different seed dispersal systems, such that *Psittacanthus* species have many bird dispersers, whereas their *Phoradendron* species are dispersed by specialists.

The extent to which other bird species contribute meaningfully to mistletoe dispersal is less certain. This role depends in part on their distributional and migration dynamics through the year, but probably most importantly on their specificity on mistletoe and the time they spend on hosts after eating mistletoe fruits (Larson, 1996;

Aukema and Martínez del Rio, 2002a). Year-round residents are typically characterized by territoriality with shorter movements, whereas seasonal migrants could be responsible for longer-distance dispersal events. Even though potential colonization could extend beyond the known distributional limits of the mistletoe, successful establishment events only occur if the right combinations of hosts and climate are also met (Lira-Noriega *et al.*, 2013). Differential vector roles in shaping the spatial structure of mistletoe populations have also been documented in the Patagonian mistletoe *Tristerix corymbosus* (García *et al.*, 2009; Amico *et al.*, 2011). While interesting, disentangling the roles of different vectors would require analyses beyond the scope of that presented here.

Other biotic interactions may also limit the mistletoe's distribution, such as roles of pollinators and vertebrate and invertebrate herbivores. Although little is known about which other species interact with *P. californicum*, it is possible that lepidopterans, weevils, coreid bugs and homopterans, feed on its branches and seeds, as in the related *Phoradendron tomentosum* when parasitizing *Prosopis glandulosa* (Whittaker, 1984). Several rodents, deer, bighorn sheep, cattle and goats are also known to feed on mistletoes. The spatial variation of these interactions could be studied and added as new hypotheses to test in this system. Nonetheless, we anticipate that dispersers and hosts will prove the most significant species in defining the mistletoe's distribution.

From the perspective of the mistletoe and the community of species with which it interacts, this study allowed us to corroborate, and to some extent generalize, the ecological dynamics and patterns of association with hosts and dispersers known from several studies at local scales and from our own observations in the field. This study offers

a broad-scale view of mistletoe infections, with hypotheses regarding conditions under which they occur (Wisz et al., 2013), and reinforces the idea that mistletoes should continue to be considered a valuable epidemiological system to understand infection patterns in vector-borne diseases and parasite–host interactions (Aukema, 2003; Mathiasen et al., 2008). This general approach could be easily applied to other systems of parasitism and disease.

Acknowledgements

We thank Sean Maher for guidance on niche overlap estimates, Mark Robbins for advice on potential mistletoe bird dispersers, Richard Felger for help with species identifications and valuable comments on background areas, and Ben Wilder for valuable comments on the manuscript. Comments from three referees and the editors helped improve the manuscript. Collecting trips were supported by a Young Researchers Award from the Global Biodiversity Information Facility (GBIF), a Tinker Award from the University of Kansas Center of Latin American Studies, and a University of Kansas Biodiversity Institute Panorama small grant award (Bunker Fund). A.L.-N. received scholarship support from Consejo Nacional de Ciencia y Tecnología, Mexico (189216).

Chapter 3

Relationship of genetic diversity and niche centrality: A survey and analysis³

³ Lira-Noriega A, Manthey JD (2014) Relationship of genetic diversity and niche centrality: A survey and analysis. *Evolution* 68: 1082-1093. Doi:10.1111/evo.12343.

Abstract

The distribution of genetic diversity within and among populations in relation to species' geographic ranges is important to understanding processes of evolution, speciation, and biogeography. One hypothesis predicts that natural populations at geographic range margins will have lower genetic diversity relative to those located centrally in species' distributions owing to a link between geographic and environmental marginality; alternatively, genetic variation may be unrelated with geographic marginality via decoupling of geographic and environmental marginality. We investigate the predictivity of geographic patterns of genetic variation based on geographic and environmental marginality using published genetic diversity data for 40 species (insects, plants, birds, mammals, worms). Only about half of species showed positive relationships between geographic and environmental marginality. Three analyses (sign test, multiple linear regression, and meta-analysis of correlation effect sizes) showed a negative relationship between genetic diversity and distance to environmental niche centroid, but no consistent relationship of genetic diversity with distance to geographic range center.

Introduction

The study of species' geographic distributions has been approached from many different perspectives in ecology, evolutionary biology, biogeography, and macroecology (Udvardy 1969; Rapoport 1982; Brown et al. 1996; Gaston 2003; Holt and Keitt 2005). Particularly important are geographic range edges, because they represent frontiers where populations interact with marginal environmental conditions, to which they may or may

not adapt (Holt 2003; Bridle and Vines 2007; Kawecki 2008; Sexton et al. 2009; Paul et al. 2011).

Along distributional limits, populations are often sparse, fragmented, and prone to local extinction (Gaston 2003); they may represent demographic sinks maintained by immigration from higher-quality core habitats, which makes them demographically and genetically dependent on other populations (Pulliam 1988). Peripheral sites may also receive gene flow that can counteract local selection pressures and local adaptation (Kawecki 2008). As a consequence, these populations may be more prone to loss of genetic diversity (Kawecki 2008; Keller et al. 2010).

This pattern has been illustrated as a hypothesized relationship between local abundance and geographic centrality, in which abundances would be higher in central populations versus peripheral ones (e.g., Brown 1984; Brussard 1984; Vucetich and Waite 2003). This idea is called the abundant-center hypothesis (Hengeveld and Haeck 1982). However, exceptions to the pattern have been reported frequently (e.g., Sagarin and Gaines 2002; Gaston 2003; Martínez-Meyer et al. 2013). Although higher genetic diversity may be expected at range centers than at range edges, empirical patterns have been mixed (Eckert et al. 2008; Kawecki 2008; Moeller et al. 2011).

The distance to the center of the geographic distribution *per se* should perhaps not be expected to cause abundance or genetic variability differences. Demographic processes may relate more directly to the quality of local conditions, as expressed by the fundamental ecological niche of the species (Hutchinson 1957, 1978; Pulliam 2000; Soberón 2010; Martínez-Meyer et al. 2013). The fundamental niche is the set of

environmental conditions under which the species shows positive population growth rates without immigration; outside of those conditions, the species shows zero or negative population growth. Under this alternative framework, populations under conditions closer to the core of the fundamental ecological niche would achieve higher growth rates or greater stability than those far from the optimum conditions (VanDerWal et al. 2009). Of special note is that environmentally 'central' conditions frequently are not located at the center of the geographic range. Therefore, an important question arises: are demographic and genetic effects of peripherality manifested more consistently in geographic or environmental spaces?

Under one hypothesis (H_0 in Fig. 3.1), geographic marginality and ecological marginality are positively linked, creating a relationship between geographic marginality and population characteristics (e.g., local abundance or genetic diversity). Alternatively, geographic marginality and ecological marginality may be decoupled (H_A in Fig. 3.1), leading to a lack of a relationship between geographic marginality and population characteristics. The key assumption behind these hypotheses is that environmental marginality causes adverse population effects. Here, environmental marginality may lead to small population sizes (i.e., an environmental version of the abundant-center hypothesis), which in turn causes population genetic processes to reduce genetic diversity. Increased genetic drift in small populations, source-sink dynamics of unsustainable populations, or strong selection in marginal environments could all contribute to environmental marginality reducing genetic diversity within a species.

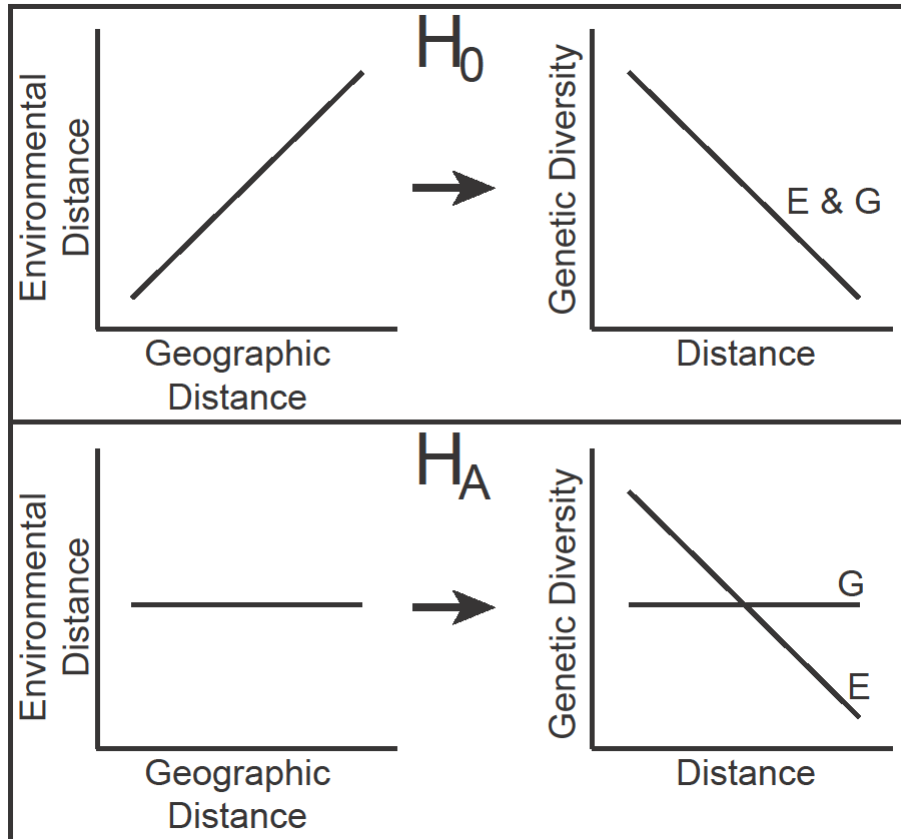


Figure 3.1 Hypothesized relationships between distance to ecological niche centroid, geographic range center, and genetic diversity. Under H_0 , environmental and geographic marginality coincide, leading both to be negatively correlated with genetic diversity. Alternatively, under H_A , environmental and geographic marginality are decoupled, leading to the lack of a relationship between genetic diversity and geographic centrality.

Little has been done to explore this ecological niche-based version of the abundant-center hypothesis, i.e., that population dynamics or genetic structure are functions of environmental conditions associated with ecological niches of species (Martínez-Meyer et al. 2013). To our knowledge, only one study has explored the central-peripheral hypothesis regarding genetic variability in relation to environmental suitability (Diniz-Filho et al. 2009). However, these authors related genetic variability to measures of environmental suitability (not centrality within the niche), which they estimated from an

average of ecological niche model suitability scores from multiple niche modeling algorithms; they found no clear relationships.

The above situation suggests that reassessment of the traditional geographic abundant-center hypothesis (Sagarin and Gaines 2002; Gaston 2003; Garner et al. 2004; Eckert et al. 2008) in terms of ecological niches is necessary. Particularly important to this point are differences between environmental conditions near the core of the geographic distribution versus those at its periphery, because these contrasting environments are where key components of selection, adaptation, and evolution are—or are not—taking place (Bridle and Vines 2007; Kawecki 2008; Bozinovic et al. 2011). Soberón and Miller (submitted) extended models originally presented by Holt and Gomulkiewicz (1997), and obtained equations for genetic variance-covariance matrices in spatially explicit population-genetic models. The main equation predicted that phenotypic variance should decrease as a function of the geographic distribution only if strong spatial covariance exists in the direction of selective pressures. This result suggests that geographic centrality will be associated with higher genetic diversity only when correlated with environmental characteristics.

Here, we test whether genetic diversity is higher near the core or at the periphery of habitable conditions (the niche) versus the geographic distribution in 40 species for which some measure of genetic variability in multiple natural populations has been published. We contrasted relationships among genetic diversity, distances to three estimates of niche centroids, and distances to seven measures of geographic range centers.

Methods

Species' occurrences and genetic diversity

We assembled data from 40 species from numerous taxonomic groups for which both genetic diversity and geographic locations of populations were reported (Table 3.1). These data come from insects (7), birds (15), mammals (3), plants (14), and an onychophoran velvet worm, distributed in North and South America, South Africa, Eurasia, the Mediterranean region, and the Arctic. The collection of data was done by searching for phylogeography papers in the Web of Science; papers with poor locality data, individuals from a single population spread over many kilometers (e.g., > 10 km between individuals in a single population), or small sample sizes for all or most populations were excluded. Genetic diversity measures were taken directly from the original publications (Table 3.1, Appendix 3.1); most indices of genetic diversity were from putatively neutral genetic markers. One assumption of this study is that the reported values of neutral genetic variation have some relationship with fitness, which has been shown in some taxa (Leimu et al. 2006; Reed and Frankham 2003), but not in others (Chapman et al. 2009).

Table 3.1 Species used in this study, their taxonomic affinities, measure of genetic diversity used (Div.), and the original publication for each species. GD = Genic diversity, AR = allelic richness, π = nucleotide diversity, HE = expected heterozygosity, AWD = average distances within populations. * after species name indicates that alternative ploidy levels were removed from analysis.

| Species | Taxonomic Group | Div. | Reference |
|----------------------------------|--------------------------------|-----------|------------------------------|
| <i>Arenaria humifusa</i> | Magnoliopsida: Caryophyllaceae | GD | Westergaard et al. 2011 |
| <i>Bombus bifarius</i> | Insecta: Apidae | AR | Lozier et al. 2011 |
| <i>Bombus bimaculatus</i> | Insecta: Apidae | AR | Lozier et al. 2011 |
| <i>Bombus impatiens</i> | Insecta: Apidae | AR | Lozier et al. 2011 |
| <i>Bombus occidentalis</i> | Insecta: Apidae | AR | Lozier et al. 2011 |
| <i>Bombus pensylvanicus</i> | Insecta: Apidae | AR | Lozier et al. 2011 |
| <i>Bombus vosnesenskii</i> | Insecta: Apidae | AR | Lozier et al. 2011 |
| <i>Cardellina pusilla</i> | Aves: Parulidae | π | Kimura et al. 2002 |
| <i>Cardellina ruber</i> | Aves: Parulidae | π | Barrera-González et al. 2012 |
| <i>Cardinalis cardinalis</i> | Aves: Cardinalidae | π | Smith et al. 2011 |
| <i>Cassiope tetragona</i> | Magnoliopsida: Ericaceae | GD | Eidesen et al. 2007b |
| <i>Certhia americana</i> | Aves: Certhiidae | π | Manthey et al. 2011 |
| <i>Dalbergia nigra</i> | Magnoliopsida: Leguminosae | π | Ribeiro et al. 2011 |
| <i>Eucryphia cordifolia</i> | Magnoliopsida: Cuconiaceae | π | Segovia et al. 2012 |
| <i>Fraxinus angustifolia</i> | Magnoliopsida: Oleaceae | AR | Temunovic et al. 2012 |
| <i>Himantoglossum hircinum</i> | Liliopsida: Orchidaceae | HE | Pfeifer et al. 2009 |
| <i>Hymenaea stigonocarpa</i> | Magnoliopsida: Fabaceae | π | Ramos et al. 2007 |
| <i>Lampornis amethystinus</i> | Aves: Trochilidae | π | Cortés-Rodríguez et al. 2008 |
| <i>Lynx rufus</i> | Mammalia: Felidae | π /AR | Reding et al. 2012 |
| <i>Melampodium leucanthum</i> * | Magnoliopsida: Asteraceae | AWD | Rebernic et al. 2010 |
| <i>Microtus miurus</i> | Mammalia: Cricetidae | π | Weksler et al. 2010 |
| <i>Microtus oeconomus</i> | Mammalia: Cricetidae | π | Galbreath and Cook 2004 |
| <i>Oxalis alpina</i> | Magnoliopsida: Oxalidaceae | π | Pérez-Alquicira et al. 2010 |
| <i>Pelecanus erythrorhynchos</i> | Aves: Pelecanidae | π | Oomen et al. 2011 |
| <i>Peripatopsis capensis</i> | Onychophorida: Peripatopsidae | π | McDonald and Daniels 2012 |
| <i>Peromyscus attwateri</i> | Mammalia: Cricetidae | π | Lack et al. 2010 |
| <i>Pheropsophus jessoensis</i> | Insecta: Carabidae | π | Li et al. 2012 |
| <i>Picooides albolarvatus</i> | Aves: Picidae | π | Alexander and Burns 2006 |
| <i>Poecile gambeli</i> | Aves: Paridae | π | Spellman et al. 2007 |
| <i>Quercus engelmannii</i> | Magnoliopsida: Fagaceae | AR | Ortego et al. 2012 |
| <i>Rhodiola alsia</i> | Magnoliopsida: Crassulaceae | π | Gao et al. 2012 |
| <i>Rubus chamaemorus</i> | Magnoliopsida: Rosaceae | GD | Ehrich et al. 2008 |
| <i>Sagina caespitosa</i> | Magnoliopsida: Caryophyllaceae | GD | Westergaard et al. 2011 |
| <i>Setophaga caerulescens</i> | Aves: Parulidae | π | Grus et al. 2009 |
| <i>Sitta carolinensis</i> | Aves: Sittidae | π | Spellman and Klicka 2007 |
| <i>Sitta pygmaea</i> | Aves: Sittidae | π | Spellman and Klicka 2006 |
| <i>Spermophilus parryii</i> | Mammalia: Sciuridae | π | Galbreath et al. 2011 |
| <i>Stipa capillata</i> | Liliopsida: Poaceae | HE | Wagner et al. 2011 |
| <i>Toxostoma redivivum</i> | Aves: Mimidae | π | Sgariglia and Burns 2003 |
| <i>Vaccinium uliginosum</i> * | Magnoliopsida: Ericaceae | GD | Eidesen et al. 2007a |

We obtained occurrence data for all species through the Global Biodiversity Information Facility (www.gbif.org), in addition to the occurrence data associated with

the phylogeographic or population genetic data from the original publication. All occurrence data were inspected carefully to detect and correct problems associated with mistaken taxonomic identification (including all lower taxonomic forms of recognized species), duplication, lack of precision, or geographically discordant localities (Chapman 2005). In the case of some plants, we eliminated populations that exhibited alternative ploidy levels (Table 3.1). Ploidy was only considered when investigating the genetic data (and not the occurrence data) because of possible inflation of genetic diversity measures with an increase in chromosomes. This only impacted two species in the analyses.

Niche characterization and distances to niche and geographic centroids

To estimate ecological niches of species and measure environmental-space distances of each population to the species' niche centroid, four steps were necessary: (1) create ecological niche models for each species, (2) extract background points and associated environmental data, (3) perform a principal components analysis on each dataset, and (4) measure multivariate Euclidean distance to niche centroids and geographic range centers.

For ecological niche modeling, 19 bioclimatic layers were obtained from the WorldClim database at a spatial resolution of 2.5' (Hijmans et al. 2005; www.worldclim.org). These layers contain worldwide precipitation and temperature information, including minima, maxima, and ranges of values. These data sets, however, were highly intercorrelated; hence, only seven were included (annual mean temperature, mean diurnal range, maximum temperature of warmest month, minimum temperature of coldest month, annual precipitation, and precipitation of wettest and driest months) for modeling, owing to high correlations between some pairs of variables ($r > 0.7$, tested in

ENMTools; Warren et al. 2008; Warren et al. 2010). Because we focus on climatic dimensions, our analyses are of the Grinnellian or scenopoetic fundamental niche, which is in essence a suite of abiotic, range-wide determinants of the population status of the species being modeled (Soberón 2007). Here, we assume that the niche we model is a good estimator of the fundamental niche, although we recognize that it is not possible to capture the true fundamental niche without physiological experiments for each species (Peterson et al. 2011).

To reduce model overfitting owing to spatially autocorrelated occurrences, we rarefied numbers of points per species using a minimum distance between points of 10'. For species with >100 occurrences, we selected 11 sets of points at random without replacement from the set of unique values of longitude and latitude, but with replacement between sets. Species' occurrences and environmental layers were then used in Maxent (Phillips et al. 2006) to build one model per set of points. We calibrated models via 11 bootstrap replications, using a threshold of $E = 10\%$ of training data to convert the models to binary (Peterson et al. 2008), with remaining parameters left as default. The median of each set of thresholded models (i.e., presence predicted in ≥ 6 of 11 models) was used as the final estimate of suitable area, considering that each thresholded model was derived from different sets of points. Because calibration areas influence outcomes of niche model predictions given differences in background sampling, and these areas should be biogeographically relevant for the species (Barve et al. 2011), we designed three calibration areas for each species: a 500 km buffer around occurrence points, and 200 and 500 km buffers around the terrestrial ecoregions (Olson et al. 2001)

in which species' occurrence points fell (labeled "500 km," "ER + 200 km," and "ER + 500 km," respectively, in tables and figures). We used these buffers to keep methodologies consistent among species, as well as to test for effects of changing the calibration areas on overall results. These polygons were used to mask environmental layers for ecological niche modeling in Maxent; niche models were calibrated for each species over three geographic areas.

To characterize ecological niches and estimate niche centroids, we created a data matrix including known occurrence data and 5000 points sampled at random from the suitable area for the species as estimated in Maxent. From this matrix, we extracted values of the 19 bioclimatic layers at each point, and then transformed the matrix via principal components analysis (PCA) based on the correlation matrix. To ensure that 5000 points, rather than a smaller number, did not impact the output we replicated this step using smaller samples of 2500, 1000, and 500 points sampled from the suitable extent for each species (see Appendix 3.1). The mean of scores along the first six principal components was used as an estimate of the species' niche centroid. From this vector, we estimated the multivariate Euclidean distance of each population for which we had genetic variation estimates. In all cases, the first six principal components explained the great majority (>95%) of the variance in the environmental data.

Geographic centrality of populations was estimated in relation to seven geographic ranges: the centroid of the minimum convex polygon encompassing all occurrence points, centroids of the three suitable areas obtained from thresholded Maxent models, and centroids of the three polygons of the calibration areas used for

niche modeling. These measures allowed us to contrast among competing hypotheses associating genetic diversity with distance to geographic or ecological niche centroids. This may be especially important because species' geographic ranges have traditionally been delimited using different approximations (Rapoport 1982), and this task is frequently accomplished via gridded outputs of ecological niche models (Fortin et al. 2005).

To identify relationships between genetic diversity and distances to ecological niche and geographic centroids, we used linear regressions between these variables, using distance to ecological niche or geographic centroids as the independent variable. We used linear regression only to derive simple patterns from the overall dataset, not attempting to derive best models, to avoid complicating comparisons between species unnecessarily. To reduce effects of outlier points in regressions, we removed points with a Cook's distance (Cook 1977) of ≥ 0.95 , followed by rerunning the linear regression.

To investigate overall trends in the data, we used three methods. First, we used a sign test across all linear regressions to determine whether negative or positive slopes were unexpectedly overrepresented in each dataset. Second, we fit a generalized linear model including all genetic diversity and distance data for each species. Distance to niche centroid and distance to geographic range center (e.g., E distance and G distance for ER + 200 km calibration area) were used as predictors of genetic diversity to disentangle the effects of each variable with the following model: genetic diversity \sim distance to niche centroid + distance to geographic range center. Prior to regression, all variables were z-standardized within each species.

Finally, we calculated mean effect sizes of correlation coefficients between genetic diversity and distance to either ecological niche centroid or geographic center (Borenstein et al. 2009). First, we transformed the correlation coefficient (r) to Fisher's z , using:

$$(1) z = 0.5 \times \ln\left(\frac{1+r}{1-r}\right)$$

which gave an effect size for each individual species. The variance of z (VZ) was calculated as:

$$(2) VZ = \frac{1}{n-3}$$

where n is the number of populations for each species. Lastly, the mean effect size was calculated as the weighted mean of each species' effect size:

$$(3) ES = \frac{\sum_{i=1}^k VZ_i z_i}{\sum_{i=1}^k VZ_i}$$

Confidence intervals were calculated with 10,000 bias-corrected bootstrap replicates. Following calculation of grand mean effect sizes and associated 95% confidence intervals, values were back transformed from Fisher's z to correlation coefficients for visualization.

For every species, we checked for separate clusters of points in both geographic and environmental space. For one species, *Stipa capillata*, we detected clearly separate clusters of points along geographic distance, which corresponded to the central and peripheral populations analyzed in the original publication (Wagner et al. 2011); in this case, we calculated linear regressions separately to understand if relationships within each cloud differed from those in the whole dataset for the species. For *Lynx rufus*, for

which both mtDNA and nuclear DNA (microsatellites) data were available (Reding et al. 2012), we repeated analyses to assess whether different molecular markers showed contrasting results. Finally, we calculated correlations between niche centrality and geographic centrality to assess the degree to which the two vary independently of one another. Spatial data were handled in ArcMap 10.1 (ESRI 2011) and R (R Core Team 2012); all statistical computation was done in R.

Results

Most species showed negative relationships between distance to niche centroid and genetic diversity; results were consistent across the three alternative training regions for niche models (Tables 3.2 and 3.3). Conversely, we found no general trend between genetic diversity and distance to geographic centroid (Tables 3.2 and 3.3). Similarly, the grand mean correlation effect sizes of distance to environmental centroid were negative and significantly different than zero, whereas effect sizes of distance to geographic center, although all negative, were not significantly different from zero (Fig. 3.2).

Table 3.2 Species used in this study, number of populations for each species (*N*), number of occurrence records used for modeling ecological niches (*N Occ.*), whether geography and environment show similar relationships with genetic diversity (*Agree*), pattern(s) observed between genetic diversity and distance to centroid of the niche (*E*), number of significant comparisons for *E* (*E**) out of three total, pattern(s) observed between genetic diversity and distance to geographic center of a species (*G*), number of significant comparisons for *G* (*G**) out of seven total. A (-) or (+) indicates negative or positive relationships, respectively, while a (+/-) indicates mixed patterns. A (C) subscript indicates conflicting patterns between model-based and other geographic center measures.

| Species | N | N Occ. | Agree | E | E* | G | G* |
|----------------------------------|----|--------|-------|-----|----|------|----|
| <i>Melampodium leucanthum</i> | 68 | 360 | X | - | | - | 6 |
| <i>Cassiope tetragona</i> | 62 | 418 | X | - | 1 | - | 2 |
| <i>Vaccinium uliginosum</i> | 54 | 833 | X | - | 2 | - | 7 |
| <i>Lynx rufus</i> | 52 | 1096 | | - | 3 | +/-c | 3c |
| <i>Stipa capillata</i> | 43 | 295 | | + | | - | |
| <i>Rubus chamaemorus</i> | 41 | 625 | | - | | +/-c | |
| <i>Spermophilus parryii</i> | 34 | 207 | X | - | 3 | - | |
| <i>Bombus bimaculatus</i> | 34 | 197 | | - | | +/- | |
| <i>Bombus bifarius</i> | 33 | 947 | | - | 3 | +/- | 3 |
| <i>Bombus impatiens</i> | 33 | 390 | | - | 3 | +/- | |
| <i>Bombus pensylvanicus</i> | 25 | 451 | X | - | 3 | - | 3 |
| <i>Poecile gambeli</i> | 25 | 396 | X | - | | - | |
| <i>Pheropsophus jessoensis</i> | 25 | 27 | | - | 3 | +/- | 1 |
| <i>Peromyscus attwateri</i> | 22 | 94 | | + | | +/- | |
| <i>Eucryphia cordifolia</i> | 22 | 32 | X | - | | - | 6 |
| <i>Cardinalis cardinalis</i> | 20 | 1458 | X | - | 3 | - | 7 |
| <i>Himantoglossum hircinum</i> | 20 | 619 | | - | | + | 1 |
| <i>Oxalis alpina</i> | 20 | 107 | X | - | | - | 6 |
| <i>Certhia americana</i> | 19 | 871 | X | + | | + | |
| <i>Dalbergia nigra</i> | 19 | 27 | X | - | | - | |
| <i>Rhodiola alsia</i> | 18 | 27 | X | + | 3 | + | 1 |
| <i>Hymenaea stigonocarpa</i> | 17 | 83 | X | + | | + | |
| <i>Peripatopsis capensis</i> | 17 | 12 | X | - | | - | |
| <i>Bombus vosnesenskii</i> | 16 | 511 | | - | | +/- | 3 |
| <i>Pelecanus erythrorhynchos</i> | 16 | 344 | X | - | | - | 1 |
| <i>Sitta carolinensis</i> | 14 | 1611 | | +/- | | + | 2 |
| <i>Microtus oeconomus</i> | 14 | 464 | X | - | | - | |
| <i>Setophaga caerulescens</i> | 14 | 395 | X | + | | + | |
| <i>Sagina caespitosa</i> | 14 | 80 | | +/- | | +/- | |
| <i>Bombus occidentalis</i> | 13 | 939 | | +/- | | + | |
| <i>Lampornis amethystinus</i> | 13 | 98 | | + | | +/- | |
| <i>Quercus engelmannii</i> | 13 | 26 | X | + | | + | |
| <i>Cardellina pusilla</i> | 12 | 855 | X | - | | - | |
| <i>Picoides albolarvatus</i> | 12 | 73 | X | - | | - | |
| <i>Fraxinus angustifolia</i> | 11 | 590 | | - | | +/- | |
| <i>Sitta pygmaea</i> | 11 | 238 | X | - | | - | |
| <i>Arenaria humifusa</i> | 11 | 59 | X | - | | - | |
| <i>Toxostoma redivivum</i> | 9 | 61 | X | + | | + | |
| <i>Cardellina ruber</i> | 9 | 44 | | - | | + | 3 |
| <i>Microtus miurus</i> | 8 | 110 | X | - | | - | |
| Total consensus positive | | | 7 | 9 | | 10 | |
| Total consensus negative | | | 18 | 28 | | 19 | |
| Total mixed pattern | | | 16 | 3 | | 11 | |

Table 3.3 Binomial tests of slopes (sign test). “# - Sig.” indicates the number of significant negative results; “# + Sig.” indicates the number of significant positive results. Training areas compared included 500 km = 500 km buffer around occurrence points, ER + 200 km = 200 km buffer around terrestrial ecoregions, and ER + 500 km = 500 km buffer around terrestrial ecoregions. MCP = minimum convex polygon. Mx = centroid estimated from Maxent prediction.

| | # Negative slopes (p-value) | # - Sig. | # + Sig. |
|------------------------|-----------------------------|----------|----------|
| Environmental Distance | | | |
| 500 km | 29 (0.0064) | 8 | 1 |
| ER + 200 km | 31 (0.0007) | 8 | 1 |
| ER + 500 km | 29 (0.0064) | 8 | 1 |
| Geographic Distance | | | |
| 500 km | 26 (0.0807) | 6 | 2 |
| ER + 200 km | 25 (0.1539) | 6 | 2 |
| ER + 500 km | 24 (0.2682) | 4 | 1 |
| MCP | 25 (0.1539) | 6 | 3 |
| 500 km (Mx) | 24 (0.2682) | 9 | 1 |
| ER + 200 km (Mx) | 24 (0.2682) | 8 | 1 |
| ER + 500 km (Mx) | 25 (0.1539) | 10 | 1 |

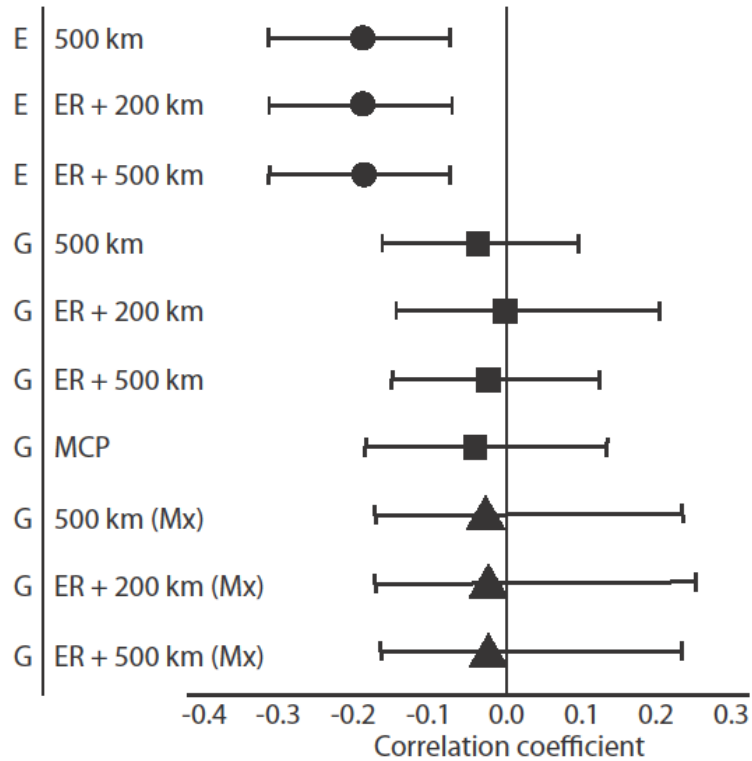


Figure 3.2 Mean grand effect sizes of the relationship between genetic diversity and either environmental (E) or geographic range (G) centrality. These are displayed for distance to environmental centroid with three different calibration areas for modeling (circles), and seven different estimates of distance to geographic center based on model calibration areas (squares) and modeled suitable areas (triangles). See methods for more details.

Overall, 24 species showed similar patterns of associations of genetic diversity between environmental and geographic space (Table 3.2). We illustrate results for two species, *Bombus bifarius* and *Lynx rufus*: in both cases, genetic diversity was negatively associated with distance to niche centroids, but patterns in relation to geographic centroids were inconsistent (Figs. 3 and 4). The mitochondrial (mtDNA) and nuclear DNA available for *Lynx rufus* yielded consistent patterns ($r = 0.41$, $P = 0.0028$; Fig. 3.4), although they differed in frequency distributions, as mtDNA was slightly biased toward east-to-west genetic structure, whereas nuclear DNA (microsatellites) was normally

distributed. In *Stipa capillata*, the species with distinct clusters in geographic space, regression analyses showed significantly negative slopes for peripheral populations for all estimates of distance to the niche centroid and to the three distances from the geographic center estimated from Maxent models, a pattern which was hidden when both central and peripheral populations were pooled together. We identified outlier points for seven species in environmental space and for ten species in geographic space; however, regression analyses following removal of outliers did not change in overall pattern (Appendix 3.1).

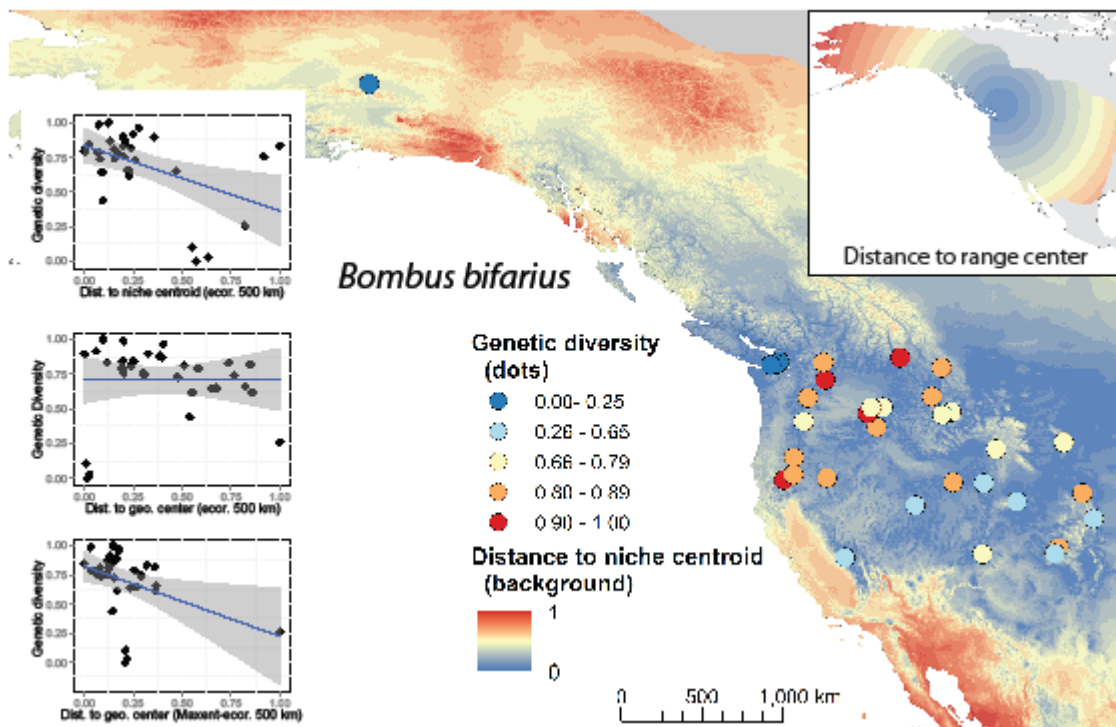


Figure 3.3 Relationships between genetic diversity and centrality in *Bombus bifarius*. Points indicate populations sampled, with warmth of colors symbolizing higher genetic diversity; the map is colored as distance to niche centroid, with warmer colors representing further distance from niche centroid. Top right inset shows the distance to the range center (based on 500 km buffer around ecoregions). Left panel shows linear regressions between genetic diversity and distance to niche or geographic centroids.

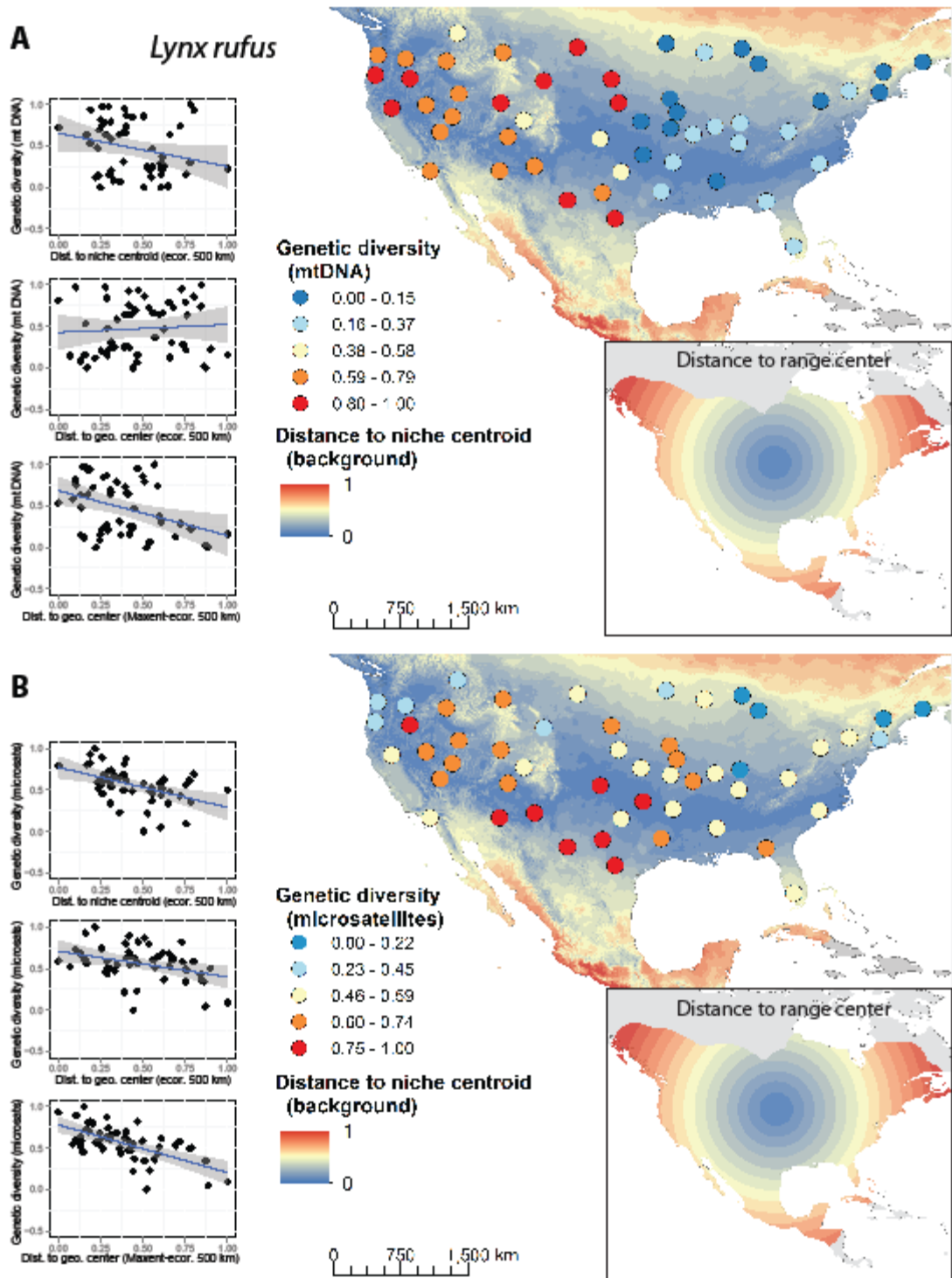


Figure 3.4 Relationships between genetic diversity and centrality in *Lynx rufus* for mitochondrial DNA (A) and microsatellites (B). Points indicate populations sampled, with warmth of colors symbolizing higher genetic diversity; the map is colored as distance to niche centroid, with warmer colors representing further distance from niche centroid. Top right inset shows the distance to the range center (500 km buffer around ecoregions). Left panel shows linear regressions between genetic diversity and distance to niche or geographic centroids.

No consistent correlation (among calibration areas) existed between distance to geographic centroid and distance to environmental centroid in all species (Appendix 3.1). Twenty-four species had consistent, positive correlations between distance to geographic and environmental centroids, with 14 to 21 of those correlations significant depending on model-calibration area. Additionally, different methods of estimating geographic centroids provided conflicting distance-diversity relationships in 11 of 40 species (Table 3.2). For example, estimating geographic centroids from minimum convex polygons versus thresholded suitability models yielded relationships with different signs between geographic centrality and genetic diversity.

Results from the generalized linear models (Table 3.4) indicated that distance to niche centroid was the only relevant predictor of genetic diversity for the dataset of points buffered with 500 km, and showed higher significance than distance to geographic range center for the datasets of ecoregions buffered by 200 and 500 km. When only cases in which slopes showing same signs were considered (Table 3.2), both distances were significant predictors. In contrast, distance to the ecological niche centroid was the only significant predictor in models of cases in which regression slopes showed contrasting patterns (Table 3.2).

Table 3.4 Results of generalized linear models using data from all species (z-standardized). Values below are the contributions in the regression model of distance to niche centroid or geographic range center to explain genetic diversity. Regressions were performed for separate datasets where distance to geographic center and distance to niche center showed consistent or mixed patterns in sign of the slope (see Table 3.2). Asterisks indicate significance at 0.05 (*), 0.01 (**), and 0.001 (***) levels. Training areas compared included 500 km = 500 km buffer around occurrence points, ER + 200 km = 200 km buffer around terrestrial ecoregions, and ER + 500 km = 500 km buffer around terrestrial ecoregions.

| Dataset | | E distance | G distance |
|-------------|-------------|------------|------------|
| 500 km | All species | -0.475*** | -0.161 |
| | Consistent | -0.330* | -0.495** |
| | Mixed | -0.628** | 0.229 |
| ER + 200 km | All species | -0.460*** | -0.247* |
| | Consistent | -0.287 | -0.570*** |
| | Mixed | -0.541** | -0.063 |
| ER + 500 km | All species | -0.478*** | -0.232* |
| | Consistent | -0.332* | -0.519*** |
| | Mixed | -0.551*** | -0.056 |

Regressions between genetic diversity and distance to geographic centroids showed no significant dependence on sample size (Table 3.5), whereas relationships between genetic diversity and distance to ecological niche centroid showed a strong relationship to sample size (Table 3.5). Limiting analyses to species with 25 or more populations sampled, 12 of 13 species showed negative relationships between genetic diversity and distance to niche centroid ($P = 0.003$, binomial test), with eight of these showing a significant relationship (Table 3.2). Conversely, only 7 of 13 species showed negative relationships between genetic diversity and distance to geographic centroid (4 of 7 significant; Table 3.2); three of which showed conflicting significant results between different geographic centroid estimates.

Table 3.5 Relationship between number of populations and *P*-values of the relationships between distance to niche centroid and distance to geographic center. Training areas compared included 500 km = 500 km buffer around occurrence points, ER + 200 km = 200 km buffer around terrestrial ecoregions, and ER + 500 km = 500 km buffer around terrestrial ecoregions. MCP = minimum convex polygon. Mx = centroid estimated from Maxent prediction.

| | R squared | <i>P</i> -value |
|------------------------|-----------|-----------------|
| Environmental Distance | | |
| 500 km | 0.2009 | 0.0037 |
| ER + 200 km | 0.2029 | 0.0035 |
| ER + 500 km | 0.1899 | 0.0049 |
| Geographic Distance | | |
| 500 km | 0.0006 | 0.8747 |
| ER + 200 km | 0.0004 | 0.8945 |
| ER + 500 km | 0.0001 | 0.9412 |
| MCP | 0.0106 | 0.5269 |
| 500 km (Mx) | 0.0886 | 0.0621 |
| ER + 200 km (Mx) | 0.0823 | 0.0726 |
| ER + 500 km (Mx) | 0.0800 | 0.0771 |

Discussion

Reviewing published phylogeographic studies for 40 species, we identified a clear pattern of negative relationships between genetic diversity and distance to ecological niche centroids, but mixed or no relationships between genetic diversity and distributional centrality. Using three methods to evaluate the entire dataset, the sign test of results of linear regressions of the two distances separately (Table 3.3), the generalized linear models combining both distances (Table 3.4), and the meta-analysis of mean effect sizes (Fig. 3.2), distance to niche centroid showed higher predictive ability of genetic diversity than distance to geographic range center. Only about half the species showed a strong correlation between environmental and geographic marginality (Appendix 3.1). This decoupling in some situations likely led to the pattern where distance to geographic range center was a predictor of genetic diversity only when it agreed in sign with environmental distance (supporting H_0 in Fig. 3.1) but showed no predictivity when

environment and geography disagreed in sign (supporting H_A in Fig. 3.1). These results support the hypothesis that peripherality within the set of habitable conditions (ecological niche) represents an important determinant of geographic patterns in species' genetic variation.

Although we found consistent negative relationships between genetic diversity and ecological niche centrality, we do not imagine that environmental conditions alter levels of genetic variation in species directly. Rather, we envision a cascade of environmental impacts on population dynamics (e.g., effective population size, gene flow, population stability), leading to changes in genetic variation likely causing observed patterns (Kawecki 2008). Two recent studies identified negative relationships between relative abundances and distances to niche centroid (Martínez-Meyer et al. 2013) or environmental suitability (VanDerWal et al. 2009), which demonstrate part of the set of causal links that we envision.

Lower genetic diversity at the periphery of the set of suitable ecological niche conditions translates into lower potential for genetic differentiation and expansion beyond environmental conditions of a species' niche, where positive feedback with population density occurs (Antonovics et al. 2001; Barton 2001). In consequence, persistence of locally-adapted genotypes may be unachievable given lower population densities and incoming gene flow, resulting in long-term stabilizing selection on niche-related traits and consequent conservatism (Haldane 1956). On broader time scales, niche stability (or lack thereof) has been shown to impact geographic variation in population genetic diversity (Carnaval et al. 2009; Ortego et al. 2012); however, it would

be difficult or impossible to measure the environmental suitability that individual populations experience through time.

It is interesting that, for many species, high levels of genetic diversity were observed in geographically distant populations. Interpreting this pattern in the context of historical and ecological evidence of species' dispersal capabilities and genetic diversity or structure, as many phylogeographic studies do, supports the hypothesis of a set of optimal conditions within which populations are more likely to survive and reproduce, with greater population stability and higher levels of genetic diversity.

Because we found a strong tendency toward greater statistical power as more populations (≥ 25) were sampled for a species, studies investigating these relationships based on fewer populations may simply have lacked statistical power to detect relationships. These results suggest that future phylogeographic studies should focus on sampling designs that incorporate not only large numbers of populations spread across geographic distributions of species, but should also represent the different environments where populations occur across species' geographic ranges. Better still, empirical studies designed explicitly to test relative effects of environmental versus geographic centrality should be developed.

Finally, as an important component of biodiversity, as well as a strong predictor of fitness (Reed and Frankham 2003), genetic diversity is an important conservation target (Primack 2006). As such, the capacity to predict genetic diversity across species' distributions may prove useful to conservation biologists. Phylogeographic studies have shown mixed results in anticipating genetic diversity patterns based on peripherality or

centrality of populations (Eckert et al. 2008; Kawecki 2008; Moeller et al. 2011). Our results, in conjunction with studies focused on abundance (VanDerWal et al. 2009; Martínez-Meyer et al. 2013), suggest that a focus on environmental centrality, rather than geographic centrality, will provide greater insight into populations as foci of conservation initiatives. Preserving populations central in a species' niche (but not necessarily central in the geographic range) may protect populations with higher abundance and that maintain relatively higher genetic diversity than populations that are environmentally peripheral.

Acknowledgements

Comments from John K. Kelly, Jorge Soberón, A. Townsend Peterson helped us to improve previous versions of this manuscript. A.L.-N. received scholarship support from Consejo Nacional de Ciencia y Tecnología (189216).

Chapter 4

**The roles of history and ecology in chloroplast
phylogeographic patterns of the vector-borne plant
parasite *Phoradendron californicum* Nutt.
(Viscaceae) in the Sonoran Desert**

Abstract

The dependence on hosts and vectors in combination with testable historical and ecological hypotheses make parasitic plants ideal systems in which to test questions in ecology and evolution regarding how different factors shape distributions of individuals and genes. Here, we describe phylogeographic patterns in the parasitic flowering plant, the desert mistletoe (*Phoradendron californicum*), based on three non-coding chloroplast DNA regions. We assess the marginal probability of 16 *a priori* hypotheses related to geologic events and ecological factors, to predict the cpDNA variation across the distribution of *P. californicum* within a Bayesian phylogenetic framework.

Complementarily, we use macrofossil record from packrat middens and niche model projections on Last Glacial Maximum climatic conditions for hosts, mistletoe, and a bird specialist to interpret phylogeographic patterns. We found patterns of variation in cpDNA haplotypes most probable under a model reflecting a series of geologic events related to formation of the Baja California Peninsula and seaways across it in the Pliocene and the Pleistocene. Alternatively, fossil record, niche projections, and haplotype distribution suggested shifting distributions of host-mistletoe interactions and evidence of host races, which might explain some of the genealogical history of the cpDNA; however, these hypotheses were not favored by the Bayesian statistical tests. Depending on molecular rate, age estimates for well-supported nodes were compatible with geologic events or climatic oscillations. Our findings suggest that variation of cpDNA across the species range results from the interplay of vicariant events, past climatic oscillations, and more dynamic factors related to ecological processes at finer scales.

Introduction

The Sonoran Desert and the Baja California Peninsula have long been considered an important area for phylogeographic research (Hafner and Riddle 2011, Munguia-Vega 2011). Many studies investigated the presence of genetic discontinuities across the region, revealing rich processes of cryptic divergence (reviewed in Munguia-Vega 2011). In general, phylogeographic breaks correspond with past geological events along the Peninsula (Munguia-Vega 2011, Riddle et al. 2000). For example, Riddle *et al.* (2000) identified three marine barriers—Late Pliocene transgressions resulting in formation of the Gulf of California, the seaway across the Isthmus of La Paz, and the Pleistocene midpeninsular seaway—as key geological events influencing the evolutionary history of the region's biota.

Most phylogeographic and biogeographic studies of the Sonoran Desert and Baja California have focused on vertebrates and insects (Munguia-Vega 2011); however, studies of plants are necessary to assess generality of the patterns reported from other groups (Clark-Tapia and Molina-Freaner 2003, Fehlberg and Ranker 2009, Garrick et al. 2009, Nason et al. 2002). While the formation of the Baja California Peninsula and development of breaks across it could explain genetic discontinuities, ecological or biological attributes could also have explanatory power regarding phylogeographic patterns (Grismer 2002). In this context, genetic structure and cohesion can be influenced by life history attributes (e.g., dispersal and hybridization; Loveless and Hamrick 1984), along with geological and historical events (Aguinagalde et al. 2005, Duminil et al. 2007, Schaal et al. 1998). Previous studies in plants have explored vicariance, fragmentation,

and postglacial range expansion (Clark-Tapia and Molina-Freaner 2003, Fehlberg and Ranker 2009, Garrick et al. 2009, Nason et al. 2002), but leaving other ecological and biological factors unexplored.

In the Sonoran and Mojave deserts, the desert mistletoe *Phoradendron californicum* Nutt. (Viscaceae) offers an ideal opportunity to explore how historical and ecological factors affect population and lineage divergence. In the first case, we can enumerate geologic events shaping patterns of genetic divergence on the Baja California Peninsula (cf. Riddle et al. 2000); in the second, *P. californicum*'s dependence almost exclusively on leguminous trees and its seed dispersal by one specialist and several generalist bird species (Aukema 2001, Larson 1996) give a comprehensive framework on what are alternative determinants of mistletoe's prevalence locally and regionally (Lira-Noriega et al. 2013, Lira-Noriega and Peterson accepted). Mistletoes are key species in ecosystems (Watson 2001), thus most attention has focused on their ecological attributes (e.g., Aukema 2003, Martínez del Rio et al. 1996, Watson 2009); however, genetic structure and phylogenetic histories suggest that both ecological and historical processes influence mistletoes divergence at multiple scales, through processes like post-glacial dispersal from Pleistocene refugia (Amico and Nickrent 2009), formation of host races (Glazner et al. 1988, Overton 1997, Zuber and Widmer 2009), and landscape fragmentation (Stanton et al. 2009).

Given evidence of divergence along the Baja California Peninsula across several taxa, and the challenge of understanding how biotic and abiotic factors influence divergence in desert mistletoe, we investigate the extent to which historical and

ecological drivers have produced the phylogeographic patterns observed. We reconstruct phylogeographic patterns in *P. californicum* with chloroplast DNA (cpDNA), and use Bayesian coalescent analyses to estimate the marginal likelihood of 16 *a priori* hypotheses corresponding to the (1) geologic events forming the Gulf of California and peninsular breaks, (2) distance to the multivariate centroid of the climatic niche, (3) distance to the center of the geographic range, (4) number of potential dispersers derived from suitability maps, (5) coincidence with the vegetation types of the Sonoran Desert, and (6) host species. This approach is complemented using ecological niche projections to Last Glacial Maximum climatic conditions for the mistletoe, most common host species, and specialist bird disperser, and fossil record of mistletoe and hosts is used to explore ecological explanations for observed genetic patterns.

Materials and Methods

Sampling

For cpDNA analysis we sampled 127 individuals from 65 populations from across the geographic range of *Phoradendron californicum* (Fig. 1; Appendix 4.1): of these, 54 populations (105 individuals) were sampled in the course of A.L.-N.'s fieldwork in Mexico and the United States in 2010 and 2012, and 11 populations from herbarium specimens, mostly from Sonora, Mexico (10 individuals), and the islands of Tiburón (9 individuals) and Ángel de la Guarda (3 individuals) in the Gulf of California. Sampling in 2012 in the southwestern United States and Baja California followed a random selection of collecting points at stratified distances with respect to distance to the multivariate mean of climatic

conditions used by the species (niche centroid) and to the geographic center of the species' range (see Lira-Noriega and Manthey 2014). At each locality, fresh apical shoots and stems of individuals were sampled randomly, without regard to host species, and dried in silica gel for DNA isolation. Vouchers for each population were pressed and deposited at the R.L. McGregor Herbarium (KANU). Latitude and longitude coordinates were derived from label data for tissues from herbaria; our localities were determined using a Garmin 60CSx global positioning device. In light of safety concerns, localities in Sonora were sampled more cursorily during 2010 fieldwork and were complemented with herbarium specimens. For the outgroup, four individuals of the sister species *P. serotinum* (Raf.) M.C. Johnst. (Ashworth 2000, Nickrent 2002) were used for analysis.

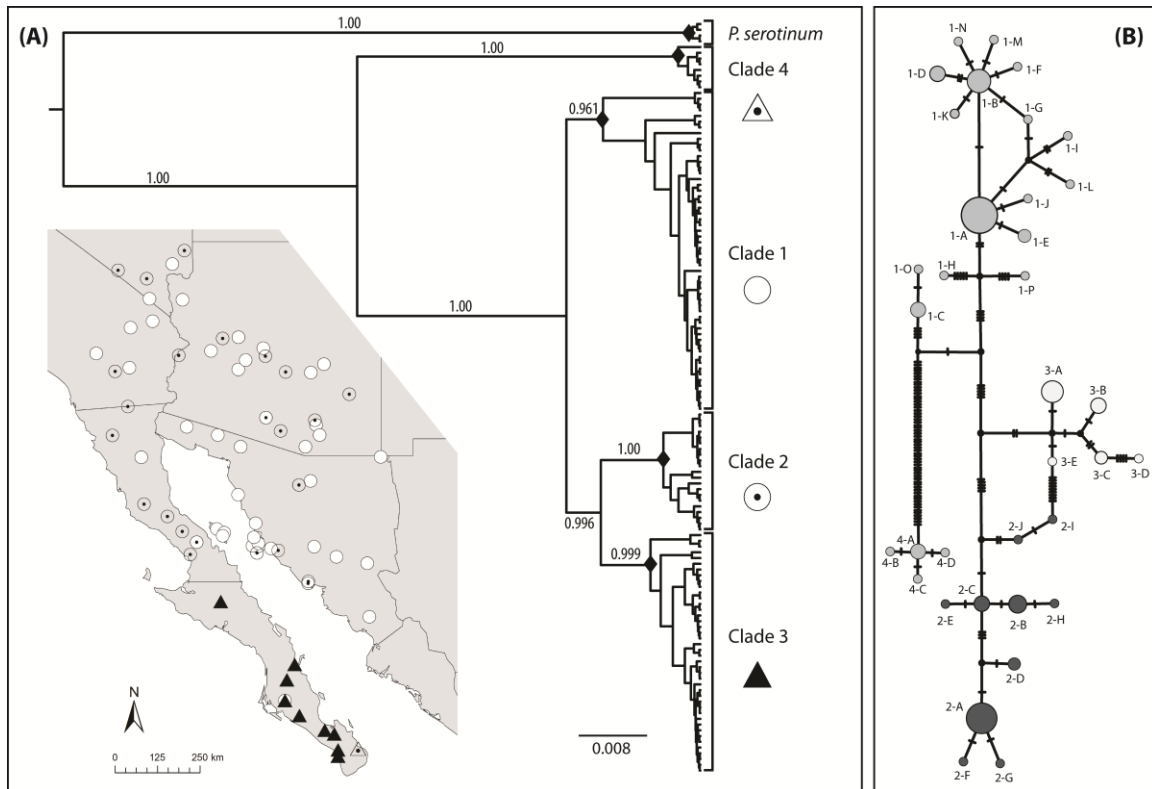


Figure 4.1 (A) Gene tree inferred from cpDNA and clades distributions. Posterior probabilities from delimited groups ($P > 0.95$) are shown on branches and significant nodes from GMYC are in black diamonds. (B) Haplotype network from the three cpDNA regions and its correspondence with clades (numbers).

DNA extraction, amplification, and sequencing

Total DNA was extracted using a modified CTAB protocol (Doyle and Doyle 1987, Mort et al. 2001). PCR amplifications were conducted in 25 μ l aliquots using Bullseye Red Taq master mix (MidSci, St. Louis, USA). CpDNA regions were amplified for 1-3 individuals per locality using *atpI/atpH* (*atpH-atpI* spacer), *trnQ(UUG)/5'rps16* (*trnQ-rps16* spacer), and *trn(UAG)/rpl32* (*trnL-rpl32* spacer), using the protocols of Shaw et al. (2007). The same primers were used in sequencing reactions. All sequencing was performed by Macrogen, Inc. (Rockville, Maryland, USA). Resulting contigs were assembled and edited using Geneious v6 (Biomatters. www.geneious.com).

Alignment and phylogenetic analyses

DNA sequences were aligned using MUSCLE v3.8.31 (Edgar 2004), and corrected visually to minimize apparent character state changes with Jalview v2.8 (Waterhouse et al. 2009). To identify haplogroups and their relationships, we estimated both haplotype networks and gene trees of sequences. Haplotype networks were constructed using PopART v1 (www.popart.otago.ac.nz/index.shtml) with parsimony network criteria implemented in TCS (Templeton et al. 1992). Individuals with missing or partially sequenced regions were excluded from analyses to avoid ambiguity produced by missing data (Joly et al. 2007). Concatenated datasets of two (*atpI-atpH + trnQ-rps16*, *trnL-rpl32 + trnQ-rps16*, *atpI-atpH + trnL-rpl32*) and three (*atpI-atpH + rpl32-trnL + trnQ-rps16*) of the cpDNA regions were analyzed to assess differences that could indicate influence of missing individuals in the estimated networks.

We estimated maximum-likelihood scores for models developed with and without a molecular-clock constraint using PAUP* v4.0b10 (Swofford 2003), and were unable to reject a strict-clock model using a likelihood ratio test ($-\ln ML_{\text{unconstrained}} = 3922.5793$, $-\ln ML_{\text{constrained}} = 4098.658$, $P_{(df=119)} \approx 1$). Accordingly, we assumed a strict molecular clock model to estimate an ultrametric gene tree for the three concatenated regions (including indels and individuals with incomplete data) within a Bayesian statistical framework. We used BEAST v1.7.5 (Drummond et al. 2012) to estimate a gene tree under a constant-size coalescent prior on trees with a $1/x$ prior on population size, a GTR + gamma model of nucleotide substitution with default priors, and set a strict-clock rate to 1.0 to estimate branch lengths in units of expected substitutions per site. We ran four independent

MCMC chains for 100 million generations each, and sampled every 20,000 generations. Mixing and burn-in were assessed using Tracer v1.5 (Rambaut and Drummond 2007) and convergence of posterior splits probability among chains was corroborated with AWTY (Are We There Yet? Nylander et al. 2008). We also estimated a time-calibrated gene tree using the same settings as above except that we used general (lognormal(2,1); $1 - 3 \times 10^{-9}$ subst. sites⁻¹ year⁻¹; Wolfe et al. 1987) and accelerated (lognormal(8.24,1); 8.24×10^{-9} subst. sites⁻¹ year⁻¹; Yang et al. 2008) priors on the strict-clock rate, because no fossil record is available to calibrate a substitution rate in *P. californicum*. Both rates priors assume increased rates of molecular substitution in *P. californicum* owing to its parasitic life strategy (Bromham et al. 2013). All four chains converged early in all analyses, and we conservatively discarded the first 1000 sampled trees (20 million generations) as burn-in when summarizing results. We summarized the retained trees using the topology of the maximum-clade credibility tree and median node ages.

Using the resulting ultrametric tree from BEAST, we inferred population structure using a general mixing Yule-coalescent (GMYC) model (Pons et al. 2006). This analysis identifies shifts in branch rates from a Yule (speciation) to coalescent (population) process (Esselstyn et al. 2012, Pons et al. 2006). Both single- and multiple-threshold hypotheses were compared to a null model (one species) using a likelihood ratio test to determine possible shift points on ultrametric trees (Esselstyn et al. 2012, Fujisawa and Barraclough 2013, Pons et al. 2006). Usually used for species delimitation with single locus, we employed GMYC to estimate whether recovered clades were divergent populations better fit by independent coalescent processes. The GMYC analysis was conducted using

the R (R Development Core Team 2013) package splits (Ezard et al. 2013), employing default settings for both single- and multiple-threshold models.

Hypothesis testing in a phylogenetic context

We estimated the marginal probability of the aligned sequences under different geographic, ecological and historical hypotheses of population divergence. We used the stepping-stone method (Xie *et al.* 2011) in BEAST (Baele et al. 2012) to estimate marginal likelihoods of 16 *a priori* hypotheses grouping individuals according to six broad categories of factors: (1) geologic events forming the Gulf of California and peninsular breaks, (2) distance in environmental space to the multivariate centroid of the species' climatic niche, (3) distance in geographic space to the center of the species' geographic range, (4) number of potential dispersers derived from suitability maps, (5) coincidence with a vegetation of the Sonoran Desert (Shreve 1951), and (6) host species. The partitioning of individuals into populations for all hypotheses is summarized in Table 4.1 and Appendix 4.1, and the methods for generating information pertaining each hypothesis are in Appendix 4.2. We used Beauti v1.7.5 to generate XML analysis files for each hypothesis. Analyses under all hypotheses shared the same settings, and differed only in how individuals were assigned to classes. This approach allowed us to estimate comparable marginal likelihoods under each hypothesis, which estimated the strength of each hypothesis relative to the one with the largest marginal likelihood using Bayes factors in a $2^{*(\ln \text{likelihood})}$ scale as $2^{*(\ln \text{likelihood of best model} - \ln \text{likelihood of alternative model})}$ (Kass and Raftery 1995). The marginal likelihood of each hypothesis was estimated by combining the stepping-stone samples from two independent runs. We

ran all *BEAST analyses for an initial 10^8 generations, sampling every 20,000 generations, followed by sampling at 100 power posteriors between the prior and posterior, where powers were evenly spaced quantiles of a Beta (0.3, 1.0) distribution. At each power posterior step, we sampled every 1000 generations for 10^8 generations (i.e., 1000 samples from each of the 100 powers). We used (1) a strict-clock model with a rate of 1.0 to estimate gene-tree branches in units of expected substitutions per site, (2) a Yule-process prior on species trees and an exponentially distributed hyperprior on the Yule birthrate with a mean of 15, (3) a piecewise constant model of population size for each branch of the species tree, (4) an exponential prior with a mean of 0.005 for the per-branch population sizes, and (5) a GTR + Gamma model of nucleotide substitution with default priors except for the shape parameter of the gamma-distributed model of among-site rate heterogeneity with an exponential prior with a mean of 1.0. Lastly, we set the ploidy to mitochondrial (= chloroplast).

Table 4.1 Summary of historical events, and ecological and geographic conditions used to group *Phoradendron californicum* populations according to 16 *a priori* established hypotheses explaining cpDNA variability.

| Hypothesis | Mapping levels |
|---|---|
| Historical (vicariant events) | |
| Historic 1 | (1) in Baja California Peninsula after northward transgression forming the Gulf of California; (2) outside Baja California Peninsula after northward transgression forming the Gulf of California. |
| Historic 2 | (1.1) trans-peninsular seaway forming the Isthmus of La Paz 3 mya; (1.2) rest of Baja California Peninsula; (2) rest of continental land. |
| Historic 4 | (1) trans-peninsular seaway forming the Isthmus of La Paz; (2) region between Isthmus of La Paz and mid-peninsular seaway break in the central Vizcaino region; (3) region between mid-peninsular seaway break in the central Vizcaino region and north of Baja California Peninsula; (4) rest of continental land. |
| Break Cabo | (breakcabo) south of break of Isthmus of La Paz break; (rest) north and rest of territory of break Isthmus of La Paz break. |
| Break mid-seaway | (breakseaway) south of mid-peninsular seaway break in the central Vizcaino region; (rest) rest of territory north of mid-peninsular seaway break in the central Vizcaino region. |
| Regionalization | |
| Vegetation (Shreve 1951) | Arizona Mountains Forest; Arizona Upland; Central Desert; Chaparral; Chihuahuan Desert; Gulf Coast; Lower Colorado Desert; Magdalena Plains; Mojave; Plains of Sonora; Sarcocaulous Shrubland; Sonoran thornscrub; Vizcaino Desert. |
| Ecoregions | Sonoran desert, Mojave desert, Baja California desert, Sonoran-Sinaloan transition subtropical dry forest, Gulf of California xeric scrub, California coastal sage and chaparral, San Lucan xeric scrub, Chihuahuan desert, Arizona Mountains forests. |
| Topographic/geographic | |
| Elevation (quartiles) | 1st (-0-357m); 2nd (358-877m); 3rd (878-1528m); 4th (1529-4239m). |
| Longitude (quartiles) | 1st (-116.58- -114.25°); 2nd (-114.26- -112.29°); 3rd (-112.30- -110.9°); 4th (-110.9- -109.05°). |
| Latitude (quartiles) | 1st (23.38-28.76°); 2nd (28.77-31.57°); 3rd (31.58-33.61°); 4th (33.62-36.76°). |
| Distance to geographic range center (quartiles) | 1st (0-367km); 2nd (368-472km); 3rd (473-610km); 4th (611-760km). |
| Ecological | |
| Distance to ecological niche centroid (quartiles) | 1st (0.40-2.38); 2nd (2.39-3.16); 3rd (3.17-4.19); 4th (4.20-11.40). |
| Host species | <i>Acacia greggii</i> , <i>A. occidentalis</i> , <i>Cercidium floridum</i> , <i>C. microphyllum</i> , <i>C. praecox</i> , <i>Larrea tridentata</i> , <i>Olneya tesota</i> , <i>Prosopis articulata</i> , <i>P. glandulosa</i> , <i>P. velutina</i> . |
| Genera | <i>Acacia</i> , <i>Cercidium</i> , <i>Larrea</i> , <i>Olneya</i> , <i>Prosopis</i> . |
| Year-round dispersers suitability (quartiles) | 1st (1-3); 2nd (3-5); 3rd (5-7); 4th (7-10). |
| Wintertime dispersers suitability (quartiles) | 1st (0-2); 2nd (2-4); 3rd (4-6); 4th (6-10). |
| Null | (in) all individuals correspond to one same category. |

Ecological niche modeling

Current and Last Glacial Maximum (LGM) climate-based suitable areas were estimated using ecological niche model transfers for the mistletoe, the five most common hosts (*Acacia greggii*, *Cercidium floridum*, *C. microphyllum*, *Prosopis glandulosa*, *P. velutina*), and the principal bird disperser (*Phainopepla nitens*). Host occurrence data were derived from herbarium specimens from across their ranges from the Global Biodiversity Information Facility (<http://www.gbif.org>) and the Southwest Environmental Information Network (<http://swbiodiversity.org/portal/index.php>); mistletoe occurrences were assembled from these sources and A.L.-N.'s fieldwork (Lira-Noriega et al. 2013). Disperser occurrences were drawn from eBird (<http://ebird.org/content/ebird/>). Numbers of unique occurrences were *A. greggii* (946), *C. floridum* (345), *C. microphyllum* (694), *Phoradendron californicum* (295), *Prosopis glandulosa* (914), *P. velutina* (1169), and *Phainopepla nitens* (15,487).

Environmental variation across the region was characterized with climate layers at a spatial resolution of 2.5' for the present from WorldClim (Hijmans et al. 2005; www.worldclim.org), and for the LGM (21 kya) from general circulation model simulation outputs from two models: the Community Climate System Model (CCSM3; Collins et al. 2006) and the Interdisciplinary Research on Climate (MIROC v3.2; Hasumi and Emori 2004). To avoid fitting models in overly dimensional environmental spaces, we reduced dimensionality to seven relatively uncorrelated 'bioclimatic' variables ($r < 0.7$; annual mean temperature, mean diurnal range, maximum temperature of warmest month, minimum temperature of coldest month, annual precipitation, precipitation of wettest

month, and precipitation of driest month). Bioclimatic variables are summaries of means and variation in temperature and precipitation, and reflect dimensions of climate relevant in delimiting species' distributions (Hijmans et al. 2005).

We designed model calibration regions separately for each species, given that ecological niche models must be calibrated and compared across regions relevant to the species in a biogeographic context. These areas should be accessible to, and likely to have been 'sampled' by, the species over relevant periods of time (Barve et al. 2011). As a simple hypothesis of the accessible area, we took the ecoregions (Olson et al. 2001) in which species' occurrence points fell, plus a 200 km buffer around them.

We used Maxent (v3.3.3.e; Phillips et al. 2006) to obtain suitability values across the region under current and past climate conditions. Prior to calibrating models in Maxent, occurrence data were rarefied spatially to leave occurrences at a minimum distance of 0.17°; this step helps to eliminate problems of spatial autocorrelation common in this type of data, and allows sampling environmental conditions evenly across the range of the species. Models were calibrated on current climate conditions, and transferred to past climate conditions via 10 bootstrap replications, each with 30% of points set aside for model testing. The remaining Maxent parameters were left as default. To convert initial model outputs to binary predictions, we used a modified least training presence threshold approach ($E = 5\%$) over the median predicted suitability across replicates (Peterson et al. 2011). Performance of binary predictions was evaluated using a one-tailed cumulative binomial test to calculate the probability of obtaining that level of

sensitivity (or better) by chance alone, based on 100 independent test points set aside at random *a priori*.

Host and mistletoe macrofossils

To understand the distributional dynamics of hosts and mistletoe through time, we assembled subfossil information from packrat middens (Appendix S3). These data were used to interpret species' distributions in synchrony with niche model projections. We were unable to use subfossil data to calibrate divergence-time because they (1) correspond to relatively recent samples of extant species and thus provide little information regarding the timing of speciation events, and (2) lack DNA data and thus cannot be used as dated tips.

Results

DNA sequences

The three cpDNA regions (*trnQ-rps16*, *trnL-rpl32*, *atpI-atpH*) were of size 552, 465, and 632 base pairs (bp), with 30, 23, and 22 variable positions, respectively. Indels were common in *trnQ-rps16*, with 61 indels, compared with 31 indels in *atpI-atpH*, and 20 in *trnL-rpl32*. Amplification of *trnQ-rps16*, was difficult due to poly A and T regions. As a result, combined cpDNA parsimony network reconstructions were based on 87 (127 total) sequences. Nonetheless, results did not suggest significant differences among datasets in the networks reconstructed (see below).

Gene tree reconstruction

The estimated ultrametric tree indicated at least four well-supported clades (posterior probability > 0.95) at deep nodes. Clade 1 (pp = 0.961) and clade 2 (pp = 0.999) each grouped individuals from across the northern Baja California Peninsula and the Sonoran Desert. A third clade (pp = 0.999) included sequences almost exclusively from southern Baja California and the Cape region (Fig. 4.1), and was sister to clade 2 (pp = 0.996). A fourth clade (pp = 1) corresponded to a single population in the eastern part of the Cape (Fig. 4.1), being placed as sister to all other clades.

The GMYC analysis favored the single-threshold (ML = -1362.186) and multiple-threshold models (ML = 1366.448) over the null model (ML = 1358.265), which suggests existence of both coalescent and Yule-like divergence processes (Fig. 4.1). The single-threshold ML model suggested presence of five clades, four corresponding to *P. californicum* in the gene tree reconstructions, while the multiple-threshold model indicated 53 clusters (Table S4.1). We favor the single-threshold model to delimit clades, based on the high support for the five clades identified in Bayesian analysis (all pp > 0.95) and known tendencies of the multiple-threshold approach to oversplit groups (Fujisawa and Barraclough 2013, Reid and Carstens 2012).

Divergence times for clades ranged 1.3-4.1 mya with the general rate, and 0.2-0.8 mya with the accelerated rate (Table 4.2). Clade 1 had the oldest most recent common ancestor (MRCA) estimates (4.1 mya and 0.8 mya), whereas clade 3 had the youngest MRCA (1.8 mya and 0.3 mya). The age of the divergence of *P. californicum* and *P. serotinum* was estimated at 16.4 and 3.4 mya.

Parsimony network

Analyses of the combined cpDNA dataset recovered three lineages that represent the clades from the Bayesian reconstruction (clades 1, 2, and 3). The 35 haplotypes detected represented 13 haplogroups and 22 singletons. The two largest haplogroups (1-A and 2-A) corresponded to clades 1 and 2, with 17 and 12 haplotypes each (Appendix S4.1). An additional group (clade 4) was detected in samples from a single population in the east part of the Cape region (population 225 in Appendix S4.1), separated by 58 steps from the main groups and connected to two haplotypes (1-O and 1-C) from clade 1 (Fig 4.1). Ambiguity was detected in the connection between clade 2 and Baja California, and also within clade 1, although neither of these ambiguities affected the structure of relationships among main groups. Networks retrieved using other combinations of cpDNA regions did not differ in the main configuration of the networks, except in the *atpI-atpH + trnQ-rps16* dataset, where ambiguities were detected (Fig. S4.2). The only difference noted between the haplotype network and the gene tree corresponds to two haplotypes not nested in clade 1 (1-C, 1-O; Fig 4.1); nevertheless, this did not alter the original configuration of the other clades.

Gene tree topology and ecological versus historical hypothesis testing

Among the 16 hypotheses of population structure, the one with largest probability of producing the cpDNA dataset corresponded to the vicariant events related to formation of the Gulf of California and subsequent breaks across the Baja California Peninsula (Table 4.3, Fig. 4.2). The $2\ln$ Bayes factors comparing this model to other hypotheses are all larger than 23.5, suggesting very strong support relative to the alternative models (Kass

and Raftery 1995). This result corresponds to a Bayes factor of $\sim 127,000$, which means the posterior odds in favor of this model over the next best model is 127,000 times greater than the prior odds.

Table 4.3 Marginal likelihood and Bayes factor of hypotheses used to test the phylogenetic relationships of the gene tree (see Table 4.1). Hypotheses are listed in order of importance according to the marginal likelihood. Bayes factor is estimated with respect to the hypothesis with largest likelihood.

| Hypothesis | Marginal likelihood | 2ln Bayes factor |
|---|---------------------|------------------|
| Historic 4 (subdivision based on major breaks resulting from geologic vicariant events) | -4339.373 | |
| Historic 2 (trans-peninsular seaway forming the Isthmus of La Paz; 3 mya) | -4351.165 | 23.585 |
| Historic 1 (northward transgression forming the Gulf of California; 3-5 mya) | -4362.646 | 46.546 |
| Vegetation (Shreve 1951) | -4363.874 | 49.002 |
| Latitude (quartiles) | -4366.716 | 54.686 |
| Distance to geographic range center (quartiles) | -4369.276 | 59.806 |
| Distance to ecological niche centroid (quartiles) | -4369.522 | 60.298 |
| Ecoregions | -4369.873 | 61.001 |
| Mid-peninsular seaway break in the central Vizcaino region | -4370.834 | 62.922 |
| Longitude (quartiles) | -4382.242 | 85.738 |
| Isthmus of La Paz break | -4385.374 | 92.002 |
| Wintertime dispersers suitability (quartiles) | -4394.777 | 110.808 |
| Elevation (quartiles) | -4403.482 | 128.218 |
| Year-round dispersers suitability (quartiles) | -4403.774 | 128.803 |
| Genera | -4410.532 | 142.318 |
| Host species | -4415.586 | 152.427 |
| Null hypothesis | -4416.835 | 154.924 |

Note: Following Kass and Raftery (1995), the Bayes factor scale of strength of evidence in favor of one hypothesis is: 0-2 (not worthy of mention), 2-6 (positive), 6-10 (strong), >10 (very strong).

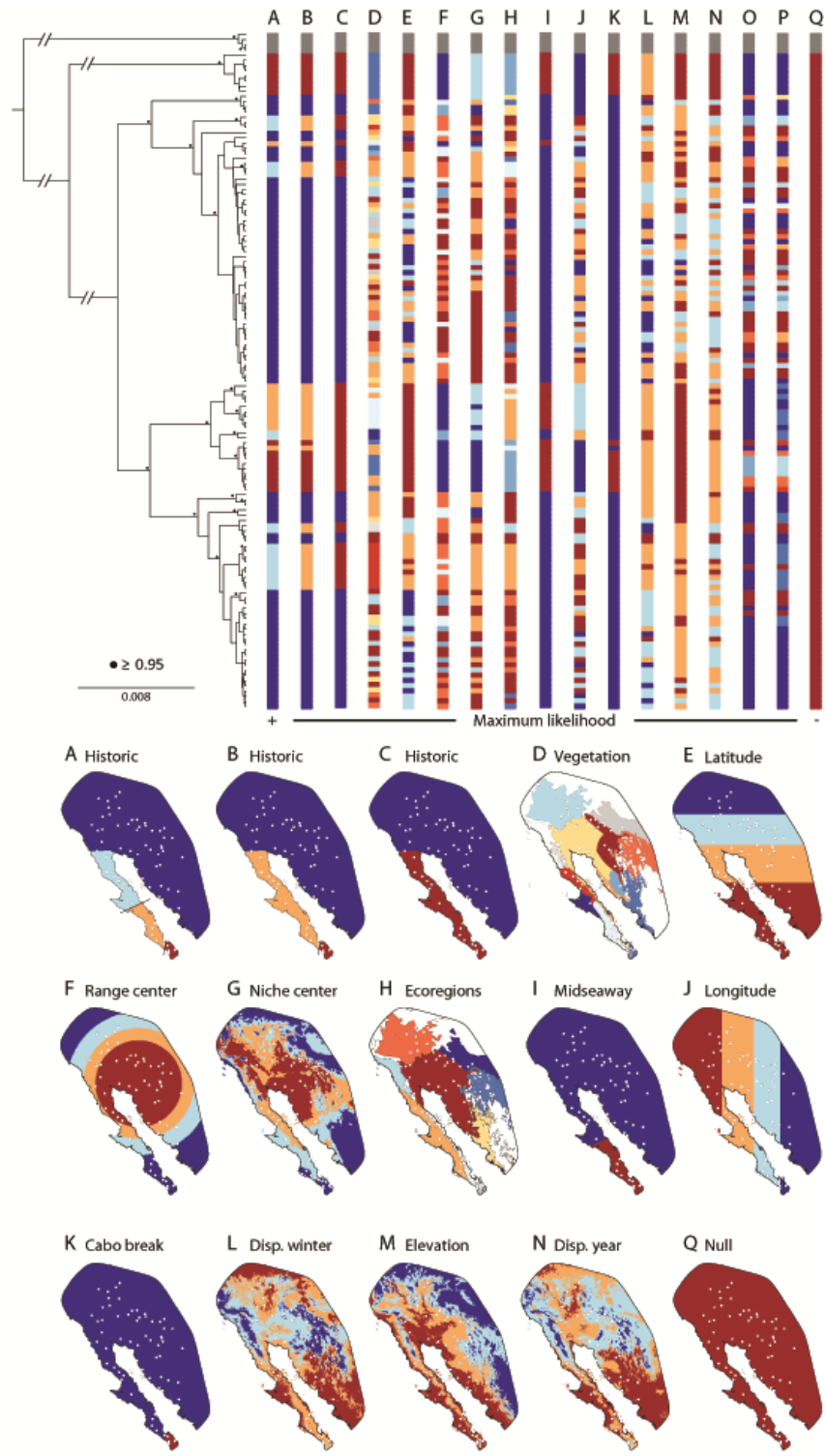


Figure 4.2 Historical, geographic, and ecological *a priori* hypotheses used to predict the cpDNA variation across the distribution of *P. californicum* in a Bayesian phylogenetic framework. Hypotheses are ordered according to their likelihood and with same color-coding between tree topology and geographic distribution. White dots on maps correspond to sampled populations.

The models with the second and third largest marginal likelihoods (B and C in Fig. 4.2) were also based on historical hypotheses nested within the best model, and correspond to the northward marine transgression related to isolation of the Cape region by the Isthmus of La Paz and formation of the Gulf of California. In order of likelihood, remaining hypotheses were Shreve's vegetation regionalization (C and D); distance to geographic range center, distance to ecological niche centroid, and ecoregions (F-H); elevation and disperser suitability (M-N); and lastly host species and the null hypothesis (P-Q). Testing these hypotheses omitting the highly divergent population 225 did not change these results (Table S4.2).

Present-Last Glacial Maximum suitability

All niche models performed significantly better than random expectations ($P < 0.001$; Appendix S4). Thresholded suitability maps for mistletoe, hosts, and the disperser for the present corresponded well to known ranges of each species (Fig. 4.3). Last Glacial Maximum predictions showed some differences in amount of area predicted as suitable for *P. californicum* and its hosts, depending on which global circulation model was used. For *P. californicum*, projections showed relatively smaller ranges mostly restricted to southwestern Arizona and parts of California in CCSM, in MIROC extending into Arizona, central Baja California, and northwestern Sonora; *P. nitens* predictions were similar in both scenarios, preserving most of its range in the present across the Sonoran Desert. Both LGM models showed suitable areas for *P. californicum* in the Lower Colorado River Valley, north of La Paz in the Cape, and in a coastal area in western Sonora. All host species except *P. glandulosa* showed reductions in distributional areas; *A. greggii* and *P.*

velutina showed similar patterns, with their ranges split in two regions, one in the Lower Colorado River Valley and the other in southern Sonora, whereas *Cercidium* species had most of their suitable areas in southern coastal Sonora. Overall, these predictions showed the largest accumulation of LGM host suitability in the Lower Colorado River Valley, along the coast of Sonora, and in the eastern Cape region in the Baja California Peninsula (Figs. 4.3 and 4.4, Fig. S4.1).

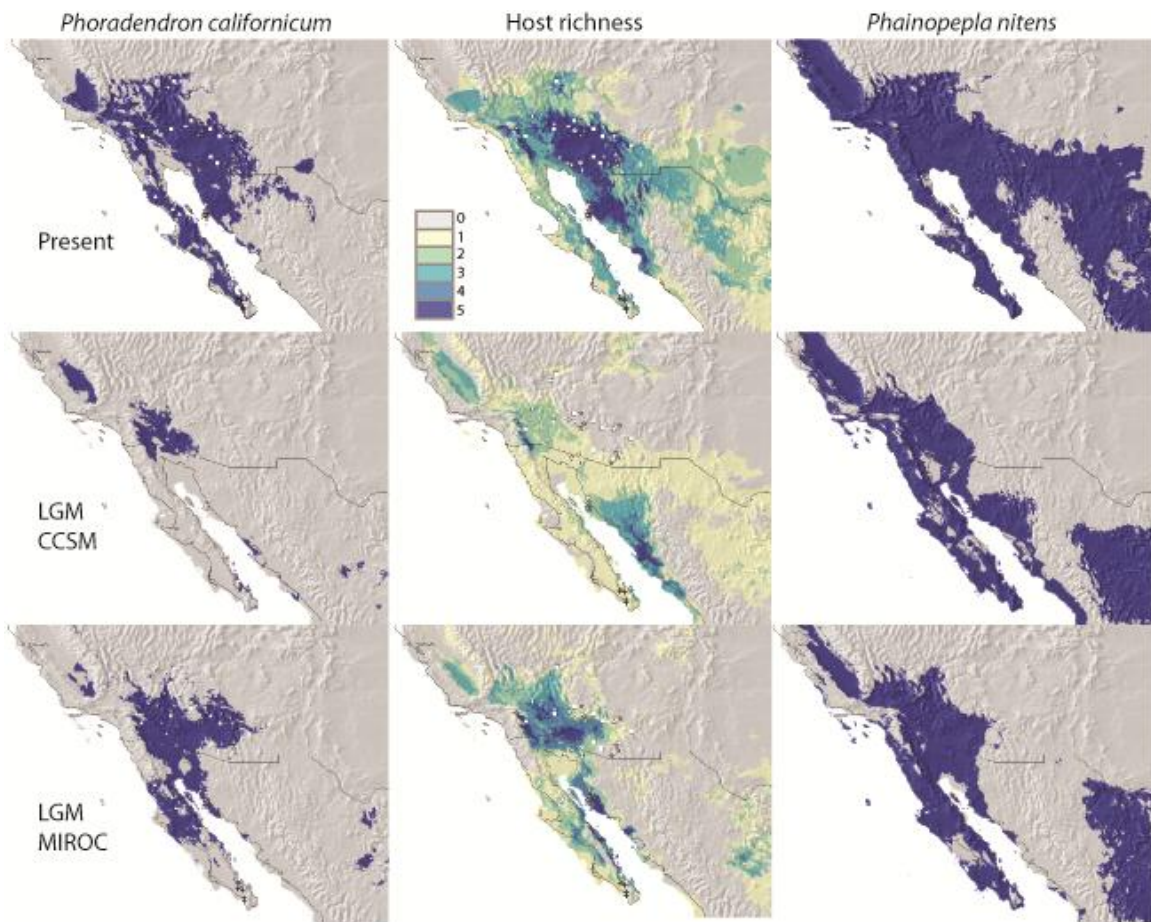


Figure 4.3 Potential distribution for the mistletoe (*Phoradendron californicum*), its hosts (richness), and disperser (*Phainopepla nitens*) under current climate and two LGM climate scenarios (CCSM and MIROC).

Host and mistletoe macrofossils

The subfossil record from packrat middens of hosts and mistletoe has been found in caves across the Sonoran and Chihuahuan deserts, indicating drastic changes in species composition and highly dynamic distributional areas related to climate oscillations (see Appendix S3). Most host fossils were from the Sonoran Desert, most abundant since 13 kya and for the mistletoe since 6.4 kya (see Appendix S3). Two of the most common host species, *A. greggii* and *P. velutina*, were the oldest in the fossil record and were also associated with two of the most frequent haplotypes (Fig. 4.4 and Fig. S4.1).

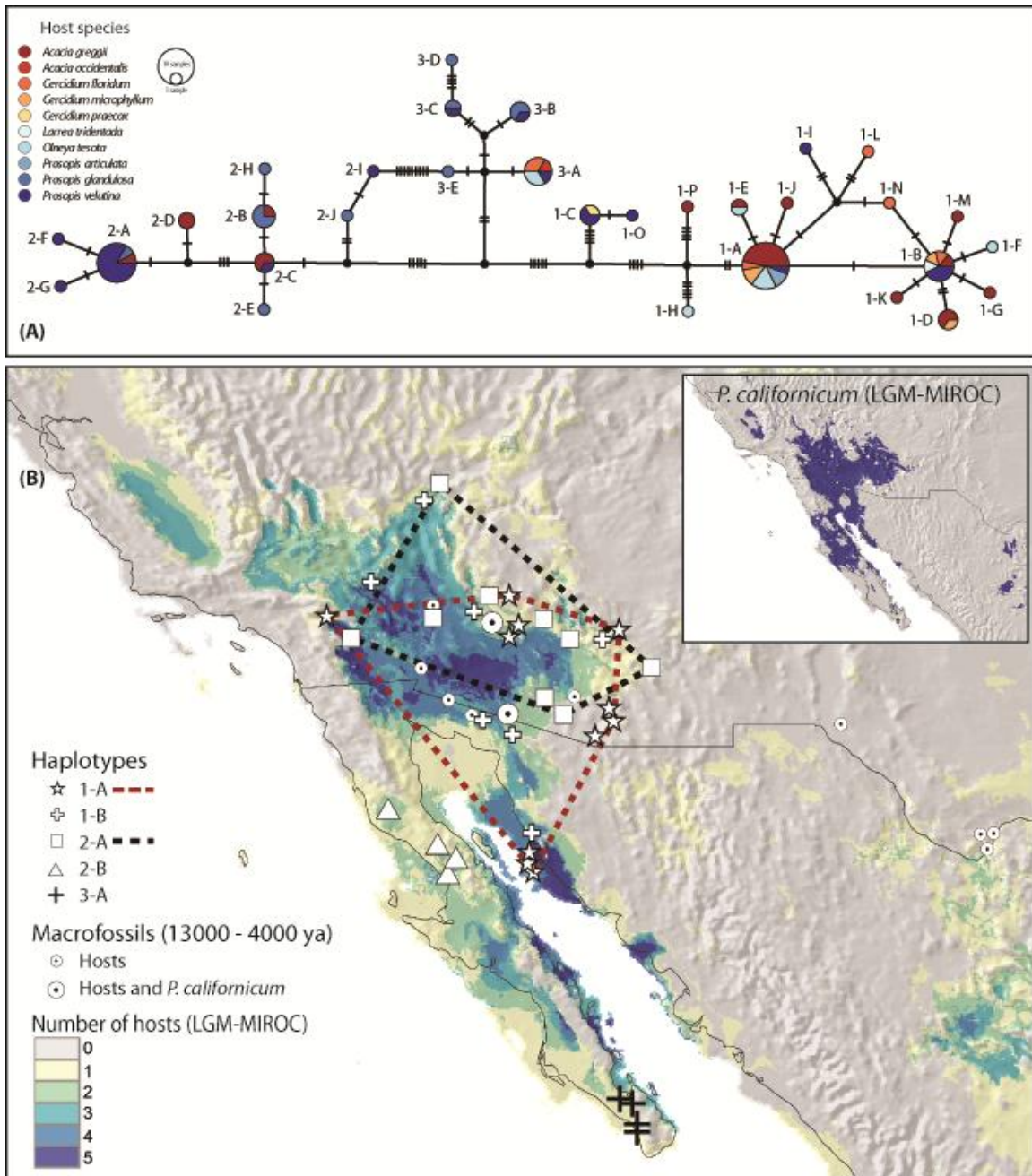


Figure 4.4 (A) *Phoradendron californicum* haplotype network for the three cpDNA concatenated regions colored by host species, excluding haplotypes from clade 4. (B) Potential distribution for mistletoe (inset) and hosts distributions during the LGM (21 kya) according to the MIROC climate scenario, showing geographic locations of most frequent haplotypes and macrofossil localities with mistletoe or hosts.

Discussion

The phylogeny of *P. californicum* inferred from cpDNA, was most probable under a model reflecting a series of geologic events related to formation of the Baja California Peninsula and seaways across it in the Pliocene and the Pleistocene. This view, however, is complemented with that of a more dynamic distributional history associated to continuous interaction with hosts in the Sonoran and Mojave deserts, as inferred from niche model projections based on Pleistocene climate and fossil record.

Mistletoe phylogeny and phylogeographic patterns

Analyses of cpDNA showed that at least four well-supported clades existed among sampled populations of *P. californicum*; 35 haplotypes were identified, with three main clades coincident between the estimated haplotype network and ultrametric tree. Both sympatry and allopatry in geographic distributions of haplotypes in *P. californicum*'s gene tree suggest that diverse processes of diversification have occurred simultaneously in the Baja California Peninsula and the Sonoran Desert region. These patterns are especially intriguing in the context of the seaway breaks hypotheses and the mechanisms of seed dispersal of *P. californicum*.

The first pattern corresponds to clades 1 and 2, which are sympatric across the northern Sonoran Desert, northern Baja California Peninsula, and southern Mojave Desert (Fig. 4.1). This distribution suggests long distance dispersal of seeds, as presence of haplotypes across the Gulf of California and their origin from non-sister clades cannot support an old vicariant event without subsequent gene flow. The fleshy fruits of *P. californicum* are dependent on birds for dispersal and germination (Larson 1996, Murphy

et al. 1993), thus we expect long-distance dispersal, or accumulation of numerous short-distance dispersal events over extended geographic regions, causing little or no signal of phylogeographic structure in the cpDNA (e.g., Duminil et al. 2007, Worth et al. 2010). The pattern exhibited between northern clades (1 and 2) would support this hypothesis, given its large distribution and lack of geographic exclusivity of haplotypes across the Gulf of California.

The second pattern is depicted by clades 2 and 3, in which clade 3 occurs exclusively in southern Baja California Peninsula, and by the separation of clade 4 in the Cape region from the rest of *P. californicum* (Fig. 4.1). In this case, the phylogeographic break between clades 2 and 3 is congruent with the midpeninsular seaway near the Vizcaíno Desert c. 1 mya. The split between clade 4 and the rest of *P. californicum* is coincident with the formation of the Isthmus of La Paz in the southern portion of the peninsula 3-4 mya, which supports vicariant divergence (Murphy and Aguirre-León 2002, Riddle et al. 2000; Fig. 4.1). Nevertheless, this clade corresponds to a single population in the eastern Cape region, which has been recognized as a botanical region distinct from the rest of the Baja California Peninsula (Shreve 1951), and is also distant from optimal niche conditions, which would correspond to both lower abundance and genetic diversity (Lira-Noriega and Manthey 2014, Martínez-Meyer et al. 2013) or niche divergence. The presence of phylogeographic breaks in the southern Baja California lineages (clades 3 and 4) suggests that limited dispersal has been sustained under conditions that promote isolation and limited post-divergence spread. However, if no changes are assumed in the dispersal capabilities among lineages, presence of deep phylogenetic breaks in the Baja

California Peninsula cannot be solely explained by vicariance, suggesting that additional biological and ecological attributes could have promoted restrictions in the dispersal of seeds.

Our estimates of node ages for the MRCA are compatible with some of the peninsular geological events for the general mutation rate (1.3-4.1 mya), but also with some of the most recent climatic oscillations for the accelerated mutation rate (0.2-0.8 mya), which suggests that vicariance cannot be an exclusive explanation for the phylogeographic patterns (Garrick et al. 2009, Grismer 2002). Given the parasitic nature of *P. californicum*, an accelerated mutation rate in chloroplast regions would be more adequate to calibrating node ages compared to other non-parasitic plants in the area (Bromham et al. 2013). This effect would be reflected in differences of at least three to six times of neutral nucleotide variability present from the three sampled non-coding chloroplast regions, compared to previous estimates from endemic plants of the Baja California Peninsula ($\pi_{psbA-trnH} = 0.0013$; Fehlbeg and Ranker 2009; Table S4.3). Therefore, it is likely that the dates estimated under accelerated rates coincide with vicariant divergence between clade 4 and the rest of *P. californicum*, and divergence between clades 2 and 3 would be mostly associated with ecological and environmental mechanisms of divergence.

Historical and ecological hypotheses

Given the preponderance of environmental and ecological factors in seed dispersal (Cain et al. 2000, Nathan 2006), these factors should be contrasted with the most parsimonious vicariant hypotheses on the phylogeographic structure in *P. californicum*. When we tested

the cpDNA topology against historical, ecological, and geographic hypotheses, patterns of lineage divergence were best explained when individuals were grouped in the four land areas that correspond to the three major seaway breaks associated with the formation of the Gulf of California and subsequent splits of the Baja California Peninsula (Riddle et al. 2000, Riddle and Hafner 2006). Assumptions of the multi-population coalescent model used to estimate marginal likelihoods of these competing hypotheses are likely violated by *P. californicum*, most notably the assumption of no post-divergence gene flow among subpopulations. However, we expect violations of this assumption would weaken support for the hypothesis based on historical vicariance. Thus, our findings support this model as the best predictor of the genealogical history of the cpDNA, suggesting that these major land areas were important in structuring populations of *P. californicum* at deeper evolutionary timescales, and coincides with findings from previous phylogeographic studies (Munguia-Vega 2011, Murphy and Aguirre-León 2002).

However, while these historic hypotheses are based on the assumption that Pliocene/Pleistocene marine transgression events were responsible for the genetic discontinuities (Lindell et al. 2006, Riddle et al. 2000), several evolutionary forces might be equally capable of explaining this pattern (Garrick et al. 2009, Grismer 2002). For example, periods of expansion and contraction of the species' range related to climate oscillations and changes in vegetation could result in similar genetic discontinuities (Comes and Kadereit 1998, Grismer 2002). Accordingly, our results do not necessarily rule out competing hypotheses, particularly at recent timescales. Rather, these processes may be more significant at finer spatial and temporal scales compared to large-scale processes

in structuring lineages (e.g., Lira-Noriega et al. 2013). This could explain, for example, why the hypothesis based on vegetation types follows the historical hypotheses in marginal likelihood, which are then followed by the hypotheses based on other ecological and geographic factors (Table 4.3, Fig. 2).

An alternative explanation to the larger-scale geologic events in genetically structuring *P. californicum* and in favor of ecological processes is supported by haplotype geographic distributions in the context of its hosts (Fig. 4.4 and Fig. S4.1). Although host species and genera explain the overall evolutionary history of the cpDNA poorly (these hypotheses had the smallest marginal likelihoods before the null hypothesis; Table 4.3), haplotype networks suggest the possibility of continuous evolutionary pathways in relation to host species. Among the 10 host species identified for the individuals used in our analysis, *Acacia greggii*, *Prosopis velutina*, and *P. glandulosa* were the most frequent hosts and perhaps drivers of haplotype differentiation, followed by the two *Cercidium* species; coincidentally, these host species and the mistletoe have been recorded in packrat middens around the Lower Colorado River Valley, allowing us to confirm their distributions and associations (Fig. 4.4 and Fig. S4.1, Appendix S4.3).

Haplotype groupings according to host species reinforce the evidence of host specialization previously reported in *P. californicum*. Using isozymes, Glazner et al. (1988) concluded genetic differences and different rates of seed establishment existed depending on whether *P. californicum* individuals were parasitic on *A. greggii* or *Prosopis glandulosa* in populations from the Mojave and Colorado deserts. Later, in a cross-establishment experiment in northern Baja California, Overton (1997) concluded that two

host-specific types existed in *P. californicum*, one that primarily infects *Acacia* and *Cercidium*, and another infecting *Prosopis*, but he did not find differences in establishment of seeds from *Acacia* or *Prosopis* on *Olneya*. These findings help to explain why haplotypes associated with clade 1 and 3-A are represented by a combination of host species corresponding mostly to *Acacia* and *Cercidium*, and haplotypes associating clade 2 to *Prosopis*, which allows us to speculate on relative roles of host distributions for the phylogeography of *P. californicum* (see Fig. 4.4 and Fig. S4.1).

Present and past distributions

Ecological niche model transfers to LGM (21 kya) conditions and macrofossils from packrat middens (13-4 kya) both indicate that *P. californicum*'s distribution was fragmented by the colder climates during the last ice age (Fig.4; Appendix S4.3). Only one host species (*P. glandulosa*) showed a potentially wider distribution across the North American deserts during the LGM, and also in a packrat midden from the Chihuahuan Desert, whereas the other four species showed large range reductions, retreating to refugia in the lower Colorado River Valley in the northern Sonoran Desert, southwestern Sonora, and parts of Baja California (Fig. 4.4 and Fig. S4.1).

Since the widest inferred climatic refugium of *P. californicum* in the LGM coincides with distributions of two common hosts (*A. greggii* and *P. velutina*), the most frequent haplotypes from the northern clades (clades 1 and 2; Figs. 1 and 4), and the disperser could range over the mistletoe distribution during LGM (see Fig. 4.3), it is possible that dispersal and gene flow could have persisted in this part of the distribution during harsher climatic conditions, supporting the cpDNA phylogeographic patterns. Additionally,

macrofossils indicate compositional changes of plant communities in the region in synchrony with paleoclimatic conditions, and the appearance of hosts and mistletoe at around 13-4 kya indicates their more recent arrival, as well as contractions and expansions of their ranges (McAuliffe and McDonald 2006, McAuliffe and Van Devender 1998, Van Devender 1990a, b).

Because ecological and biological features of seed dispersal cannot be assimilated into cpDNA phylogeographic patterns without considering environmental changes, as they can be strongly correlated to climatic shifts (Aguinagalde et al. 2005), the combined lines of evidence from the phylogenetic analysis, the hypothesis testing, and past distributions allow for better interpretation of the distribution and history in *P. californicum*. In this paper, we covered as much of the phylogeographic pattern as was feasible by sampling many populations and genes across the range of *P. californicum*, rather than large numbers of individuals per population. This dataset should be adequate to test a series of hypotheses and detect and understand potential distributional breaks. We presented a novel use of multi-population coalescent models to test among *a priori* hypotheses based on potential historical and ecological processes of population differentiation. This approach allowed us to compare the probability of the sequence data under each hypothesis while integrating out uncertainty in the gene tree, population history, and demographic parameters. Similar approaches have been used for delimiting species (Grummer et al. 2013). Although we were limited to a single locus, by integrating over the genealogical and population history, the results should accurately reflect the posterior uncertainty conditional on our data. This approach is easily extended to multi-

locus data and provides a useful tool for testing among competing models of phylogeographical history in an objective statistical framework.

Acknowledgments

The authors thank Ben Wilder for obtaining samples from Tiburón and Angel de la Guarda islands, Richard Felger and Pedro Peña for help with regionalization of the Sonoran Desert, Joseph D. Manthey for advice on molecular analyses, and Farzana Ahmed for help with DNA extractions. Comments from A. Townsend Peterson, Richard Glor and Emily McTavish helped us to improve previous version of the manuscript. We thank curators from ASU for permission to sample loaned specimens and from KANU for supporting this project. A Young Researchers Award from the Global Biodiversity Information Facility (GBIF), a Tinker Award from the University of Kansas Center of Latin American Studies, and a University of Kansas Biodiversity Institute Panorama small grant award (Bunker Fund) supported collecting trips. A.L.-N. received scholarship support from Consejo Nacional de Ciencia y Tecnología, Mexico (189216).

References

- Acevedo P, Jiménez-Valverde A, Lobo JM, Real R (2012) Delimiting the geographical background in species distribution modelling. *Journal of Biogeography* **39**, 1383-1390.
- Aguinagalde I, Hampe A, Mohanty A, Martin JP, Duminil J, Petit RJ (2005) Effects of life-history traits and species distribution on genetic structure at maternally inherited markers in European trees and shrubs. *Journal of Biogeography* **32**, 329-339.
- Alexander MP, Burns KJ (2006) Intraspecific phylogeography and adaptive divergence in the White-headed Woodpecker. *Condor* **108**, 489-508.
- Allouche O, Steinitz O, Rotem D, Rosenfeld A, Kadmon R (2008) Incorporating distance constraints into species distribution models. *Journal of Applied Ecology* **45**, 599-609.
- Amico GC, Nickrent DL (2009) Population structure and phylogeography of the mistletoes *Tristerix corymbosus* and *T. aphyllus* (Loranthaceae) using chloroplast DNA sequence variation. *American Journal of Botany* **96**, 1571-1580.
- Amico GC, Rodriguez-Cabal MA, Aizen MA (2011) Geographic variation in fruit colour is associated with contrasting seed disperser assemblages in a south-Andean mistletoe. *Ecography* **34**, 318-326.
- Anderson, R (1981) Population ecology of infectious disease agents. Pages 318-355 in May R, editor. *Theoretical ecology. Principles and applications*. Blackwell Scientific Publications, Oxford.
- Anderson RP, Peterson AT, Gómez-Laverde M (2003) Using niche-based GIS modeling to test geographic predictions of competitive exclusion and competitive release in South American pocket mice. *Oikos* **98**, 3-16.
- Araujo MB, Luoto M (2007) The importance of biotic interactions for modelling species distributions under climate change. *Global Ecology and Biogeography* **16**, 743-753.
- Ashworth VETM (2000) Phylogenetic relationships in phoradendreae (Viscaceae) inferred from three regions of the nuclear ribosomal cistron. I. Major lineages and paraphyly of phoradendron. *Systematic Botany* **25**, 349-370.
- Aukema JE (2003) Vectors, viscin, and Viscaceae: Mistletoes as parasites, mutualists, and resources. *Frontiers in Ecology* **1**, 212-219.
- Aukema JE, Martínez del Rio C (2002a) Where does a fruit-eating bird deposit mistletoe seeds? Seed deposition patterns and an experiment. *Ecology* **83**, 3489-3496.

- Aukema JE, Martínez del Rio C. (2002b) Variation in mistletoe seed deposition: Effects of intra- and interspecific host characteristics. *Ecography* **25**, 139-144.
- Aukema JE (2001) *Dispersal and spatial distribution of the desert mistletoe, Phoradendron californicum, at multiple scales: Patterns, processes and mechanisms*. Ph.D. Thesis University of Arizona, Tucson, AZ.
- Aukema JE (2004) Distribution and dispersal of desert mistletoes is scale-dependent, hierarchically nested. *Ecography* **27**, 137-144.
- Baatz M, Benz U, Dehghani S, Heynen M, Höltje A, Hofmann P, Lingenfelder I, Mimler M, Sohlbach M, Weber M, Willhauck G (2003) *eCognition 3 user guide*. Definiens Imaging, Munich, Germany.
- Baele G, Lemey P, Bedford T, Rambaut A, Suchard MA, Alekseyenko AV (2012) Improving the accuracy of demographic and molecular clock model comparison while accommodating phylogenetic uncertainty. *Molecular Biology and Evolution* **29**, 2157-2167.
- Barrera-Guzmán AO, Mila B, Sánchez-González LA, Navarro-Sigüenza AG (2012) Speciation in an avian complex endemic to the mountains of Middle America (*Ergaticus*, Ayes: Parulidae). *Molecular Phylogenetics and Evolution* **62**, 907-920.
- Barve N, Barve V, Jiménez-Valverde A, Lira-Noriega A, Maher SP, Peterson AT, Soberón J, Villalobos F (2011) The crucial role of the accessible area in ecological niche modeling and species distribution modeling. *Ecological Modelling* **222**, 1810-1819.
- Begon M, Townsend CR, Harper JL (2006) *Ecology: From individuals to ecosystems*, 4th edn. Blackwell Publishing, Oxford, UK.
- Borenstein M, Hedges LV, Higgins JPT, Rothstein HR (2009) *Introduction to meta-analysis*. John Wiley and Sons, Chichester, UK.
- Bozinovic F, Calosi P, Spicer JJ. 2011. Physiological correlates of geographic range in animals. *Annual Review of Ecology, Evolution and Systematics* **42**, 155-179.
- Bridle JR, Vines TH (2007) Limits to evolution at range margins: When and why does adaptation fail? *Trends in Ecology and Evolution* **22**, 140-147.
- Bromham L, Cowman P, Lanfear R (2013) Parasitic plants have increased rates of molecular evolution across all three genomes. *BMC Evolutionary Biology* **13**, 126.
- Brotens L, De Caceres M, Fall A, Fortin MJ (2012) Modeling bird species distribution change in fire prone Mediterranean landscapes: Incorporating species dispersal and landscape dynamics. *Ecography* **35**, 458-467.
- Brown JH (1984) On the relationship between abundance and distribution of species. *American Naturalist* **124**, 255-279.

- Brown JH, Stevens GC, Kaufman DM (1996) The geographic range: Size, shape, boundaries, and internal structure. *Annual Review of Ecology and Systematics* **27**, 597-623.
- Brussard PF (1984) Geographic patterns and environmental gradients—the central–marginal model in *Drosophila* revisited. *Annual Review of Ecology and Systematics* **15**, 25-64.
- Buckley LB, Urban MC, Angilletta MJ, Crozier LG, Rissler LJ, Sears MW (2010) Can mechanism inform species' distribution models? *Ecology Letters* **13**, 1041-1054.
- Cabral JS, Schurr FM (2010) Estimating demographic models for the range dynamics of plant species. *Global Ecology and Biogeography* **19**, 85-97.
- Cain ML, Milligan BG, Strand AE (2000) Long-distance seed dispersal in plant populations. *American Journal of Botany* **87**, 1217-1227.
- Callaway RM, Reinhart KO, Moore GW, Moore DJ, Pennings SC (2002) Epiphyte host preferences and host traits: Mechanisms for species-specific interactions. *Oecologia* **132**, 221-230.
- Carlo TA, Morales JM (2008) Inequalities in fruit-removal and seed dispersal: Consequences of bird behaviour, neighbourhood density and landscape aggregation. *Journal of Ecology* **96**, 609-618.
- Carnaval AC, Hickerson MJ, Haddad CFB, Rodrigues MT, Moritz C (2009) Stability predicts genetic diversity in the Brazilian Atlantic forest hotspot. *Science* **323**, 785-789.
- Chapman AD (2005) Principles and methods of data cleaning—primary species and species-occurrence data, version 1.0. Global Biodiversity Information Facility, Copenhagen.
- Chapman JR, Nakagawa S, Coltman DW, Slate J, Sheldon BC (2009) A quantitative review of heterozygosity-fitness correlations in animal populations. *Molecular Ecology* **18**, 2746-2765.
- Chu M, Walsberg GE (1999) Phainopepla (*Phainopepla nitens*). The birds of North America, No. 415 (ed. by A. Poole & F. Gill). Birds of North America Inc., Philadelphia, PA.
- Clark-Tapia R, Molina-Freaner F (2003) The genetic structure of a columnar cactus with a disjunct distribution: *Stenocereus gummosus* in the Sonoran desert. *Heredity* **90**, 443-450.
- Clay K, Dement D, Rejmanek M (1985) Experimental evidence for host races in mistletoe (*Phoradendron tomentosum*). *American Journal of Botany* **72**, 1225-1231.
- Collins WD, Bitz CM, Blackmon ML, Bonan GB, Bretherton CS, Carton JA, Chang P, Doney SC, Hack JJ, Henderson TB, Kiehl JT, Large WG, McKenna DS, Santer BD, Smith RD

- (2006) The Community Climate System Model version 3 (CCSM3). *Journal of Climate* **19**, 2122-2143.
- Comes HP, Kadereit JW (1998) The effect of quaternary climatic changes on plant distribution and evolution. *Trends in Plant Science* **3**, 432-438.
- Cook RD (1977) Detection of influential observation in linear–regression. *Technometrics* **19**, 15-18.
- Cortes-Rodriguez N, Hernandez-Baños BE, Navarro-Siguenza AG, Peterson AT, Garcia-Moreno J (2008) Phylogeography and population genetics of the Amethyst-throated Hummingbird (*Lampornis amethystinus*). *Molecular Phylogenetics and Evolution* **48**, 1-11.
- Cowles RB (1936) The relation of birds to seed dispersal of the desert mistletoe. *Madroño* **3**, 352-356.
- Cunningham HR, Rissler LJ, Apodaca JJ (2009) Competition at the range boundary in the slimy salamander: Using reciprocal transplants for studies on the role of biotic interactions in spatial distributions. *Journal of Animal Ecology*, **78**, 52-62.
- de Souza Muñoz M, de Giovanni R, de Siqueira M, Sutton T, Brewer P, Pereira R, Canhos D, Canhos V (2011) openModeller: A generic approach to species' potential distribution modelling. *Geoinformatica* **15**, 111-135.
- Dimmit MA (2000) Biomes and communities of the Sonoran Desert region. in S. J. Phillips and P. Wentworth Comus, editors. *A natural history of the Sonoran Desert*. Arizona-Sonora Desert Museum Press and University of California Press, Berkeley and Los Angeles, California.
- Diniz J, Nabout JC, Bini LM, Soares TN, Telles MPD, de Marco P, Collevatti RG (2009) Niche modelling and landscape genetics of *Caryocar brasiliense* ("Pequi" tree: Caryocaraceae) in Brazilian Cerrado: An integrative approach for evaluating central-peripheral population patterns. *Tree Genetics & Genomes* **5**, 617-627.
- Dissanayake STM, Onal H, Westervelt JD, Balbach HE (2012) Incorporating species relocation in reserve design models: An example from Ft. Benning GA. *Ecological Modelling*, **224**, 65-75.
- Doyle JJ, Doyle JD (1987) A rapid DNA isolation procedure for small quantities of fresh leaf tissue. *Phytochemical Bulletin* **19**, 11-15.
- Drummond AJ, Suchard MA, Xie D, Rambaut A (2012) Bayesian Phylogenetics with BEAUti and the BEAST 1.7. *Molecular Biology and Evolution* **29**, 1969-1973.
- Duminil J, Fineschi S, Hampe A, Jordano P, Salvini D, Vendramin GG, Petit RJ (2007) Can population genetic structure be predicted from life-history traits? *American Naturalist* **169**, 662-672.
- Easterling D R, Karl TR, Lawrimore JH, Del Greco SA (1999) United States historical climatology network daily temperature, precipitation, and snow data for 1871-

1997. ORNL/CDIAC-118, NDP-070. Carbon Dioxide Information Analysis Center, Oak Ridge National Laboratory, U.S. Department of Energy, Oak Ridge, Tennessee.
- Eckert CG, Samis KE, Loughheed SC (2008) Genetic variation across species' geographical ranges: The central-marginal hypothesis and beyond. *Molecular Ecology* **17**, 1170-1188.
- Edgar RC (2004) MUSCLE: Multiple sequence alignment with high accuracy and high throughput. *Nucleic Acids Research* **32**, 1792-1797.
- Ehrich D, Alsos IG, Brochmann C (2008) Where did the northern peatland species survive the dry glacials: Cloudberry (*Rubus chamaemorus*) as an example. *Journal of Biogeography* **35**, 801-814.
- Eidesen PB, Alsos IG, Popp M, Stensrud O, Suda J, Brochmann C (2007) Nuclear vs. plastid data: Complex Pleistocene history of a circumpolar key species. *Molecular Ecology* **16**, 3902-3925.
- Eidesen PB, Carlsen T, Molau U, Brochmann C (2007) Repeatedly out of Beringia: *Cassiope tetragona* embraces the arctic. *Journal of Biogeography* **34**, 1559-1574.
- Elith J, Graham CH, Anderson RP, Dudik M, Ferrier S, Guisan A, Hijmans RJ, Huettmann F, Leathwick JR, Lehmann A, Li J, Lohmann LG, Loiselle BA, Manion G, Moritz C, Nakamura M, Nakazawa Y, Overton JM, Peterson AT, Phillips SJ, Richardson K, Scachetti-Pereira R, Schapire RE, Soberon J, Williams S, Wisz MS, Zimmermann NE (2006) Novel methods improve prediction of species' distributions from occurrence data. *Ecography* **29**, 129-151.
- ESRI. 2011. ArcGIS Desktop: Release 10. Redlands, California. Environmental Systems Research Institute.
- Esselstyn JA, Evans BJ, Sedlock JL, Khan FAA, Heaney LR (2012) Single-locus species delimitation: A test of the mixed Yule-coalescent model, with an empirical application to Philippine round-leaf bats. *Proceedings of the Royal Society B-Biological Sciences* **279**, 3678-3686.
- Ezard T, Fujisawa T, Barraclough TC (2013) splits: Species' Limits by Threshold Statistics. R package version 1.0-18/45. <http://R-Forge.R-project.org/projects/splits/>.
- Fehlberg SD, Ranker TA (2009) Evolutionary history and phylogeography of *Encelia farinosa* (Asteraceae) from the Sonoran, Mojave, and Peninsular Deserts. *Molecular Phylogenetics and Evolution* **50**, 326-335.
- Fischer G, Nachtergaele F, Prieler S, van Velthuizen HT, Verelst L, Wiberg D (2008) Global agro-ecological zones assessment for agriculture. International Institute for Applied Systems Analysis, Laxenburg, Austria and FAO, Rome, Italy.
- Fortin MJ, Keitt TH, Maurer BA, Taper ML, Kaufman DM, Blackburn TM (2005) Species' geographic ranges and distributional limits: Pattern analysis and statistical issues. *Oikos* **108**, 7-17.

- Fujisawa T, Barraclough TG (2013) Delimiting species using Single-Locus Data and the Generalized Mixed Yule Coalescent Approach: A revised method and evaluation on simulated data sets. *Systematic Biology* **62**, 707-724.
- Galbreath KE, Cook JA (2004) Genetic consequences of Pleistocene glaciations for the tundra vole (*Microtus oeconomus*) in Beringia. *Molecular Ecology* **13**, 135-148.
- Galbreath KE, Cook JA, Eddingsaas AA, DeChaine EG. 2011. Diversity and demography in Beringia: Multilocus tests of paleodistribution models reveal the complex history of Arctic ground squirrels. *Evolution* **65**, 1879-1896.
- Gao QB, Zhang DJ, Duan YZ, Zhang FQ, Li YH, Fu PC, Chen SL (2012) Intraspecific divergences of *Rhodiola alsia* (Crassulaceae) based on plastid DNA and internal transcribed spacer fragments. *Botanical Journal of the Linnean Society* **168**, 204-215.
- Garcia D, Rodriguez-Cabal MA, Amico GC (2009) Seed dispersal by a frugivorous marsupial shapes the spatial scale of a mistletoe population. *Journal of Ecology* **97**, 217-229.
- Garcillán PP, Ezcurra E (2003) Biogeographic regions and β -diversity of woody dryland legumes in the Baja California peninsula. *Journal of Vegetation Science* **14**, 859-868.
- Garner TWJ, Pearman PB, Angelone S (2004) Genetic diversity across a vertebrate species' range: A test of the central-peripheral hypothesis. *Molecular Ecology* **13**, 1047-1053.
- Garrick RC, Nason JD, Meadows CA, Dyer RJ (2009) Not just vicariance: Phylogeography of a Sonoran Desert euphorb indicates a major role of range expansion along the Baja peninsula. *Molecular Ecology* **18**, 1916-1931.
- Gaston KJ (2003) *The structure and dynamics of geographic ranges*. Oxford University Press, Oxford, UK.
- Gaston KJ, Genney DR, Thurlow M, Hartley SE (2004) The geographical range structure of the holly leaf-miner. IV. Effects of variation in host-plant quality. *Journal of Animal Ecology* **73**, 911-924.
- Genini J, Côrtes MC, Guimarães PR, Galetti M (2012) Mistletoes play different roles in a modular host-parasite network. *Biotropica* **44**, 171-178.
- Glazner JT, Devlin B, Ellstrand NC (1988) Biochemical and morphological evidence for host race evolution in Desert Mistletoe, *Phoradendron californicum* (Viscaceae). *Plant Systematics and Evolution* **161**, 13-21.
- Grismer L (2002) A re-evaluation of the evidence for a mid-Pleistocene mid-peninsular seaway in Baja California: A reply to Riddle et al. *Herpetological Review* **33**, 15-16.

- Grummer JA, Bryson RW, Reeder TW (2013) Species delimitation using Bayes factors: Simulations and application to the *Sceloporus scalaris* species group (Squamata: Phrynosomatidae). *Systematic Biology* **62**, 1069-1089.
- Grus WE, Graves GR, Glenn TC (2009) Geographic variation in the mitochondrial control region of Black-throated Blue Warblers (*Dendroica caerulescens*). *Auk* **126**, 198-210.
- Guisan A, Zimmermann NE (2000) Predictive habitat distribution models in ecology. *Ecological Modelling* **135**, 147-186.
- Hafner DJ, Riddle BR (2011) Boundaries and barriers of North American warm deserts: An evolutionary perspective. In Upchurch P, McGowan A, Slater C (eds) *Palaeogeography and palaeobiogeography: Biodiversity in space and time*. CRC Press.
- Hagen A (2003) Fuzzy set approach to assessing similarity of categorical maps. *International Journal of Geographical Information Science* **17**, 235-249.
- Haigh SL (1996) Saltcedar (*Tamarix ramosissima*), an uncommon host for desert mistletoe (*Phoradendron californicum*). *Great Basin Naturalist* **56**, 186-187.
- Haldane JBS (1956) The Relation between density regulation and natural selection. *Proceedings of the Royal Society Series B-Biological Sciences* **145**, 306-308.
- Hastings A, Petrovskii S, Morozov A (2011) Spatial ecology across scales. *Biology Letters* **7**, 163-165.
- Hasumi H, Emori S (2004) K-1 coupled gcm (miroc) description. Center for Climate System Research, University of Tokyo, Tokyo.
- Heibl C, Calenge C (2013) phyloclim: Integrating phylogenetics and climatic niche modeling. R package version 0.9-3. Available at: <http://cran.r-project.org/web/packages/phyloclim>.
- Heikkinen RK, Luoto M, Virkkala R, Pearson RG, Korber JH (2007) Biotic interactions improve prediction of boreal bird distributions at macro-scales. *Global Ecology and Biogeography* **16**, 754-763.
- Hengeveld R, Haack J (1982) The distribution of abundance. I. Measurements. *Journal of Biogeography* **9**, 303-316.
- Hijmans RJ, Cameron SE, Parra JL, Jones PG, Jarvis A (2005) Very high resolution interpolated climate surfaces for global land areas. *International Journal of Climatology* **25**, 1965-1978.
- Holt RD (2003) On the evolutionary ecology of species' ranges. *Evolutionary Ecology Research* **5**, 159-178.

- Holt RD, Gomulkiewicz R (1997) The evolution of species' niches: A population dynamic perspective. In Othmer H, Adler F, Lewis M, Dallon J (eds) *Case studies in mathematical modelling: Ecology, physiology, and cell biology*, pp. 25-50. Prentice-Hall, Englewood Cliffs, New Jersey.
- Holt RD, Keitt TH (2005) Species' borders: A unifying theme in ecology. *Oikos* **108**, 3-6.
- Homer CCH, Yang L, Wylie B, Coan M (2004) Development of a 2001 National Landcover Database for the United States. *Photogrammetric Engineering and Remote Sensing* **70**, 829-840.
- Hutchinson GE (1957) Population Studies - Animal Ecology and Demography - Concluding Remarks. *Cold Spring Harbor Symposia on Quantitative Biology* **22**, 415-427.
- Hutchinson GE (1978) *An introduction to population ecology*. Yale University Press, New Haven, USA.
- Jackson ST, Overpeck JT (2000) Responses of plant populations and communities to environmental changes of the late Quaternary. *Paleobiology* **26**, 194-220.
- James FC, Johnston RF, Wamer NO, Niemi GJ, Boecklen WJ (1984) The Grinnellian niche of the Wood Thrush. *American Naturalist* **124**, 17-30.
- Jerome CA, Ford BA (2002) The discovery of three genetic races of the dwarf mistletoe *Arceuthobium americanum* (Viscaceae) provides insight into the evolution of parasitic angiosperms. *Molecular Ecology* **11**, 387-405.
- Joly S, Stevens MI, van Vuuren BJ (2007) Haplotype networks can be misleading in the presence of missing data. *Systematic Biology* **56**, 857-862.
- Kass RE, Raftery AE (1995) Bayes factors. *Journal of the American Statistical Association* **90**, 773-795.
- Kavanagh PH, Burns KC (2012) Mistletoe macroecology: Spatial patterns in species diversity and host use across Australia. *Biological Journal of the Linnean Society* **106**, 459-468.
- Kawecki TJ (2008) Adaptation to marginal habitats. *Annual Review of Ecology and Systematics* **39**, 321-342.
- Kearney M, Porter W (2009) Mechanistic niche modelling: Combining physiological and spatial data to predict species' ranges. *Ecology Letters* **12**, 334-350.
- Kearney M, Wintle BA, Porter W (2010) Correlative and mechanistic models of species distribution provide congruent forecasts under climate change. *Conservation Letters* **3**, 203-213.

- Keller SR, Olson MS, Silim S, Schroeder W, Tiffin P (2010) Genomic diversity, population structure, and migration following rapid range expansion in the Balsam Poplar, *Populus balsamifera*. *Molecular Ecology* **19**, 1212-1226.
- Kimura M, Clegg SM, Lovette IJ, Holder KR, Girman DJ, Mila B, Wade P, Smith TB (2002) Phylogeographical approaches to assessing demographic connectivity between breeding and overwintering regions in a Nearctic-Neotropical warbler (*Wilsonia pusilla*). *Molecular Ecology* **11**, 1605-1616.
- Kuijt, J. (2003) Monograph of *Phoradendron* (Viscaceae). *Systematic Botany Monographs* **66**, 1-643.
- Lack JB, Pfau RS, Wilson GM (2010) Demographic history and incomplete lineage sorting obscure population genetic structure of the Texas mouse (*Peromyscus attwateri*). *Journal of Mammalogy* **91**, 314-325.
- Laliberte AS, Rango A, Havstad KM, Paris JF, Beck RF, McNeely R, Gonzalez AL (2004) Object-oriented image analysis for mapping shrub encroachment from 1937 to 2003 in southern New Mexico. *Remote Sensing of Environment* **93**, 198-210.
- Larson DL (1996) Seed dispersal by specialist versus generalist foragers: The plant's perspective. *Oikos* **76**, 113-120.
- Lavorel S, Stafford Smith MS, Reid N (1999) Spread of mistletoes (*Amyema preissii*) in fragmented Australian woodlands: A simulation study. *Landscape ecology* **14**, 147-160.
- Lei SA (1999) Age, size and water status of *Acacia gregii* influencing the infection and reproductive success of *Phoradendron californicum*. *American Midland Naturalist* **141**, 358-365.
- Leimu R, Mutikainen P, Koricheva J, Fischer M (2006) How general are positive relationships between plant population size, fitness, and genetic variation? *Journal of Ecology* **94**, 942-952.
- Lemieux CJ, Beechey TJ, Scott DJ, Gray PA (2011) The state of climate change adaptation in Canada's protected areas sector. *Canadian Geographer* **55**, 301-317.
- Levin SA (1992) The problem of pattern and scale in ecology. *Ecology* **73**, 1943-1967.
- Levin SA, Pacala SW (1997) Theories of simplification and scaling of spatially distributed species. Pages 271-295 in Tilman D, Kareiva P, editors. *Spatial ecology: The role of space in population dynamics and interspecific interactions*. Princeton University Press, Princeton, New Jersey, USA.
- Li XC, Yin H, Li K, Gao XY (2012) Population genetic structure and historical demography of the ground beetle *Pheropsophus jessoensis* from the Tsinling–Dabashan

- Mountains, central China based on mitochondrial DNA analysis. *Zoological Science* **29**, 238-246.
- Liaw A, Wiener M (2002) Classification and regression by randomForest. *R News* **2**, 18--22.
- Lindell J, Ngo A, Murphy RW (2006) Deep genealogies and the mid-peninsular seaway of Baja California. *Journal of Biogeography* **33**, 1327-1331.
- Lira-Noriega A, Manthey JD (2014) Relationship of genetic diversity and niche centrality: A survey and analysis. *Evolution* doi:10.1111/evo.12343.
- Lira-Noriega A, Peterson AT (In press) Range-wide ecological niche comparisons of parasite, hosts and dispersers in a vector-borne plant parasite system. *Journal of Biogeography*.
- Lira-Noriega A, Soberón J, Miller CP (2013) Process-based and correlative modeling of desert mistletoe distribution: A multiscalar approach. *Ecosphere* **4**, art99.
- Liu CR, Berry PM, Dawson TP, Pearson RG (2005) Selecting thresholds of occurrence in the prediction of species distributions. *Ecography* **28**, 385-393.
- Liu RS, Martínez del Rio C, Wu JH (2011) Spatiotemporal variation of mistletoes: A dynamic modeling approach. *Bulletin of Mathematical Biology* **73**, 1794-1811.
- Loveless MD, Hamrick JL (1984) Ecological determinants of genetic-structure in plant-populations. *Annual Review of Ecology and Systematics* **15**, 65-95.
- Lozier JD, Strange JP, Stewart IJ, Cameron SA (2011) Patterns of range-wide genetic variation in six North American bumble bee (Apidae: *Bombus*) species. *Molecular Ecology* **20**, 4870-4888.
- MacArthur RH (1972) *Geographical ecology: Patterns in the distribution of species*. Harper and Row, New York, USA.
- Mackey BG, Lindenmayer DB (2001) Towards a hierarchical framework for modelling the spatial distribution of animals. *Journal of Biogeography* **28**, 1147-1166.
- Maher SP, Ellis C, Gage KL, Ensore RE, Peterson AT (2010) Range-wide determinants of plague distribution in North America. *American Journal of Tropical Medicine and Hygiene* **83**, 736-742.
- Manthey JD, Klicka J, Spellman GM (2011) Cryptic diversity in a widespread North American songbird: Phylogeography of the Brown Creeper (*Certhia americana*). *Molecular Phylogenetics and Evolution* **58**, 502-512.
- Marquardt ES, Pennings SC (2010) Constraints on host use by a parasitic plant. *Oecologia*, **164**, 177-184.

- Martínez del Rio C, Silva A, Medel R, Hourdequin M (1996) Seed dispersers as disease vectors: Bird transmission of mistletoe seeds to plant hosts. *Ecology* **77**, 912-921.
- Martínez-Meyer E, Díaz-Porras D, Peterson AT, Yáñez-Arenas C (2013) Ecological niche structure and rangewide abundance patterns of species. *Biology Letters* **9**, 20120637.
- Mathiasen RL, Nickrent DL, Shaw DC, Watson DM (2008) Mistletoes: Pathology, systematics, ecology and management. *Plant Disease* **92**, 988-1006.
- McAuliffe JR, McDonald EV (2006) Holocene environmental change and vegetation contraction in the Sonoran Desert. *Quaternary Research* **65**, 204-215.
- McAuliffe JR, Van Devender TR (1998) A 22,000-year record of vegetation change in the north-central Sonoran Desert. *Palaeogeography Palaeoclimatology Palaeoecology* **141**, 253-275.
- McDonald DE, Daniels SR (2012) Phylogeography of the Cape velvet worm (Onychophora: *Peripatopsis capensis*) reveals the impact of Pliocene/Pleistocene climatic oscillations on Afromontane forest in the Western Cape, South Africa. *Journal of Evolutionary Biology* **25**, 824-835.
- Moeller DA, Geber MA, Tiffin P (2011) Population genetics and the evolution of geographic range limits in an annual plant. *American Naturalist* **178**, S44-S61.
- Monahan WB (2009) A mechanistic niche model for measuring species' distributional responses to seasonal temperature gradients. *PloS ONE* **4**:e7921.
- Montaño-Centellas FA (2013) Effectiveness of mistletoe seed dispersal by tyrant flycatchers in a mixed Andean landscape. *Biotropica* **45**, 209-216.
- Morand S, Krasnov BR (eds) (2010) *The biogeography of host-parasite interactions*. Oxford University Press, New York.
- Morin X, Thuiller W (2009) Comparing niche- and process-based models to reduce prediction uncertainty in species range shifts under climate change. *Ecology* **90**, 1301-1313.
- Mort ME, Soltis DE, Soltis PS, Francisco-Ortega J, Santos-Guerra A (2001) Phylogenetic relationships and evolution of Crassulaceae inferred from matK sequence data. *American Journal of Botany* **88**, 76-91.
- Munguia-Vega A (2011) *Habitat fragmentation in small vertebrates from the Sonoran Desert in Baja California*. The University of Arizona.
- Murphy RW, Aguirre-León G (2002) The nonavian reptiles: Origins and evolution. In Case TJ, Cody ML, Ezcurra E (eds) *A new island biogeography of the Sea of Cortéz*, pp. 181-220. Oxford University Press, New York.

- Murphy SR, Reid N, Yan ZG, Venables WN (1993) Differential passage time of mistletoe fruits through the gut of honeyeaters and flowerpeckers: Effects on seedling establishment. *Oecologia* **93**, 171-176.
- Nason JD, Hamrick JL, Fleming TH (2002) Historical vicariance and postglacial colonization effects on the evolution of genetic structure in *Lophocereus*, a Sonoran Desert columnar cactus. *Evolution* **56**, 2214-2226.
- Nathan R (2006) Long-distance dispersal of plants. *Science* **313**, 786-788.
- Nickrent DL (2002) Mistletoe phylogenetics: Current relationships gained from analysis of DNA sequences. *Proceedings of the forty-eighth western international forest disease work conference*, 48-57.
- Nickrent DL, Stell AL (1990) Electrophoretic evidence for genetic differentiation in two host races of hemlock dwarf mistletoe (*Arceuthobium tsugense*). *Biochemical Systematics and Ecology* **18**, 267-280.
- Norton DA, Smith MS (1999) Why might roadside mulgas be better mistletoe hosts? *Australian Journal of Ecology* **24**, 193-198.
- Norton DA, Ladley JJ, Owen HJ (1997) Distribution and population structure of the loranthaceous mistletoes *Alepis flavida*, *Peraxilla colensoi*, and *Peraxilla tetrapetala* within two New Zealand Nothofagus forests. *New Zealand Journal of Botany*, 35, 323-336.
- Nylander JAA, Wilgenbusch JC, Warren DL, Swofford DL (2008) AWTY (are we there yet?): A system for graphical exploration of MCMC convergence in Bayesian phylogenetics. *Bioinformatics* **24**, 581-583.
- Olson DM, Dinerstein E, Wikramanayake ED, Burgess ND, Powell GVN, Underwood EC, D'Amico JA, Itoua I, Strand HE, Morrison JC, Loucks CJ, Allnutt TF, Ricketts TH, Kura Y, Lamoreux JF, Wettengel, WW, Hedao P, Kassem KR (2001) Terrestrial ecoregions of the world: A new map of life on Earth. *BioScience* **51**, 933-938.
- Oomen RA, Reudink MW, Nocera JJ, Somers CM, Green MC, Kyle CJ (2011) Mitochondrial evidence for panmixia despite perceived barriers to gene flow in a widely distributed waterbird. *Journal of Heredity* **102**, 584-+.
- Ortego J, Riordan EC, Gugger PF, Sork VL (2012) Influence of environmental heterogeneity on genetic diversity and structure in an endemic southern Californian oak. *Molecular Ecology* **21**, 3210-3223.
- Overton JM (1997) Host specialization and partial reproductive isolation in desert mistletoe (*Phoradendron californicum*). *Southwestern Naturalist* **42**, 201-209.
- Overton JM (1994) Dispersal and infection in mistletoe metapopulations. *Journal of Ecology* **82**, 711-723.

- Overton JM (1996) Spatial autocorrelation and dispersal in mistletoes: Field and simulation results. *Vegetatio* **125**, 83-98.
- Paul JR, Sheth SN, Angert AL (2011) Quantifying the impact of gene flow on phenotype-environment mismatch: A demonstration with the scarlet monkeyflower *Mimulus cardinalis*. *American Naturalist* **178**, S62-S79.
- Pearson RG, Dawson TP (2003) Predicting the impacts of climate change on the distribution of species: Are bioclimate envelope models useful? *Global Ecology and Biogeography* **12**, 361-371.
- Pearson RG, Raxworthy CJ, Nakamura M, Peterson AT (2007) Predicting species distributions from small numbers of occurrence records: A test case using cryptic geckos in Madagascar. *Journal of Biogeography* **34**, 102-117.
- Pérez-Alquicira J, Molina-Freaner FE, Piñero D, Weller SG, Martínez-Meyer E, Rozas J, Domínguez CA (2010) The role of historical factors and natural selection in the evolution of breeding systems of *Oxalis alpina* in the Sonoran desert 'Sky Islands'. *Journal of Evolutionary Biology* **23**, 2163-2175.
- Peterson AT, Soberón J, Pearson RG, Anderson RP, Martínez-Meyer E, Nakamura M, and Araújo MB. (2011) *Ecological niches and geographic distributions* Princeton University Press, Princeton, New Jersey, USA.
- Peterson AT, Papeş M, Soberón J (2008) Rethinking receiver operating characteristic analysis applications in ecological niche modeling. *Ecological Modelling* **213**, 63-72.
- Peterson AT, Papeş M, Eaton M. (2007) Transferability and model evaluation in ecological niche modeling: A comparison of GARP and Maxent. *Ecography* **30**, 550-560.
- Pfeifer M, Schatz B, Pico FX, Passalacqua NG, Fay MF, Carey PD, Jeltsch F (2009) Phylogeography and genetic structure of the orchid *Himantoglossum hircinum* (L.) Spreng. across its European central-marginal gradient. *Journal of Biogeography* **36**, 2353-2365.
- Phillips SJ, Anderson RP, Schapire RE (2006) Maximum entropy modeling of species geographic distributions. *Ecological Modelling* **190**, 231-259.
- Pons J, Barraclough TG, Gomez-Zurita J, Cardoso A, Duran DP, Hazell S, Kamoun S, Sumlin WD, Vogler AP (2006) Sequence-based species delimitation for the DNA taxonomy of undescribed insects. *Systematic Biology* **55**, 595-609.
- Primack R (2006) *Essentials of conservation biology*. Sinauer, Sunderland, Massachusetts.
- Pulliam HR (1988) Sources, sinks, and population regulation. *American Naturalist* **132**, 652-661.

- Pulliam HR (2000) On the relationship between niche and distribution. *Ecology Letters* **3**:349-361.
- R Development Core Team (2013) R: A language and environment for statistical computing. R Foundation for Statistical Computing, Vienna, Austria: R Foundation for Statistical Computing.
- R Development Core Team (2011) R: A language and environment for statistical computing. R Foundation for Statistical Computing, Vienna, Austria: R Foundation for Statistical Computing.
- R Development Core Team (2012) A language and environment for statistical computing. R Foundation for Statistical Computing, Vienna, Austria: R Foundation for Statistical Computing.
- Rambaut A, Drummond A (2007) Tracer v 1.5. Available from <http://beast.bio.ed.ac.uk/Tracer>.
- Ramos ACS, Lemos-Filho JP, Ribeiro RA, Santos FR, Lovato MB (2007) Phylogeography of the tree *Hymenaea stigonocarpa* (Fabaceae : Caesalpinioideae) and the influence of quaternary climate changes in the Brazilian cerrado. *Annals of Botany* **100**, 1219-1228.
- Rangel TF, Diniz-Filho JAF, Bini LM (2010) SAM: A comprehensive application for spatial analysis in macroecology. *Ecography* **33**, 6-50.
- Rapoport EH (1982) *Areography: Geographical strategies of species*. Pergamon Press, Oxford.
- Rawsthorne J, Watson DM, Roshier DA (2012) The restricted seed rain of a mistletoe specialist. *Journal of Avian Biology* **43**, 9-14.
- Real R, Barbosa AM, Rodriguez A, Garcia FJ, Vargas JM, Palomo LJ, Delibes M (2009) Conservation biogeography of ecologically interacting species: The case of the Iberian lynx and the European rabbit. *Diversity and Distributions* **15**, 390-400.
- Rebernick CA, Schneeweiss GM, Bardy KE, Schonswetter P, Villaseñor JL, Obermayer R, Stuessy TF, Weiss-Schneeweiss, H (2010) Multiple Pleistocene refugia and Holocene range expansion of an abundant southwestern American desert plant species (*Melampodium leucanthum*, Asteraceae). *Molecular Ecology* **19**, 3421-3443.
- Reding DM, Bronikowski AM, Johnson WE, Clark WR (2012) Pleistocene and ecological effects on continental-scale genetic differentiation in the bobcat (*Lynx rufus*). *Molecular Ecology* **21**, 3078-3093.
- Reed DH, Frankham R (2003) Correlation between fitness and genetic diversity. *Conservation Biology* **17**, 230-237.

- Reid NM, Carstens BC (2012) Phylogenetic estimation error can decrease the accuracy of species delimitation: A Bayesian implementation of the general mixed Yule-coalescent model. *BMC Evolutionary Biology* **12**, 196.
- Reid N (1991) Coevolution of mistletoes and frugivorous birds. *Australian Journal of Ecology* **16**, 457-469.
- Ribeiro RA, Lemos JP, Ramos ACS, Lovato MB (2011) Phylogeography of the endangered rosewood *Dalbergia nigra* (Fabaceae): Insights into the evolutionary history and conservation of the Brazilian Atlantic Forest. *Heredity* **106**, 46-57.
- Riddle B, Hafner D, Alexander L, Jaeger J (2000) Cryptic vicariance in the historical assembly of a Baja California peninsular desert biota. *Proceedings of the National Academy of Sciences of the United States of America* **97**, 14438-14443.
- Riddle BR, Hafner DJ (2006) A step-wise approach to integrating phylogeographic and phylogenetic biogeographic perspectives on the history of a core North American warm deserts biota. *Journal of Arid Environments* **66**, 435-461.
- Rist L, Uma Shaanker R, Ghazoul J (2011) The spatial distribution of mistletoe in a southern Indian tropical forest at multiple scales. *Biotropica* **43**, 50-57.
- Roberts DR, Hamann A (2012) Predicting potential climate change impacts with bioclimate envelope models: A palaeoecological perspective. *Global Ecology and Biogeography* **21**, 121-133.
- Robertson MP, Peter CI, Villet MH, Ripley BS (2003) Comparing models for predicting species' potential distributions: A case study using correlative and mechanistic predictive modelling techniques. *Ecological Modelling* **164**, 153-167.
- Sagarin RD, Gaines SD (2002) The 'abundant centre' distribution: To what extent is it a biogeographical rule? *Ecology Letters* **5**, 137-147.
- Sauer JR, Hines JE, Fallon J, Pardieck KL, Ziolkowski Jr DJ, Link WA (2011) The North American Breeding Bird Survey, Results and Analysis 1966-2010. Version 12.07.2011. USGS Patuxent Wildlife Research Center, Laurel, Maryland.
- Schaal BA, Hayworth DA, Olsen KM, Rauscher JT, Smith WA (1998) Phylogeographic studies in plants: Problems and prospects. *Molecular Ecology* **7**, 465-474.
- Schurr FM, Pagel J, Cabral JS, Groeneveld J, Bykova O, O'Hara RB, Hartig F, Kissling WD, Linder HP, Midgley GF, Schroder B, Singer A, Zimmermann NE (2012) How to understand species' niches and range dynamics: A demographic research agenda for biogeography. *Journal of Biogeography* **39**, 2146-2162.
- Segovia RA, Pérez MF, Hinojosa LF (2012) Genetic evidence for glacial refugia of the temperate tree *Eucryphia cordifolia* (Cunoniaceae) in southern South America. *American Journal of Botany* **99**, 121-129.

- Sexton JP, McIntyre PJ, Angert AL, Rice KJ (2009) Evolution and ecology of species range limits. *Annual Review of Ecology Evolution and Systematics* **40**, 415-436.
- Sgariglia EA, Burns KJ (2003) Phylogeography of the California Thrasher (*Toxostoma redivivum*) based on nested-clade analysis of mitochondrial-DNA variation. *Auk* **120**, 346-361.
- Shaw J, Lickey EB, Schilling EE, Small RL (2007) Comparison of whole chloroplast genome sequences to choose noncoding regions for phylogenetic studies in angiosperms: The tortoise and the hare III. *American Journal of Botany* **94**, 275-288.
- Shreve F (1951) *Vegetation of the Sonoran Desert*. Publ. Carnegie Inst. Washington No. 591. Reprinted as vol. 1, Shreve F, Wiggins IL *Vegetation and flora of the Sonoran Desert*. Stanford University Press, Stanford, CA.
- Smith BT, Escalante P, Banos BEH, Navarro-Sigüenza AG, Rohwer S, Klicka J (2011) The role of historical and contemporary processes on phylogeographic structure and genetic diversity in the Northern Cardinal, *Cardinalis cardinalis*. *BMC Evolutionary Biology* **11**.
- Soberón J (2007) Grinnellian and Eltonian niches and geographic distributions of species. *Ecology Letters* **10**, 1115-1123.
- Soberón JM (2010) Niche and area of distribution modeling: A population ecology perspective. *Ecography* **33**, 159-167.
- Soberón J, Nakamura M (2009) Niches and distributional areas: Concepts, methods, and assumptions. *Proceedings of the National Academy of Sciences of the United States of America* **106**, 19644-19650.
- Soberón J, Peterson AT (2005) Interpretation of models of fundamental ecological niches and species' distributional areas. *Biodiversity Informatics* **2**, 1-10.
- Spellman GM, Klicka J (2006) Testing hypotheses of Pleistocene population history using coalescent simulations: Phylogeography of the pygmy nuthatch (*Sitta pygmaea*). *Proceedings of the Royal Society B-Biological Sciences* **273**, 3057-3063.
- Spellman GM, Klicka J (2007) Phylogeography of the white-breasted nuthatch (*Sitta carolinensis*): Diversification in North American pine and oak woodlands. *Molecular Ecology* **16** 1729-1740.
- Spellman GM, Riddle B, Klicka J (2007) Phylogeography of the mountain chickadee (*Poecile gambeli*): Diversification, introgression, and expansion in response to Quaternary climate change. *Molecular Ecology* **16** 1055-1068.
- Stanton S, Honnay O, Jacquemyn H, Roldan-Ruiz I (2009) A comparison of the population genetic structure of parasitic *Viscum album* from two landscapes differing in degree of fragmentation. *Plant Systematics and Evolution* **281**, 161-169.
- Swofford DL (2003) PAUP* Phylogenetic analysis using parsimony (*and other methods). Version 4. Sinauer Associates.

- Templeton AR, Crandall KA, Sing CF (1992) A Cladistic-Analysis of Phenotypic Associations with Haplotypes Inferred from Restriction Endonuclease Mapping and DNA-Sequence Data .3. Cladogram Estimation. *Genetics* **132**, 619-633.
- Temunovic M, Franjic J, Satovic Z, Grgurev M, Frascaria-Lacoste N, Fernandez-Manjarre JF (2012) Environmental heterogeneity explains the genetic structure of continental and Mediterranean populations of *Fraxinus angustifolia* Vahl. *Plos One*, **7**
- Thuiller W, Albert CH, Dubuis A, Randin C, Guisan A (2010) Variation in habitat suitability does not always relate to variation in species' plant functional traits. *Biology Letters* **6**, 120-123.
- Torres NM, De Marco P, Santos T, Silveira L, Jacomo ATD, Diniz JAF (2012) Can species distribution modelling provide estimates of population densities? A case study with jaguars in the Neotropics. *Diversity and Distributions* **18**, 615-627.
- Udvardy MDF (1969) *Dynamic zoogeography*. Van Nostrand Reinhold Company, New York.
- Van Devender TR (1990a) Late Quaternary vegetation and climate of the Chihuahuan Desert, United States and Mexico. In Betancourt JL, Van Devender TR, Martin PS (eds) *Pacrat middens: The last 40,000 years of biotic change*, pp. 104-133. The University of Arizona Press, Tucson, AZ.
- Van Devender TR (1990b) Late Quaternary vegetation and climate of the Sonoran Desert, United States and Mexico. In Betancourt JL, Van Devender TR, Martin PS (eds) *Pacrat middens: The last 40,000 years of biotic change*, pp. 134-165. The University of Arizona Press, Tucson, AZ.
- Vandermeer JH, Goldberg DE (2003) *Population ecology: First principles*. Princeton University Press, New Jersey, USA.
- VanDerWal J, Shoo LP, Johnson CN, Williams SE (2009) Abundance and the environmental niche: Environmental suitability estimated from niche models predicts the upper limit of local abundance. *American Naturalist* **174**, 282-291.
- Visser H, de Nijs T (2006) The Map Comparison Kit. *Environmental Modelling & Software* **21**, 346-358.
- Vucetich JA, Waite TA (2003) Spatial patterns of demography and genetic processes across the species' range: Null hypotheses for landscape conservation genetics. *Conservation Genetics* **4**, 639-645.
- Wagner V, Durka W, Hensen I (2011) Increased genetic differentiation but no reduced genetic diversity in peripheral vs. central populations of a steppe grass. *American Journal of Botany* **98**, 1173-1179.
- Walsberg GE (1975) Digestive adaptations of *Phainopepla nitens* associated with the eating of mistletoe berries. *Condor* **77**, 169-174.

- Warren DL, Glor RE, Turelli M (2010) ENMTools: A toolbox for comparative studies of environmental niche models. *Ecography* **33**, 607-611.
- Warren DL, Glor RE, Turelli M (2008) Environmental niche equivalency versus conservatism: Quantitative approaches to niche evolution. *Evolution* **62**, 2868-2883.
- Waterhouse AM, Procter JB, Martin DMA, Clamp M, Barton GJ (2009) Jalview Version 2-a multiple sequence alignment editor and analysis workbench. *Bioinformatics* **25**, 1189-1191.
- Watson DM (2001) Mistletoe - a keystone resource in forests and woodlands worldwide. *Annual Review of Ecology and Systematics* **32**, 219-249.
- Watson DM (2009) Determinants of parasitic plant distribution: The role of host quality. *Botany-Botanique* **87**, 16-21.
- Weksler M, Lanier HC, Olson LE (2010) Eastern Beringian biogeography: Historical and spatial genetic structure of singing voles in Alaska. *Journal of Biogeography* **37**, 1414-1431.
- Westergaard KB, Alsos IG, Popp M, Engelskjøn T, Flatberg KI, Brochmann C (2011) Glacial survival may matter after all: Nunatak signatures in the rare European populations of two west-arctic species. *Molecular Ecology* **20**, 376-393.
- Whittaker PL (1984) The insect fauna of mistletoe (*Phoradendron tomentosum*, Loranthaceae) in southern Texas. *The Southwestern Naturalist* **29**, 435-444.
- Whittaker RJ, Willis KJ, Field R (2001) Scale and species richness: Towards a general, hierarchical theory of species diversity. *Journal of Biogeography* **28**, 453-470.
- Wiens JA (1989) Spatial scaling in ecology. *Functional Ecology* **3**, 385-397.
- Wiens JA (2000) Ecological heterogeneity: An ontogeny of concepts and approaches. Pages 9-31 in Hutchings MJ, John EA, Stewart AJA editors. *The ecological consequences of environmental heterogeneity: The 40th symposium of the British Ecological Society*, held at the University of Sussex, 23-25 March 1999. Blackwell Science, Sussex, UK.
- Wilson KA, Westphal MI, Possingham HP, Elith J (2005) Sensitivity of conservation planning to different approaches to using predicted species distribution data. *Biological Conservation* **122**, 99-112.
- Wisz MS, Pottier J, Kissling WD, Pellissier L, Lenoir J, Damgaard CF, Dormann CF, Forchhammer MC, Grytnes JA, Guisan A, Heikkinen RK, Høye TT, Kuhn I, Luoto M, Maiorano L, Nilsson MC, Normand S, Ockinger E, Schmidt NM, Termansen M, Timmermann A, Wardle DA, Aastrup P, Svenning JC (2013) The role of biotic interactions in shaping distributions and realised assemblages of species: Implications for species distribution modelling. *Biological Reviews* **88**, 15-30.

- Wolfe KH, Li WH, Sharp PM (1987) Rates of nucleotide substitution vary greatly among plant mitochondrial, chloroplast, and nuclear DNA. *Proceedings of the National Academy of Sciences United States of America* **84**, 9054-9058.
- Wood SN (2011) Fast stable restricted maximum likelihood and marginal likelihood estimation of semiparametric generalized linear models. *Journal of the Royal Statistical Society Series B-Statistical Methodology* **73**, 3-36.
- Worth JRP, Jordan GJ, Marthick JR, Mckinnon GE, Vaillancourt RE (2010) Chloroplast evidence for geographic stasis of the Australian bird-dispersed shrub *Tasmannia lanceolata* (Winteraceae). *Molecular Ecology* **19**, 2949-2963.
- Xie W, Lewis PO, Fan Y, Kuo L, Chen MH (2011) Improving marginal likelihood estimation for Bayesian phylogenetic model selection. *Systematic Biology* **60**,150-160.
- Yang F-S, Li Y-F, Ding XIN, Wang X-Q (2008) Extensive population expansion of *Pedicularis longiflora* (Orobanchaceae) on the Qinghai-Tibetan Plateau and its correlation with the Quaternary climate change. *Molecular Ecology* **17**, 5135-5145.
- Zuber D, Widmer A (2009) Phylogeography and host race differentiation in the European mistletoe (*Viscum album* L.). *Molecular Ecology* **18**, 1946-1962.

Appendices

Appendix 1.1 Derivation of the formulas for the process-based model.

We modeled population dynamics of mistletoes using formalism borrowed from metapopulation theory. We consider a grid of cells of maximum resolution, corresponding to the typical area under an average-sized legume tree, on the order of 20 m². We now construct coarser-resolution grids that contain maximum-resolution cells, asking for the proportion of the coarse-resolution cells that is occupied by infected trees (number of high-resolution infected cells/total number of cells in the coarse-resolution unit), that is, by trees with at least one individual of mistletoe. Let $i = 1, 2, 3 \dots n$ denote the coarse-resolution cells in the grid. Then the following equation is proposed (Hanski 1999):

$$\frac{dp_i}{dt} = c_i(1 - p_i) - e_i p_i,$$

where p_i is the probability of species presence in cell i , dp_i/dt is its time derivative; c_i is the colonization rate in cell i and e_i is the extinction rate in cell i . In words, the growth rate of the proportion of space occupied by the mistletoe in the i -th cell increases proportionally to a colonization rate c_i and in inverse proportion to an extinction rate e_i .

Now, imagine that the grid is coarsened, such that inside a new larger cell J (we use a capital letter to denote an aggregate of smaller cells) is a collection of the higher-resolution cells i . This can be achieved by using square cells and doubling the side of the

cells in the grid: one doubling contains 4 smaller cells, another doubling contains 16 smaller cells, and so on.

We are interested in the mean value of the occupied proportion of a cell:

$$\bar{p}_J = \frac{1}{|J|} \sum_{i \in J} p_i,$$

and therefore:

$$\frac{d\bar{p}_J}{dt} = \frac{d}{dt} \frac{1}{|J|} \sum_{i \in J} p_i = \frac{1}{|J|} \left(\sum_{i \in J} c_i (1 - p_i) - \sum_{i \in J} e_i p_i \right) = \frac{1}{|J|} \left(\sum_{i \in J} c_i - \sum_{i \in J} c_i p_i - \sum_{i \in J} e_i p_i \right).$$

Now, we make the reasonable assumption that, inside every larger cell J , the values of colonization rate and extinction rates can be approximated as their averages over the smaller cells:

$$\frac{d\bar{p}_J}{dt} = \frac{1}{|J|} \left(\sum_{i \in J} c_i - \sum_{i \in J} c_i p_i - \sum_{i \in J} e_i p_i \right) = \bar{c}_J - \bar{c}_J \bar{p}_J - \bar{e}_J \bar{p}_J,$$

which, in the steady state, implies:

$$\bar{p}_J^* = \frac{\bar{c}_J}{\bar{c}_J + \bar{e}_J}.$$

The equations for the colonization and extinction rates are postulated after consideration of the BAM diagram: colonization is proportional to the abundance of birds and trees in cell J , and inversely related to the distance to other occupied cells (Hanski 1999):

$$\bar{c}_J = \beta_2 \sum_{K=1}^n L_K \exp\left(\frac{-d_{J,K} \beta_0}{1 + \beta_1 b_K}\right),$$

where β_0 and β_1 represent parameters to be fitted, $d_{J,K}$ is a measure of distance (Euclidean, corrected by topography) between cells J and K ; b_K is the density of birds present in cell K , and L_K is the number of trees in cell K . These three last quantities are obtained from data (see Methods for more detail).

The extinction rate in cell J is assumed to be a function of the distance from the centroid of the fundamental niche of the species to the environmental data in the cell, as represented in an ellipsoid:

$$\bar{e}_J = f \left[(\mathbf{x}_J - \boldsymbol{\mu})^T \boldsymbol{\Sigma}^{-1} (\mathbf{x}_J - \boldsymbol{\mu}) \right],$$

where the parameters $\boldsymbol{\mu}$ and $\boldsymbol{\Sigma}$ represent fitted values that define a multi-normal distribution of optimal, ideal environmental preferences. The values of x_J represent the observed environmental values in the cell J .

Table S1.1. Summary of model performance. For each model it is shown the area predicted as suitable or unsuitable after using a minimum training presence threshold and the partial AUC ratio statistics.

| Resolution | Model | Area 0 | Area 1 | AUC min | AUC max | AUC mean | AUC s.d. |
|------------|---------|---------|---------|---------|---------|----------|----------|
| 1 km | process | 178579 | 1181774 | 0.973 | 1.156 | 1.030 | 0.026 |
| | g_dh | 1076124 | 290319 | 1.122 | 1.550 | 1.321 | 0.069 |
| | g_c | 704875 | 662533 | 1.045 | 1.299 | 1.132 | 0.051 |
| | g_cdh | 1051953 | 314490 | 1.142 | 1.601 | 1.418 | 0.082 |
| | gm_dh | 694012 | 672431 | 1.035 | 1.270 | 1.089 | 0.026 |
| | gm_c | 561353 | 806055 | 1.029 | 1.328 | 1.073 | 0.027 |
| | gm_cdh | 825443 | 541000 | 1.041 | 1.265 | 1.089 | 0.026 |
| | m_dh | 538460 | 827983 | 1.110 | 1.530 | 1.297 | 0.087 |
| | m_c | 226380 | 1141028 | 1.048 | 1.270 | 1.110 | 0.042 |
| m_cdh | 492828 | 873615 | 1.092 | 1.556 | 1.242 | 0.063 | |
| 5 km | process | 15471 | 38806 | 1.096 | 1.247 | 1.180 | 0.019 |
| | g_dh | 42135 | 12142 | 1.049 | 1.428 | 1.111 | 0.034 |
| | g_c | 25470 | 28807 | 1.032 | 1.281 | 1.091 | 0.035 |
| | g_cdh | 41897 | 12380 | 1.040 | 1.348 | 1.107 | 0.035 |
| | gm_dh | 26332 | 27651 | 1.036 | 1.570 | 1.239 | 0.089 |
| | gm_c | 22009 | 32268 | 1.038 | 1.276 | 1.130 | 0.049 |
| | gm_cdh | 36712 | 17271 | 1.184 | 1.599 | 1.397 | 0.088 |
| | m_dh | 18661 | 35322 | 1.114 | 1.617 | 1.276 | 0.081 |
| | m_c | 11120 | 43157 | 1.068 | 1.332 | 1.129 | 0.031 |
| m_cdh | 33715 | 20268 | 1.099 | 1.510 | 1.360 | 0.084 | |
| 10 km | process | 2817 | 10764 | 1.106 | 1.272 | 1.203 | 0.024 |
| | g_dh | 10880 | 2701 | 1.043 | 1.309 | 1.099 | 0.030 |
| | g_c | 10567 | 3014 | 1.025 | 1.240 | 1.073 | 0.026 |
| | g_cdh | 10008 | 3573 | 1.071 | 1.552 | 1.165 | 0.062 |
| | gm_dh | 6099 | 7482 | 1.125 | 1.604 | 1.344 | 0.095 |
| | gm_c | 5731 | 7850 | 1.044 | 1.296 | 1.125 | 0.051 |
| | gm_cdh | 8471 | 5110 | 1.073 | 1.635 | 1.259 | 0.129 |
| | m_dh | 4583 | 8998 | 1.050 | 1.575 | 1.288 | 0.083 |
| | m_c | 3331 | 10250 | 1.094 | 1.267 | 1.149 | 0.036 |
| m_cdh | 6775 | 6806 | 1.068 | 1.532 | 1.245 | 0.054 | |
| 20 km | process | 542 | 2866 | 1.082 | 1.278 | 1.188 | 0.030 |
| | g_dh | 2724 | 684 | 1.053 | 1.357 | 1.124 | 0.040 |
| | g_c | 1591 | 1817 | 1.028 | 1.279 | 1.087 | 0.035 |
| | g_cdh | 2670 | 738 | 1.052 | 1.614 | 1.122 | 0.042 |
| | gm_dh | 1472 | 1935 | 1.089 | 1.558 | 1.280 | 0.105 |
| | gm_c | 1070 | 2337 | 1.022 | 1.254 | 1.070 | 0.028 |
| | gm_cdh | 2345 | 1062 | 1.030 | 1.454 | 1.089 | 0.037 |
| | m_dh | 746 | 2617 | 1.112 | 1.546 | 1.270 | 0.065 |
| | m_c | 951 | 2412 | 1.081 | 1.330 | 1.182 | 0.031 |
| m_cdh | 1340 | 2023 | 1.111 | 1.624 | 1.272 | 0.074 | |
| 50 km | process | 157 | 377 | 1.124 | 1.285 | 1.227 | 0.027 |
| | g_dh | 436 | 91 | 1.018 | 1.074 | 1.038 | 0.008 |
| | g_c | 189 | 345 | 1.019 | 1.214 | 1.075 | 0.033 |
| | g_cdh | 408 | 119 | 1.039 | 1.256 | 1.094 | 0.028 |
| | gm_dh | 137 | 397 | 1.002 | 1.420 | 1.056 | 0.053 |
| | gm_c | 196 | 338 | 1.033 | 1.241 | 1.133 | 0.055 |
| | gm_cdh | 352 | 182 | 1.077 | 1.563 | 1.249 | 0.098 |
| | m_dh | 143 | 384 | 1.105 | 1.571 | 1.289 | 0.101 |
| | m_c | 136 | 398 | 1.103 | 1.257 | 1.178 | 0.024 |
| m_cdh | 212 | 322 | 1.167 | 1.595 | 1.337 | 0.085 | |

Figure S1.1 Example binary maps for different models and sets of environmental.

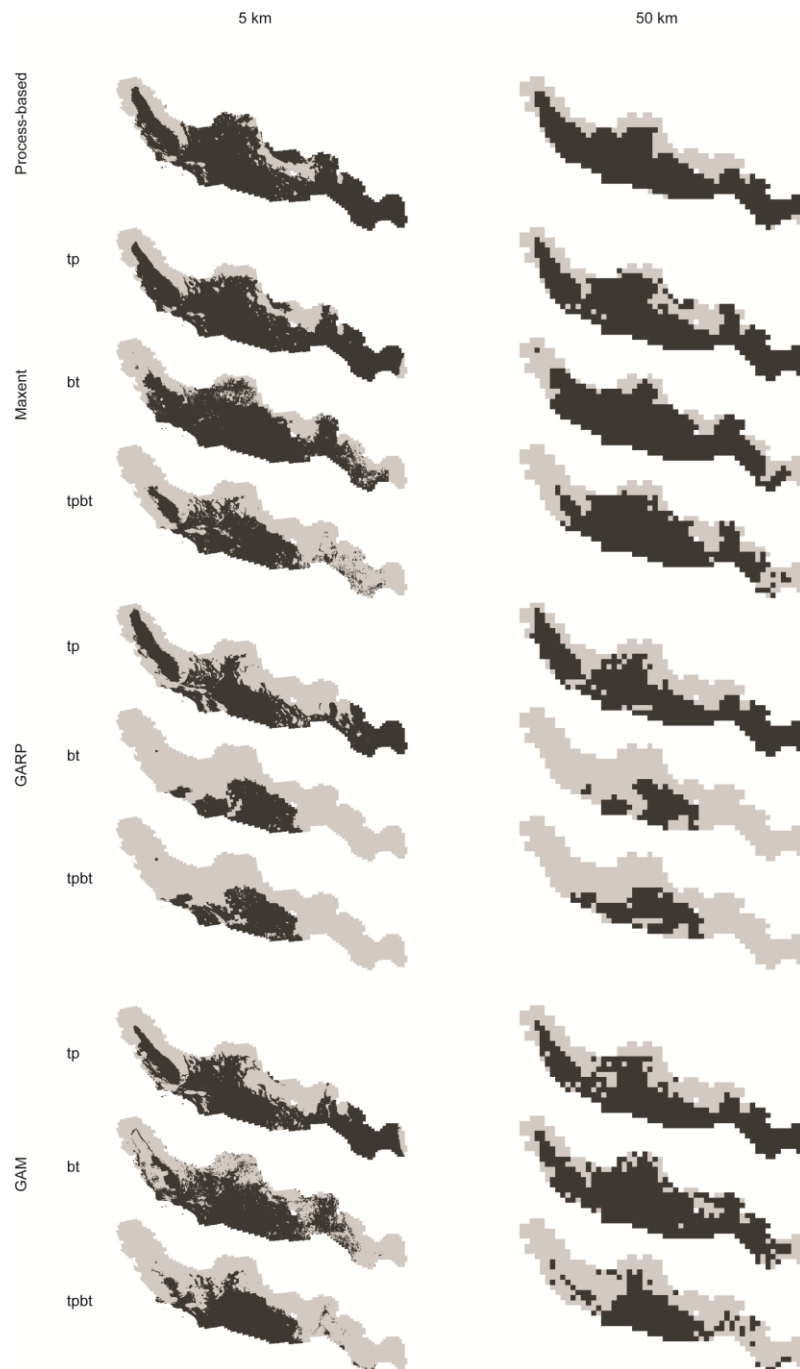


Figure S1.1 Example binary maps for different models and sets of environmental predictors at the resolutions of 5 and 50 km. Binary predictions were generated using a minimum training presence threshold.

Figure S1.2 Example of map comparison with fuzzy Kappa statistic.

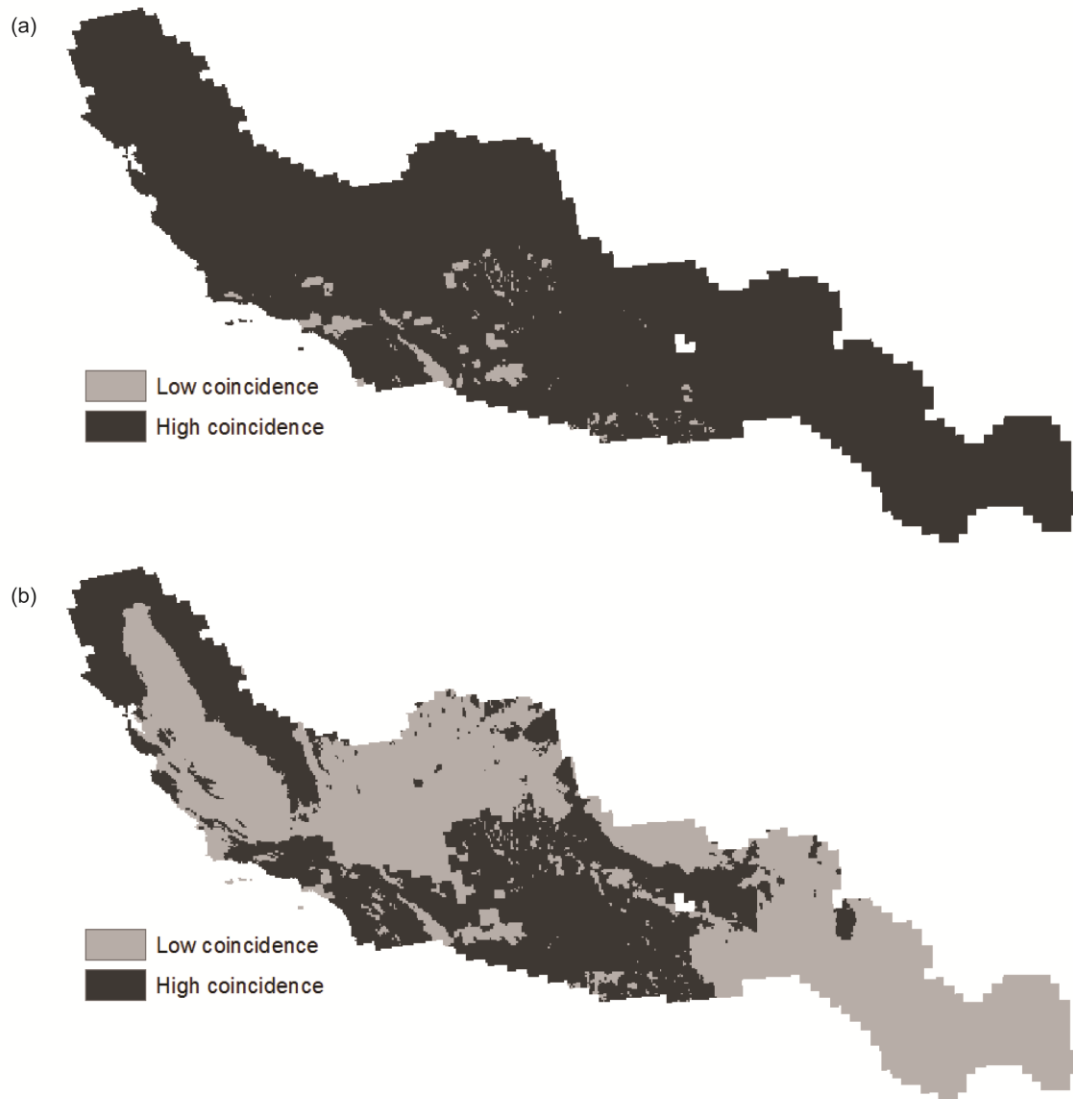


Figure S1.2 Example of map comparison with fuzzy Kappa statistic. In (a), note an overall high coincidence between two maps (in this case GARP disperser + host versus GARP climate + disperser + host), and in (b), note an example of low coincidence (GARP climate + disperser + host versus Maxent climate) at a resolution of 5 km.

Appendix 2.1 Model evaluation.

| Dispersers models | Area 0 | Area 1 | Prob. presence | Trials | Successes | P value |
|---|---------|--------|----------------|--------|-----------|-------------|
| <i>Bombycilla cedrorum</i> year-round | 852077 | 369828 | 0.302665101 | 100 | 85 | $P < 0.001$ |
| <i>Bombycilla cedrorum</i> winter | 878446 | 343459 | 0.281084863 | 100 | 87 | $P < 0.001$ |
| <i>Turdus migratorius</i> year-round | 654438 | 695037 | 0.515042517 | 100 | 96 | $P < 0.001$ |
| <i>Turdus migratorius</i> winter | 1068742 | 280733 | 0.208031271 | 100 | 94 | $P < 0.001$ |
| Hosts overall | 141687 | 159738 | 0.529942772 | 100 | 100 | $P < 0.001$ |
| <i>Phoradendron californicum</i> (mistletoe) | 52979 | 24782 | 0.318694461 | 60 | 60 | $P < 0.001$ |
| <i>Melanerpes uropygialis</i> year-round | 125740 | 20265 | 0.138796617 | 100 | 95 | $P < 0.001$ |
| <i>Melanerpes uropygialis</i> winter | 115414 | 30591 | 0.209520222 | 100 | 64 | $P < 0.001$ |
| <i>Mimus polyglottos</i> year-round | 537241 | 276777 | 0.340013366 | 99 | 95 | $P < 0.001$ |
| <i>Mimus polyglottos</i> winter | 542948 | 271070 | 0.333002464 | 96 | 86 | $P < 0.001$ |
| <i>Myadestes townsendi</i> year-round | 809985 | 187892 | 0.188291743 | 100 | 90 | $P < 0.001$ |
| <i>Myadestes townsendi</i> winter | 847374 | 150503 | 0.150823198 | 100 | 78 | $P < 0.001$ |
| <i>Phainopepla nitens</i> year-round | 206097 | 84569 | 0.290949062 | 100 | 94 | $P < 0.001$ |
| <i>Phainopepla nitens</i> winter | 197028 | 93638 | 0.322149821 | 100 | 96 | $P < 0.001$ |
| <i>Sialis currucoides</i> year-round | 849502 | 267653 | 0.23958448 | 100 | 88 | $P < 0.001$ |
| <i>Sialis currucoides</i> winter | 989582 | 127573 | 0.114194539 | 100 | 82 | $P < 0.001$ |
| <i>Sialia mexicana</i> year-round | 277017 | 132639 | 0.323781417 | 100 | 90 | $P < 0.001$ |
| <i>Sialia mexicana</i> winter | 367000 | 42656 | 0.104126389 | 100 | 77 | $P < 0.001$ |
| <i>Sialia sialis</i> year-round | 505821 | 301210 | 0.373232255 | 100 | 96 | $P < 0.001$ |
| <i>Sialia sialis</i> winter | 566506 | 240525 | 0.298036878 | 100 | 99 | $P < 0.001$ |
| <i>Toxostoma curvirostre</i> year-round | 151930 | 142866 | 0.484626657 | 100 | 98 | $P < 0.001$ |
| <i>Toxostoma curvirostre</i> winter | 219811 | 74985 | 0.254362339 | 100 | 89 | $P < 0.001$ |
| Hosts models (*species with < 14 occurrence localities) | | | | | | |
| <i>Acacia constricta</i> mistletoe-infected* | | | | | | $P < 0.001$ |
| <i>Acacia constricta</i> overall | 100077 | 37909 | 0.27473077 | 100 | 89 | $P < 0.001$ |
| <i>Acacia greggii</i> mistletoe-infected | 127697 | 11636 | 0.083512162 | 50 | 46 | $P < 0.001$ |
| <i>Acacia greggii</i> overall | 51610 | 87723 | 0.629592415 | 100 | 91 | $P < 0.001$ |
| <i>Cercidium floridum</i> mistletoe-infected* | | | | | | $P < 0.001$ |
| <i>Cercidium floridum</i> overall | 47971 | 17015 | 0.261825624 | 99 | 78 | $P < 0.001$ |
| <i>Cercidium microphyllum</i> mistletoe-infected | 33316 | 7166 | 0.177016946 | 10 | 6 | $P < 0.001$ |
| <i>Cercidium microphyllum</i> overall | 22738 | 17744 | 0.438318265 | 100 | 91 | $P < 0.001$ |
| <i>Larrea tridentata</i> mistletoe-infected* | | | | | | $P = 0.001$ |
| <i>Larrea tridentata</i> overall | 117968 | 73107 | 0.382608923 | 100 | 95 | $P < 0.001$ |
| <i>Olneya tesota</i> mistletoe-infected | 35380 | 12130 | 0.255314671 | 15 | 10 | $P < 0.001$ |
| <i>Olneya tesota</i> overall | 34448 | 13062 | 0.274931593 | 100 | 90 | $P < 0.001$ |
| <i>Prosopis glandulosa</i> mistletoe-infected | 268096 | 24224 | 0.08286809 | 14 | 13 | $P < 0.001$ |
| <i>Prosopis glandulosa</i> overall | 169737 | 122583 | 0.419345238 | 99 | 79 | $P < 0.001$ |
| <i>Prosopis velutina</i> mistletoe-infected | 114227 | 23994 | 0.173591567 | 20 | 19 | $P < 0.001$ |
| <i>Prosopis velutina</i> overall | 121153 | 17068 | 0.123483407 | 100 | 65 | $P < 0.001$ |

Appendix 3.1 Genetic diversity measures and estimates of distances to geographic range center and niche centroid.

See Supporting Information—Appendix S1—online in Lira-Noriega A, Manthey JD (2014)

Relationship of genetic diversity and niche centrality: A survey and analysis. *Evolution*

doi:10.1111/evo.12343

Appendix 4.1 Information on individuals and localities sampled in this study.

Partitioning of individuals into populations according to each hypothesis (see Table 4.1)

and DNA sequences GenBank accession numbers.

| Species | Individual | Haplotype (atpH-trnQ-rpl32) | GMYC Clade | Longitude | Latitude |
|----------------------------------|------------|-----------------------------|------------|---------------|----------------|
| <i>Phoradendron californicum</i> | 102_1 | | Clade 2 | -114.30697780 | 29.33219111000 |
| <i>Phoradendron californicum</i> | 102_2 | 2-B | Clade 2 | -114.30697780 | 29.33219111000 |
| <i>Phoradendron californicum</i> | 103_1 | 1-F | Clade 1 | -114.30297380 | 35.46136375000 |
| <i>Phoradendron californicum</i> | 105_1 | | Clade 1 | -114.57432360 | 36.40676364000 |
| <i>Phoradendron californicum</i> | 105_2 | 1-B | Clade 1 | -114.57432360 | 36.40676364000 |
| <i>Phoradendron californicum</i> | 122_1 | 1-G | Clade 1 | -115.09608860 | 34.89494143000 |
| <i>Phoradendron californicum</i> | 127_1 | | Clade 2 | -115.32215000 | 30.05752667000 |
| <i>Phoradendron californicum</i> | 127_2 | 2-B | Clade 2 | -115.32215000 | 30.05752667000 |
| <i>Phoradendron californicum</i> | 129_1 | | Clade 1 | -115.39546670 | 31.29550000000 |
| <i>Phoradendron californicum</i> | 129_2 | 1-H | Clade 1 | -115.39546670 | 31.29550000000 |
| <i>Phoradendron californicum</i> | 136_1 | 1-B | Clade 1 | -115.67687750 | 34.72310000000 |
| <i>Phoradendron californicum</i> | 139_1 | 2-E | Clade 2 | -115.74916150 | 32.63717231000 |
| <i>Phoradendron californicum</i> | 141_1 | | Clade 2 | -116.00600630 | 36.24183000000 |
| <i>Phoradendron californicum</i> | 141_2 | 2-F | Clade 2 | -116.00600630 | 36.24183000000 |
| <i>Phoradendron californicum</i> | 188_1 | 2-D | Clade 2 | -115.25048800 | 36.02206600000 |
| <i>Phoradendron californicum</i> | 188_2 | 2-D | Clade 2 | -115.25048800 | 36.02206600000 |
| <i>Phoradendron californicum</i> | 194_1 | | Clade 1 | -110.67438500 | 31.88360625000 |
| <i>Phoradendron californicum</i> | 194_2 | 1-A | Clade 1 | -110.67438500 | 31.88360625000 |
| <i>Phoradendron californicum</i> | 195_1 | | Clade 2 | -110.79938910 | 32.27710091000 |
| <i>Phoradendron californicum</i> | 195_2 | 2-G | Clade 2 | -110.79938910 | 32.27710091000 |
| <i>Phoradendron californicum</i> | 201_1 | | Clade 2 | -109.88880380 | 32.96205000000 |
| <i>Phoradendron californicum</i> | 201_2 | 2-A | Clade 2 | -109.88880380 | 32.96205000000 |
| <i>Phoradendron californicum</i> | 202_1 | 1-A | Clade 1 | -110.55802290 | 33.76069286000 |
| <i>Phoradendron californicum</i> | 202_2 | 1-A | Clade 1 | -110.55802290 | 33.76069286000 |
| <i>Phoradendron californicum</i> | 203_1 | | Clade 1 | -110.90547500 | 33.53866625000 |
| <i>Phoradendron californicum</i> | 203_2 | 1-B | Clade 1 | -110.90547500 | 33.53866625000 |
| <i>Phoradendron californicum</i> | 207_1 | 2-A | Clade 2 | -111.57298730 | 33.55313909000 |
| <i>Phoradendron californicum</i> | 208_1 | 2-A | Clade 2 | -111.70510670 | 31.99469667000 |
| <i>Phoradendron californicum</i> | 208_2 | 2-A | Clade 2 | -111.70510670 | 31.99469667000 |
| <i>Phoradendron californicum</i> | 210_1 | 2-A | Clade 2 | -112.10957380 | 33.97068750000 |
| <i>Phoradendron californicum</i> | 210_2 | 2-A | Clade 2 | -112.10957380 | 33.97068750000 |
| <i>Phoradendron californicum</i> | 211_1 | | Clade 1 | -112.16423140 | 34.18046143000 |
| <i>Phoradendron californicum</i> | 212_1 | | Clade 1 | -112.82303000 | 34.46984333000 |
| <i>Phoradendron californicum</i> | 212_2 | 1-A | Clade 1 | -112.82303000 | 34.46984333000 |
| <i>Phoradendron californicum</i> | 213_1 | | Clade 2 | -113.24104000 | 34.44217000000 |
| <i>Phoradendron californicum</i> | 213_2 | 2-A | Clade 2 | -113.24104000 | 34.44217000000 |
| <i>Phoradendron californicum</i> | 214_1 | 1-A | Clade 1 | -112.82561630 | 33.61804625000 |
| <i>Phoradendron californicum</i> | 217_1 | | Clade 2 | -114.40233500 | 33.98812500000 |
| <i>Phoradendron californicum</i> | 217_2 | 2-A | Clade 2 | -114.40233500 | 33.98812500000 |
| <i>Phoradendron californicum</i> | 218_1 | 1-I | Clade 1 | -115.70857330 | 33.66317667000 |
| <i>Phoradendron californicum</i> | 219_1 | | Clade 2 | -116.08397000 | 33.56963400000 |
| <i>Phoradendron californicum</i> | 219_2 | 2-A | Clade 2 | -116.08397000 | 33.56963400000 |
| <i>Phoradendron californicum</i> | 220_1 | 1-A | Clade 1 | -116.58552290 | 34.04408857000 |
| <i>Phoradendron californicum</i> | 220_2 | 1-J | Clade 1 | -116.58552290 | 34.04408857000 |
| <i>Phoradendron californicum</i> | 221_1 | 2-C | Clade 2 | -116.15641000 | 31.87195333000 |
| <i>Phoradendron californicum</i> | 221_2 | 2-C | Clade 2 | -116.15641000 | 31.87195333000 |
| <i>Phoradendron californicum</i> | 222_1 | | Clade 2 | -114.70249330 | 29.72847667000 |
| <i>Phoradendron californicum</i> | 222_2 | 2-H | Clade 2 | -114.70249330 | 29.72847667000 |

| | | | | | |
|----------------------------------|-------|-----|---------|---------------|----------------|
| <i>Phoradendron californicum</i> | 223_1 | | Clade 2 | -114.09635430 | 28.72225571000 |
| <i>Phoradendron californicum</i> | 223_2 | 2-B | Clade 2 | -114.09635430 | 28.72225571000 |
| <i>Phoradendron californicum</i> | 224_1 | 3-A | Clade 3 | -110.28621710 | 23.97682143000 |
| <i>Phoradendron californicum</i> | 224_3 | 3-A | Clade 3 | -110.28621710 | 23.97682143000 |
| <i>Phoradendron californicum</i> | 224_4 | | Clade 3 | -110.28621710 | 23.97682143000 |
| <i>Phoradendron californicum</i> | 225_1 | | Clade 4 | -109.68301860 | 23.59140429000 |
| <i>Phoradendron californicum</i> | 225_2 | 4-B | Clade 4 | -109.68301860 | 23.59140429000 |
| <i>Phoradendron californicum</i> | 225_3 | | Clade 4 | -109.68301860 | 23.59140429000 |
| <i>Phoradendron californicum</i> | 225_4 | 4-C | Clade 4 | -109.68301860 | 23.59140429000 |
| <i>Phoradendron californicum</i> | 225_5 | 4-E | Clade 4 | -109.68301860 | 23.59140429000 |
| <i>Phoradendron californicum</i> | 225_6 | 4-A | Clade 4 | -109.68301860 | 23.59140429000 |
| <i>Phoradendron californicum</i> | 225_7 | 4-A | Clade 4 | -109.68301860 | 23.59140429000 |
| <i>Phoradendron californicum</i> | 225_8 | 4-A | Clade 4 | -109.68301860 | 23.59140429000 |
| <i>Phoradendron californicum</i> | 226_1 | | Clade 3 | -110.18610570 | 23.38923000 |
| <i>Phoradendron californicum</i> | 226_2 | 3-A | Clade 3 | -110.18610570 | 23.38923000 |
| <i>Phoradendron californicum</i> | 226_3 | 3-A | Clade 3 | -110.18610570 | 23.38923000 |
| <i>Phoradendron californicum</i> | 226_4 | | Clade 3 | -110.18610570 | 23.38923000 |
| <i>Phoradendron californicum</i> | 227_1 | | Clade 3 | -110.18839330 | 23.55277667000 |
| <i>Phoradendron californicum</i> | 227_2 | 3-A | Clade 3 | -110.18839330 | 23.55277667000 |
| <i>Phoradendron californicum</i> | 229_1 | 3-D | Clade 3 | -111.33271750 | 25.81722000 |
| <i>Phoradendron californicum</i> | 229_2 | 3-C | Clade 3 | -111.33271750 | 25.81722000 |
| <i>Phoradendron californicum</i> | 230_1 | 3-C | Clade 1 | -115.17554780 | 35.48816333000 |
| <i>Phoradendron californicum</i> | 32_1 | 3-A | Clade 3 | -110.53916140 | 24.07610286000 |
| <i>Phoradendron californicum</i> | 36_1 | 1-A | Clade 1 | -110.76835780 | 32.14887889000 |
| <i>Phoradendron californicum</i> | 36_2 | 1-A | Clade 1 | -110.76835780 | 32.14887889000 |
| <i>Phoradendron californicum</i> | 37a_1 | | Clade 1 | -110.91354000 | 30.66852000 |
| <i>Phoradendron californicum</i> | 38a_1 | | Clade 2 | -111.22122000 | 30.56300 |
| <i>Phoradendron californicum</i> | 38a_2 | 2-C | Clade 2 | -111.22122000 | 30.56300 |
| <i>Phoradendron californicum</i> | 38a_3 | | Clade 2 | -111.22122000 | 30.56300 |
| <i>Phoradendron californicum</i> | 40_1 | 1-A | Clade 1 | -111.05250380 | 31.57505875000 |
| <i>Phoradendron californicum</i> | 40_2 | 1-A | Clade 1 | -111.05250380 | 31.57505875000 |
| <i>Phoradendron californicum</i> | 43a_1 | | Clade 1 | -112.76312000 | 31.57463000 |
| <i>Phoradendron californicum</i> | 43a_2 | 1-B | Clade 1 | -112.76312000 | 31.57463000 |
| <i>Phoradendron californicum</i> | 44_1 | | Clade 3 | -111.20883830 | 24.46257833000 |
| <i>Phoradendron californicum</i> | 44_2 | 3-B | Clade 3 | -111.20883830 | 24.46257833000 |
| <i>Phoradendron californicum</i> | 44_3 | 3-B | Clade 3 | -111.20883830 | 24.46257833000 |
| <i>Phoradendron californicum</i> | 47a_1 | | Clade 2 | -111.76702000 | 28.83073000 |
| <i>Phoradendron californicum</i> | 49_1 | | Clade 3 | -111.53967830 | 25.41103000 |
| <i>Phoradendron californicum</i> | 49_2 | | Clade 3 | -111.53967830 | 25.41103000 |
| <i>Phoradendron californicum</i> | 50_1 | | Clade 3 | -111.59258800 | 24.86047800 |
| <i>Phoradendron californicum</i> | 50_2 | 3-B | Clade 3 | -111.59258800 | 24.86047800 |
| <i>Phoradendron californicum</i> | 50_3 | | Clade 3 | -111.59258800 | 24.86047800 |
| <i>Phoradendron californicum</i> | 51a_3 | | Clade 1 | -110.82043000 | 28.92869000 |
| <i>Phoradendron californicum</i> | 53a_2 | | Clade 1 | -110.23153000 | 28.65977000 |
| <i>Phoradendron californicum</i> | 56a_1 | 1-C | Clade 1 | -109.41152000 | 28.49273000 |
| <i>Phoradendron californicum</i> | 56a_2 | 1-C | Clade 1 | -109.41152000 | 28.49273000 |
| <i>Phoradendron californicum</i> | 66_1 | | Clade 1 | -112.09338750 | 32.34311250 |
| <i>Phoradendron californicum</i> | 66_2 | 2-A | Clade 2 | -112.09338750 | 32.34311250 |
| <i>Phoradendron californicum</i> | 74_1 | 1-A | Clade 1 | -112.63009250 | 33.86492000 |
| <i>Phoradendron californicum</i> | 74_2 | 1-A | Clade 1 | -112.63009250 | 33.86492000 |
| <i>Phoradendron californicum</i> | 84_1 | | Clade 3 | -113.29310380 | 27.48149923000 |
| <i>Phoradendron californicum</i> | 84_2 | 3-E | Clade 3 | -113.29310380 | 27.48149923000 |
| <i>Phoradendron californicum</i> | 88_1 | 1-B | Clade 1 | -113.54735200 | 34.11079600 |
| <i>Phoradendron californicum</i> | 93_1 | | Clade 1 | -113.92711000 | 29.04822571000 |
| <i>Phoradendron californicum</i> | 93_2 | 2-B | Clade 2 | -113.92711000 | 29.04822571000 |
| <i>Phoradendron californicum</i> | 97_1 | 2-A | Clade 2 | -114.25198250 | 36.76251500 |
| <i>Phoradendron californicum</i> | 97_2 | 2-A | Clade 2 | -114.25198250 | 36.76251500 |

| | | | | | |
|----------------------------------|-------|-----|----------|---------------|----------------|
| <i>Phoradendron californicum</i> | L1 | 1-C | Clade 1 | -109.35555560 | 27.0777778000 |
| <i>Phoradendron californicum</i> | L10 | 1-B | Clade 1 | -113.36666670 | 31.8833333000 |
| <i>Phoradendron californicum</i> | L11 | 1-D | Clade 1 | -113.2 | 29.3 |
| <i>Phoradendron californicum</i> | L12 | 1-M | Clade 1 | -114.19166670 | 32.10000 |
| <i>Phoradendron californicum</i> | L13 | 1-B | Clade 1 | -112.36666670 | 29.55000 |
| <i>Phoradendron californicum</i> | L14 | 1-A | Clade 1 | -112.41293000 | 29.17944800 |
| <i>Phoradendron californicum</i> | L15 | 1-A | Clade 1 | -112.45000 | 28.95000 |
| <i>Phoradendron californicum</i> | L16 | | Clade 2 | -112.33299800 | 28.76577800 |
| <i>Phoradendron californicum</i> | L17 | 1-A | Clade 1 | -112.45000 | 28.95000 |
| <i>Phoradendron californicum</i> | L18 | | Clade 2 | -112.33299800 | 28.76577800 |
| <i>Phoradendron californicum</i> | L19 | 1-A | Clade 1 | -112.33299800 | 28.76577800 |
| <i>Phoradendron californicum</i> | L2 | | Clade 1 | -112.29533000 | 28.94167100 |
| <i>Phoradendron californicum</i> | L20 | 1-A | Clade 1 | -112.41293000 | 29.17944800 |
| <i>Phoradendron californicum</i> | L21 | 1-D | Clade 1 | -113.39558330 | 29.4004444000 |
| <i>Phoradendron californicum</i> | L22 | 1-D | Clade 1 | -113.24041000 | 29.21788000 |
| <i>Phoradendron californicum</i> | L3 | 1-N | Clade 1 | -112.83138890 | 30.30388889000 |
| <i>Phoradendron californicum</i> | L4 | 2-I | Clade 2 | -110.979199 | 27.961632 |
| <i>Phoradendron californicum</i> | L5 | 1-E | Clade 1 | -112.29533000 | 29.01628300 |
| <i>Phoradendron californicum</i> | L6 | 1-O | Clade 1 | -109.05583330 | 31.3072222000 |
| <i>Phoradendron californicum</i> | L7 | 1-E | Clade 1 | -111.9625 | 28.883333 |
| <i>Phoradendron californicum</i> | L8 | 2-J | Clade 2 | -110.97277780 | 28.01166667000 |
| <i>Phoradendron californicum</i> | L9 | 1-P | Clade 1 | -110.97277780 | 28.01166667000 |
| <i>Phoradendron serotinum</i> | pser1 | | Outgroup | -110.57870000 | 32.98010000 |
| <i>Phoradendron serotinum</i> | pser2 | | Outgroup | -110.57870000 | 32.98010000 |
| <i>Phoradendron serotinum</i> | pser3 | | Outgroup | -110.57870000 | 32.98010000 |
| <i>Phoradendron serotinum</i> | pser4 | | Outgroup | -110.57870000 | 32.98010000 |

| Individual | Historic1 | Historic2 | Historic3 | Historic4 | BreakCabo | BreakMidseaway | LongQuart | LatQuart | GeoDistQuart |
|------------|-----------|-----------|-----------|-----------|-----------|----------------|-----------|----------|--------------|
| 102_1 | hist1_1 | hist2_1.2 | hist3_1.3 | hist4_3 | rest | breakseaway | longq_1 | latq_2 | gdist_2 |
| 102_2 | hist1_1 | hist2_1.2 | hist3_1.3 | hist4_3 | rest | breakseaway | longq_1 | latq_2 | gdist_2 |
| 103_1 | hist1_2 | hist2_2 | hist3_2 | hist4_4 | rest | rest | longq_1 | latq_4 | gdist_3 |
| 105_1 | hist1_2 | hist2_2 | hist3_2 | hist4_4 | rest | rest | longq_1 | latq_4 | gdist_4 |
| 105_2 | hist1_2 | hist2_2 | hist3_2 | hist4_4 | rest | rest | longq_1 | latq_4 | gdist_4 |
| 122_1 | hist1_2 | hist2_2 | hist3_2 | hist4_4 | rest | rest | longq_1 | latq_4 | gdist_3 |
| 127_1 | hist1_1 | hist2_1.2 | hist3_1.3 | hist4_3 | rest | breakseaway | longq_1 | latq_2 | gdist_2 |
| 127_2 | hist1_1 | hist2_1.2 | hist3_1.3 | hist4_3 | rest | breakseaway | longq_1 | latq_2 | gdist_2 |
| 129_1 | hist1_1 | hist2_1.2 | hist3_1.3 | hist4_3 | rest | breakseaway | longq_1 | latq_2 | gdist_2 |
| 129_2 | hist1_1 | hist2_1.2 | hist3_1.3 | hist4_3 | rest | breakseaway | longq_1 | latq_2 | gdist_2 |
| 136_1 | hist1_2 | hist2_2 | hist3_2 | hist4_4 | rest | rest | longq_1 | latq_4 | gdist_3 |
| 139_1 | hist1_2 | hist2_2 | hist3_2 | hist4_4 | rest | rest | longq_1 | latq_3 | gdist_2 |
| 141_1 | hist1_2 | hist2_2 | hist3_2 | hist4_4 | rest | rest | longq_1 | latq_4 | gdist_4 |
| 141_2 | hist1_2 | hist2_2 | hist3_2 | hist4_4 | rest | rest | longq_1 | latq_4 | gdist_4 |
| 188_1 | hist1_2 | hist2_2 | hist3_2 | hist4_4 | rest | rest | longq_1 | latq_4 | gdist_4 |
| 188_2 | hist1_2 | hist2_2 | hist3_2 | hist4_4 | rest | rest | longq_1 | latq_4 | gdist_4 |
| 194_1 | hist1_2 | hist2_2 | hist3_2 | hist4_4 | rest | rest | longq_4 | latq_3 | gdist_1 |
| 194_2 | hist1_2 | hist2_2 | hist3_2 | hist4_4 | rest | rest | longq_4 | latq_3 | gdist_1 |
| 195_1 | hist1_2 | hist2_2 | hist3_2 | hist4_4 | rest | rest | longq_4 | latq_3 | gdist_1 |
| 195_2 | hist1_2 | hist2_2 | hist3_2 | hist4_4 | rest | rest | longq_4 | latq_3 | gdist_1 |
| 201_1 | hist1_2 | hist2_2 | hist3_2 | hist4_4 | rest | rest | longq_4 | latq_3 | gdist_2 |
| 201_2 | hist1_2 | hist2_2 | hist3_2 | hist4_4 | rest | rest | longq_4 | latq_3 | gdist_2 |
| 202_1 | hist1_2 | hist2_2 | hist3_2 | hist4_4 | rest | rest | longq_4 | latq_4 | gdist_2 |
| 202_2 | hist1_2 | hist2_2 | hist3_2 | hist4_4 | rest | rest | longq_4 | latq_4 | gdist_2 |
| 203_1 | hist1_2 | hist2_2 | hist3_2 | hist4_4 | rest | rest | longq_3 | latq_3 | gdist_1 |
| 203_2 | hist1_2 | hist2_2 | hist3_2 | hist4_4 | rest | rest | longq_3 | latq_3 | gdist_1 |
| 207_1 | hist1_2 | hist2_2 | hist3_2 | hist4_4 | rest | rest | longq_3 | latq_3 | gdist_1 |

| | | | | | | | | | |
|-------|---------|-----------|-----------|---------|------|-------------|---------|--------|---------|
| 47a_1 | hist1_2 | hist2_2 | hist3_2 | hist4_4 | rest | rest | longq_3 | latq_2 | gdist_2 |
| 49_1 | hist1_1 | hist2_1.2 | hist3_1.2 | hist4_2 | rest | breakseaway | longq_3 | latq_1 | gdist_5 |
| 49_2 | hist1_1 | hist2_1.2 | hist3_1.2 | hist4_2 | rest | breakseaway | longq_3 | latq_1 | gdist_5 |
| 50_1 | hist1_1 | hist2_1.2 | hist3_1.2 | hist4_2 | rest | breakseaway | longq_3 | latq_1 | gdist_5 |
| 50_2 | hist1_1 | hist2_1.2 | hist3_1.2 | hist4_2 | rest | breakseaway | longq_3 | latq_1 | gdist_5 |
| 50_3 | hist1_1 | hist2_1.2 | hist3_1.2 | hist4_2 | rest | breakseaway | longq_3 | latq_1 | gdist_5 |
| 51a_3 | hist1_2 | hist2_2 | hist3_2 | hist4_4 | rest | rest | longq_4 | latq_2 | gdist_3 |
| 53a_2 | hist1_2 | hist2_2 | hist3_2 | hist4_4 | rest | rest | longq_4 | latq_1 | gdist_3 |
| 56a_1 | hist1_2 | hist2_2 | hist3_2 | hist4_4 | rest | rest | longq_4 | latq_1 | gdist_4 |
| 56a_2 | hist1_2 | hist2_2 | hist3_2 | hist4_4 | rest | rest | longq_4 | latq_1 | gdist_4 |
| 66_1 | hist1_2 | hist2_2 | hist3_2 | hist4_4 | rest | rest | longq_3 | latq_3 | gdist_1 |
| 66_2 | hist1_2 | hist2_2 | hist3_2 | hist4_4 | rest | rest | longq_3 | latq_3 | gdist_1 |
| 74_1 | hist1_2 | hist2_2 | hist3_2 | hist4_4 | rest | rest | longq_2 | latq_4 | gdist_1 |
| 74_2 | hist1_2 | hist2_2 | hist3_2 | hist4_4 | rest | rest | longq_2 | latq_4 | gdist_1 |
| 84_1 | hist1_1 | hist2_1.2 | hist3_1.3 | hist4_3 | rest | breakseaway | longq_2 | latq_1 | gdist_4 |
| 84_2 | hist1_1 | hist2_1.2 | hist3_1.3 | hist4_3 | rest | breakseaway | longq_2 | latq_1 | gdist_4 |
| 88_1 | hist1_2 | hist2_2 | hist3_2 | hist4_4 | rest | rest | longq_2 | latq_4 | gdist_1 |
| 93_1 | hist1_1 | hist2_1.2 | hist3_1.3 | hist4_3 | rest | breakseaway | longq_2 | latq_2 | gdist_2 |
| 93_2 | hist1_1 | hist2_1.2 | hist3_1.3 | hist4_3 | rest | breakseaway | longq_2 | latq_2 | gdist_2 |
| 97_1 | hist1_2 | hist2_2 | hist3_2 | hist4_4 | rest | rest | longq_1 | latq_4 | gdist_4 |
| 97_2 | hist1_2 | hist2_2 | hist3_2 | hist4_4 | rest | rest | longq_1 | latq_4 | gdist_4 |
| L1 | hist1_2 | hist2_2 | hist3_2 | hist4_4 | rest | rest | longq_4 | latq_1 | gdist_5 |
| L10 | hist1_2 | hist2_2 | hist3_2 | hist4_4 | rest | rest | longq_2 | latq_3 | gdist_1 |
| L11 | hist1_1 | hist2_1.2 | hist3_1.3 | hist4_3 | rest | breakseaway | longq_2 | latq_2 | gdist_2 |
| L12 | hist1_2 | hist2_2 | hist3_2 | hist4_4 | rest | rest | longq_2 | latq_3 | gdist_1 |
| L13 | hist1_2 | hist2_2 | hist3_2 | hist4_4 | rest | rest | longq_2 | latq_2 | gdist_2 |
| L14 | hist1_2 | hist2_2 | hist3_2 | hist4_4 | rest | rest | longq_2 | latq_2 | gdist_2 |
| L15 | hist1_2 | hist2_2 | hist3_2 | hist4_4 | rest | rest | longq_2 | latq_2 | gdist_2 |
| L16 | hist1_2 | hist2_2 | hist3_2 | hist4_4 | rest | rest | longq_2 | latq_1 | gdist_2 |
| L17 | hist1_2 | hist2_2 | hist3_2 | hist4_4 | rest | rest | longq_2 | latq_2 | gdist_2 |
| L18 | hist1_2 | hist2_2 | hist3_2 | hist4_4 | rest | rest | longq_2 | latq_1 | gdist_2 |
| L19 | hist1_2 | hist2_2 | hist3_2 | hist4_4 | rest | rest | longq_2 | latq_1 | gdist_2 |
| L2 | hist1_2 | hist2_2 | hist3_2 | hist4_4 | rest | rest | longq_2 | latq_2 | gdist_2 |
| L20 | hist1_2 | hist2_2 | hist3_2 | hist4_4 | rest | rest | longq_2 | latq_2 | gdist_2 |
| L21 | hist1_1 | hist2_1.2 | hist3_1.3 | hist4_3 | rest | breakseaway | longq_2 | latq_2 | gdist_2 |
| L22 | hist1_1 | hist2_1.2 | hist3_1.3 | hist4_3 | rest | breakseaway | longq_2 | latq_2 | gdist_2 |
| L3 | hist1_2 | hist2_2 | hist3_2 | hist4_4 | rest | rest | longq_2 | latq_2 | gdist_1 |
| L4 | hist1_2 | hist2_2 | hist3_2 | hist4_4 | rest | rest | longq_3 | latq_1 | gdist_3 |
| L5 | hist1_2 | hist2_2 | hist3_2 | hist4_4 | rest | rest | longq_2 | latq_2 | gdist_2 |
| L6 | hist1_2 | hist2_2 | hist3_2 | hist4_4 | rest | rest | longq_4 | latq_2 | gdist_3 |
| L7 | hist1_2 | hist2_2 | hist3_2 | hist4_4 | rest | rest | longq_2 | latq_2 | gdist_2 |
| L8 | hist1_2 | hist2_2 | hist3_2 | hist4_4 | rest | rest | longq_3 | latq_1 | gdist_3 |
| L9 | hist1_2 | hist2_2 | hist3_2 | hist4_4 | rest | rest | longq_3 | latq_1 | gdist_3 |
| pser1 | out | out | out | out | out | out | out | out | out |
| pser2 | out | out | out | out | out | out | out | out | out |
| pser3 | out | out | out | out | out | out | out | out | out |
| pser4 | out | out | out | out | out | out | out | out | out |

| Individual | NicheDistQuart | Vegetation | Ecoregions |
|------------|----------------|----------------|------------------------|
| 102_1 | edistq_2 | Central Desert | Baja California desert |
| 102_2 | edistq_2 | Central Desert | Baja California desert |
| 103_1 | edistq_2 | Mojave | Mojave desert |
| 105_1 | edistq_2 | Mojave | Mojave desert |
| 105_2 | edistq_2 | Mojave | Mojave desert |
| 122_1 | edistq_2 | Mojave | Mojave desert |

| | | | |
|-------|----------|----------------------------|---------------------------------------|
| 127_1 | edistq_2 | Central Desert | Baja California desert |
| 127_2 | edistq_2 | Central Desert | Baja California desert |
| 129_1 | edistq_1 | Lower Colorado Desert | Sonoran desert |
| 129_2 | edistq_1 | Lower Colorado Desert | Sonoran desert |
| 136_1 | edistq_1 | Mojave | Mojave desert |
| 139_1 | edistq_1 | Lower Colorado Desert | Sonoran desert |
| 141_1 | edistq_2 | Mojave | Mojave desert |
| 141_2 | edistq_2 | Mojave | Mojave desert |
| 188_1 | edistq_2 | Mojave | Mojave desert |
| 188_2 | edistq_2 | Mojave | Mojave desert |
| 194_1 | edistq_1 | Chihuahuan Desert | Chihuahuan desert |
| 194_2 | edistq_1 | Chihuahuan Desert | Chihuahuan desert |
| 195_1 | edistq_1 | Arizona Upland | Sonoran desert |
| 195_2 | edistq_1 | Arizona Upland | Sonoran desert |
| 201_1 | edistq_1 | Chihuahuan Desert | Chihuahuan desert |
| 201_2 | edistq_1 | Chihuahuan Desert | Chihuahuan desert |
| 202_1 | edistq_3 | Arizona Mountains Forest | Arizona Mountains forests |
| 202_2 | edistq_3 | Arizona Mountains Forest | Arizona Mountains forests |
| 203_1 | edistq_2 | Arizona Mountains Forest | Arizona Mountains forests |
| 203_2 | edistq_2 | Arizona Mountains Forest | Arizona Mountains forests |
| 207_1 | edistq_1 | Arizona Upland | Sonoran desert |
| 208_1 | edistq_1 | Arizona Upland | Sonoran desert |
| 208_2 | edistq_1 | Arizona Upland | Sonoran desert |
| 210_1 | edistq_1 | Arizona Upland | Sonoran desert |
| 210_2 | edistq_1 | Arizona Upland | Sonoran desert |
| 211_1 | edistq_1 | Arizona Mountains Forest | Arizona Mountains forests |
| 212_1 | edistq_2 | Arizona Upland | Sonoran desert |
| 212_2 | edistq_2 | Arizona Upland | Sonoran desert |
| 213_1 | edistq_1 | Arizona Upland | Sonoran desert |
| 213_2 | edistq_1 | Arizona Upland | Sonoran desert |
| 214_1 | edistq_1 | Lower Colorado Desert | Sonoran desert |
| 217_1 | edistq_2 | Lower Colorado Desert | Sonoran desert |
| 217_2 | edistq_2 | Lower Colorado Desert | Sonoran desert |
| 218_1 | edistq_1 | Lower Colorado Desert | Sonoran desert |
| 219_1 | edistq_2 | Lower Colorado Desert | Sonoran desert |
| 219_2 | edistq_2 | Lower Colorado Desert | Sonoran desert |
| 220_1 | edistq_1 | Mojave | Mojave desert |
| 220_2 | edistq_1 | Mojave | Mojave desert |
| 221_1 | edistq_2 | Chaparral | California coastal sage and chaparral |
| 221_2 | edistq_2 | Chaparral | California coastal sage and chaparral |
| 222_1 | edistq_2 | Central Desert | Baja California desert |
| 222_2 | edistq_2 | Central Desert | Baja California desert |
| 223_1 | edistq_2 | Central Desert | Baja California desert |
| 223_2 | edistq_2 | Central Desert | Baja California desert |
| 224_1 | edistq_4 | Gulf Coast | San Lucan xeric scrub |
| 224_3 | edistq_4 | Gulf Coast | San Lucan xeric scrub |
| 224_4 | edistq_4 | Gulf Coast | San Lucan xeric scrub |
| 225_1 | edistq_3 | Sarcocaulouscent Shrubland | San Lucan xeric scrub |
| 225_2 | edistq_3 | Sarcocaulouscent Shrubland | San Lucan xeric scrub |
| 225_3 | edistq_3 | Sarcocaulouscent Shrubland | San Lucan xeric scrub |
| 225_4 | edistq_3 | Sarcocaulouscent Shrubland | San Lucan xeric scrub |
| 225_5 | edistq_3 | Sarcocaulouscent Shrubland | San Lucan xeric scrub |
| 225_6 | edistq_3 | Sarcocaulouscent Shrubland | San Lucan xeric scrub |
| 225_7 | edistq_3 | Sarcocaulouscent Shrubland | San Lucan xeric scrub |
| 225_8 | edistq_3 | Sarcocaulouscent Shrubland | San Lucan xeric scrub |
| 226_1 | edistq_4 | Sarcocaulouscent Shrubland | San Lucan xeric scrub |
| 226_2 | edistq_4 | Sarcocaulouscent Shrubland | San Lucan xeric scrub |

| | | | |
|-------|----------|------------------------|--|
| 226_3 | edistq_4 | Sarcocaulous Shrubland | San Lucan xeric scrub |
| 226_4 | edistq_4 | Sarcocaulous Shrubland | San Lucan xeric scrub |
| 227_1 | edistq_4 | Sarcocaulous Shrubland | San Lucan xeric scrub |
| 227_2 | edistq_4 | Sarcocaulous Shrubland | San Lucan xeric scrub |
| 229_1 | edistq_3 | Gulf Coast | Gulf of California xeric scrub |
| 229_2 | edistq_3 | Gulf Coast | Gulf of California xeric scrub |
| 230_1 | edistq_2 | Mojave | Mojave desert |
| 32_1 | edistq_4 | Gulf Coast | Gulf of California xeric scrub |
| 36_1 | edistq_1 | Arizona Upland | Sonoran desert |
| 36_2 | edistq_1 | Arizona Upland | Sonoran desert |
| 37a_1 | edistq_2 | Chihuahuan Desert | Chihuahuan desert |
| 38a_1 | edistq_1 | Arizona Upland | Sonoran desert |
| 38a_2 | edistq_1 | Arizona Upland | Sonoran desert |
| 38a_3 | edistq_1 | Arizona Upland | Sonoran desert |
| 40_1 | edistq_1 | Chihuahuan Desert | Chihuahuan desert |
| 40_2 | edistq_1 | Chihuahuan Desert | Chihuahuan desert |
| 43a_1 | edistq_1 | Lower Colorado Desert | Sonoran desert |
| 43a_2 | edistq_1 | Lower Colorado Desert | Sonoran desert |
| 44_1 | edistq_3 | Magdalena Plains | Baja California desert |
| 44_2 | edistq_3 | Magdalena Plains | Baja California desert |
| 44_3 | edistq_3 | Magdalena Plains | Baja California desert |
| 47a_1 | edistq_2 | Gulf Coast | Sonoran desert |
| 49_1 | edistq_3 | Magdalena Plains | Baja California desert |
| 49_2 | edistq_3 | Magdalena Plains | Baja California desert |
| 50_1 | edistq_4 | Magdalena Plains | Baja California desert |
| 50_2 | edistq_4 | Magdalena Plains | Baja California desert |
| 50_3 | edistq_4 | Magdalena Plains | Baja California desert |
| 51a_3 | edistq_2 | Plains of Sonora | Sonoran desert |
| 53a_2 | edistq_3 | Sonoran thornscrub | Sonoran-Sinaloan transition subtropical dry forest |
| 56a_1 | edistq_4 | Sonoran thornscrub | Sonoran-Sinaloan transition subtropical dry forest |
| 56a_2 | edistq_4 | Sonoran thornscrub | Sonoran-Sinaloan transition subtropical dry forest |
| 66_1 | edistq_1 | Arizona Upland | Sonoran desert |
| 66_2 | edistq_1 | Arizona Upland | Sonoran desert |
| 74_1 | edistq_1 | Arizona Upland | Sonoran desert |
| 74_2 | edistq_1 | Arizona Upland | Sonoran desert |
| 84_1 | edistq_3 | Vizcaino Desert | Baja California desert |
| 84_2 | edistq_3 | Vizcaino Desert | Baja California desert |
| 88_1 | edistq_1 | Lower Colorado Desert | Sonoran desert |
| 93_1 | edistq_2 | Central Desert | Baja California desert |
| 93_2 | edistq_2 | Central Desert | Baja California desert |
| 97_1 | edistq_3 | Mojave | Mojave desert |
| 97_2 | edistq_3 | Mojave | Mojave desert |
| L1 | edistq_3 | Sonoran thornscrub | Sonoran-Sinaloan transition subtropical dry forest |
| L10 | edistq_1 | Lower Colorado Desert | Sonoran desert |
| L11 | edistq_2 | Gulf Coast | Gulf of California xeric scrub |
| L12 | edistq_1 | Lower Colorado Desert | Sonoran desert |
| L13 | edistq_1 | Gulf Coast | Sonoran desert |
| L14 | edistq_1 | Gulf Coast | Sonoran desert |
| L15 | edistq_1 | Gulf Coast | Sonoran desert |
| L16 | edistq_2 | Gulf Coast | Sonoran desert |
| L17 | edistq_1 | Gulf Coast | Sonoran desert |
| L18 | edistq_2 | Gulf Coast | Sonoran desert |
| L19 | edistq_2 | Gulf Coast | Sonoran desert |
| L2 | edistq_1 | Gulf Coast | Sonoran desert |
| L20 | edistq_1 | Gulf Coast | Sonoran desert |
| L21 | edistq_2 | Gulf Coast | Gulf of California xeric scrub |
| L22 | edistq_2 | Gulf Coast | Gulf of California xeric scrub |

| | | | |
|-------|----------|-------------------|-------------------|
| L3 | edistq_1 | Gulf Coast | Sonoran desert |
| L4 | edistq_4 | Gulf Coast | Sonoran desert |
| L5 | edistq_1 | Gulf Coast | Sonoran desert |
| L6 | edistq_2 | Chihuahuan Desert | Chihuahuan desert |
| L7 | edistq_1 | Gulf Coast | Sonoran desert |
| L8 | edistq_4 | Gulf Coast | Sonoran desert |
| L9 | edistq_4 | Gulf Coast | Sonoran desert |
| pser1 | out | out | out |
| pser2 | out | out | out |
| pser3 | out | out | out |
| pser4 | out | out | out |

| Individual | DispYearQuart | DispWinterQuart | AltQuart | Host | Genera | Null |
|------------|---------------|-----------------|----------|---------------------|-----------|------|
| 102_1 | dispovq_3 | dispwinterq_2 | altq_2 | Prosopis glandulosa | Prosopis | in |
| 102_2 | dispovq_3 | dispwinterq_2 | altq_2 | Prosopis glandulosa | Prosopis | in |
| 103_1 | dispovq_2 | dispwinterq_2 | altq_3 | Acacia greggii | Acacia | in |
| 105_1 | dispovq_2 | dispwinterq_3 | altq_3 | Acacia greggii | Acacia | in |
| 105_2 | dispovq_2 | dispwinterq_3 | altq_3 | Acacia greggii | Acacia | in |
| 122_1 | dispovq_1 | dispwinterq_2 | altq_2 | Acacia greggii | Acacia | in |
| 127_1 | dispovq_2 | dispwinterq_2 | altq_2 | Prosopis glandulosa | Prosopis | in |
| 127_2 | dispovq_2 | dispwinterq_2 | altq_2 | Prosopis glandulosa | Prosopis | in |
| 129_1 | dispovq_3 | dispwinterq_3 | altq_2 | Olneya tesota | Olneya | in |
| 129_2 | dispovq_3 | dispwinterq_3 | altq_2 | Olneya tesota | Olneya | in |
| 136_1 | dispovq_2 | dispwinterq_2 | altq_3 | Prosopis velutina | Prosopis | in |
| 139_1 | dispovq_2 | dispwinterq_3 | altq_1 | Prosopis glandulosa | Prosopis | in |
| 141_1 | dispovq_3 | dispwinterq_2 | altq_2 | Prosopis velutina | Prosopis | in |
| 141_2 | dispovq_3 | dispwinterq_2 | altq_2 | Prosopis velutina | Prosopis | in |
| 188_1 | dispovq_2 | dispwinterq_3 | altq_2 | Acacia greggii | Acacia | in |
| 188_2 | dispovq_2 | dispwinterq_3 | altq_2 | Acacia greggii | Acacia | in |
| 194_1 | dispovq_4 | dispwinterq_4 | altq_3 | Acacia greggii | Acacia | in |
| 194_2 | dispovq_4 | dispwinterq_4 | altq_3 | Acacia greggii | Acacia | in |
| 195_1 | dispovq_3 | dispwinterq_4 | altq_2 | Prosopis velutina | Prosopis | in |
| 195_2 | dispovq_3 | dispwinterq_4 | altq_2 | Prosopis velutina | Prosopis | in |
| 201_1 | dispovq_3 | dispwinterq_3 | altq_2 | Prosopis velutina | Prosopis | in |
| 201_2 | dispovq_3 | dispwinterq_3 | altq_2 | Prosopis velutina | Prosopis | in |
| 202_1 | dispovq_4 | dispwinterq_4 | altq_4 | Acacia greggii | Acacia | in |
| 202_2 | dispovq_4 | dispwinterq_4 | altq_4 | Acacia greggii | Acacia | in |
| 203_1 | dispovq_3 | dispwinterq_4 | altq_3 | Prosopis velutina | Prosopis | in |
| 203_2 | dispovq_3 | dispwinterq_4 | altq_3 | Prosopis velutina | Prosopis | in |
| 207_1 | dispovq_2 | dispwinterq_3 | altq_2 | Prosopis velutina | Prosopis | in |
| 208_1 | dispovq_3 | dispwinterq_4 | altq_3 | Prosopis velutina | Prosopis | in |
| 208_2 | dispovq_3 | dispwinterq_4 | altq_3 | Prosopis velutina | Prosopis | in |
| 210_1 | dispovq_3 | dispwinterq_3 | altq_2 | Prosopis velutina | Prosopis | in |
| 210_2 | dispovq_3 | dispwinterq_3 | altq_2 | Prosopis velutina | Prosopis | in |
| 211_1 | dispovq_3 | dispwinterq_4 | altq_3 | Acacia greggii | Acacia | in |
| 212_1 | dispovq_3 | dispwinterq_3 | altq_3 | Acacia greggii | Acacia | in |
| 212_2 | dispovq_3 | dispwinterq_3 | altq_3 | Acacia greggii | Acacia | in |
| 213_1 | dispovq_3 | dispwinterq_3 | altq_2 | Acacia greggii | Acacia | in |
| 213_2 | dispovq_3 | dispwinterq_3 | altq_2 | Acacia greggii | Acacia | in |
| 214_1 | dispovq_3 | dispwinterq_3 | altq_2 | Cercidium floridum | Cercidium | in |
| 217_1 | dispovq_2 | dispwinterq_3 | altq_1 | Prosopis velutina | Prosopis | in |
| 217_2 | dispovq_2 | dispwinterq_3 | altq_1 | Prosopis velutina | Prosopis | in |
| 218_1 | dispovq_3 | dispwinterq_3 | altq_2 | Cercidium floridum | Cercidium | in |
| 219_1 | dispovq_2 | dispwinterq_3 | altq_1 | Prosopis glandulosa | Prosopis | in |
| 219_2 | dispovq_2 | dispwinterq_3 | altq_1 | Prosopis glandulosa | Prosopis | in |

| | | | | | | |
|-------|-----------|---------------|--------|------------------------|-----------|----|
| 220_1 | dispovq_3 | dispwinterq_4 | altq_2 | Acacia greggii | Acacia | in |
| 220_2 | dispovq_3 | dispwinterq_4 | altq_2 | Acacia greggii | Acacia | in |
| 221_1 | dispovq_3 | dispwinterq_4 | altq_2 | Acacia greggii | Acacia | in |
| 221_2 | dispovq_3 | dispwinterq_4 | altq_2 | Acacia greggii | Acacia | in |
| 222_1 | dispovq_3 | dispwinterq_2 | altq_2 | Prosopis glandulosa | Prosopis | in |
| 222_2 | dispovq_3 | dispwinterq_2 | altq_2 | Prosopis glandulosa | Prosopis | in |
| 223_1 | dispovq_1 | dispwinterq_2 | altq_1 | Prosopis glandulosa | Prosopis | in |
| 223_2 | dispovq_1 | dispwinterq_2 | altq_1 | Prosopis glandulosa | Prosopis | in |
| 224_1 | dispovq_2 | dispwinterq_2 | altq_1 | Cercidium floridum | Cercidium | in |
| 224_3 | dispovq_2 | dispwinterq_2 | altq_1 | Cercidium floridum | Cercidium | in |
| 224_4 | dispovq_2 | dispwinterq_2 | altq_1 | Cercidium floridum | Cercidium | in |
| 225_1 | dispovq_1 | dispwinterq_2 | altq_1 | Prosopis velutina | Prosopis | in |
| 225_2 | dispovq_1 | dispwinterq_2 | altq_1 | Prosopis velutina | Prosopis | in |
| 225_3 | dispovq_1 | dispwinterq_2 | altq_1 | Prosopis velutina | Prosopis | in |
| 225_4 | dispovq_1 | dispwinterq_2 | altq_1 | Prosopis velutina | Prosopis | in |
| 225_5 | dispovq_1 | dispwinterq_2 | altq_1 | Prosopis velutina | Prosopis | in |
| 225_6 | dispovq_1 | dispwinterq_2 | altq_1 | Prosopis velutina | Prosopis | in |
| 225_7 | dispovq_1 | dispwinterq_2 | altq_1 | Prosopis velutina | Prosopis | in |
| 225_8 | dispovq_1 | dispwinterq_2 | altq_1 | Prosopis velutina | Prosopis | in |
| 226_1 | dispovq_2 | dispwinterq_2 | altq_1 | Olneya tesota | Olneya | in |
| 226_2 | dispovq_2 | dispwinterq_2 | altq_1 | Olneya tesota | Olneya | in |
| 226_3 | dispovq_2 | dispwinterq_2 | altq_1 | Olneya tesota | Olneya | in |
| 226_4 | dispovq_2 | dispwinterq_2 | altq_1 | Olneya tesota | Olneya | in |
| 227_1 | dispovq_2 | dispwinterq_2 | altq_1 | Acacia occidentalis | Acacia | in |
| 227_2 | dispovq_2 | dispwinterq_2 | altq_1 | Acacia occidentalis | Acacia | in |
| 229_1 | dispovq_2 | dispwinterq_2 | altq_1 | Prosopis glandulosa | Prosopis | in |
| 229_2 | dispovq_2 | dispwinterq_2 | altq_1 | Prosopis glandulosa | Prosopis | in |
| 230_1 | dispovq_3 | dispwinterq_2 | altq_3 | Acacia greggii | Acacia | in |
| 32_1 | dispovq_2 | dispwinterq_2 | altq_1 | Prosopis velutina | Prosopis | in |
| 36_1 | dispovq_3 | dispwinterq_4 | altq_2 | Prosopis articulata | Prosopis | in |
| 36_2 | dispovq_3 | dispwinterq_4 | altq_2 | Prosopis articulata | Prosopis | in |
| 37a_1 | dispovq_1 | dispwinterq_1 | altq_2 | Cercidium microphyllum | Cercidium | in |
| 38a_1 | dispovq_1 | dispwinterq_1 | altq_2 | Prosopis velutina | Prosopis | in |
| 38a_2 | dispovq_1 | dispwinterq_1 | altq_2 | Prosopis velutina | Prosopis | in |
| 38a_3 | dispovq_1 | dispwinterq_1 | altq_2 | Prosopis velutina | Prosopis | in |
| 40_1 | dispovq_3 | dispwinterq_4 | altq_3 | Acacia greggii | Acacia | in |
| 40_2 | dispovq_3 | dispwinterq_4 | altq_3 | Acacia greggii | Acacia | in |
| 43a_1 | dispovq_3 | dispwinterq_4 | altq_2 | Prosopis velutina | Prosopis | in |
| 43a_2 | dispovq_3 | dispwinterq_4 | altq_2 | Prosopis velutina | Prosopis | in |
| 44_1 | dispovq_2 | dispwinterq_2 | altq_1 | Prosopis glandulosa | Prosopis | in |
| 44_2 | dispovq_2 | dispwinterq_2 | altq_1 | Prosopis glandulosa | Prosopis | in |
| 44_3 | dispovq_2 | dispwinterq_2 | altq_1 | Prosopis glandulosa | Prosopis | in |
| 47a_1 | dispovq_1 | dispwinterq_2 | altq_1 | Prosopis velutina | Prosopis | in |
| 49_1 | dispovq_1 | dispwinterq_2 | altq_1 | Prosopis velutina | Prosopis | in |
| 49_2 | dispovq_1 | dispwinterq_2 | altq_1 | Prosopis velutina | Prosopis | in |
| 50_1 | dispovq_2 | dispwinterq_2 | altq_1 | Prosopis velutina | Prosopis | in |
| 50_2 | dispovq_2 | dispwinterq_2 | altq_1 | Prosopis velutina | Prosopis | in |
| 50_3 | dispovq_2 | dispwinterq_2 | altq_1 | Prosopis velutina | Prosopis | in |
| 51a_3 | dispovq_1 | dispwinterq_1 | altq_1 | Prosopis velutina | Prosopis | in |
| 53a_2 | dispovq_1 | dispwinterq_2 | altq_2 | Prosopis velutina | Prosopis | in |
| 56a_1 | dispovq_1 | dispwinterq_2 | altq_2 | Prosopis velutina | Prosopis | in |
| 56a_2 | dispovq_1 | dispwinterq_2 | altq_2 | Prosopis velutina | Prosopis | in |
| 66_1 | dispovq_3 | dispwinterq_3 | altq_2 | Prosopis velutina | Prosopis | in |
| 66_2 | dispovq_3 | dispwinterq_3 | altq_2 | Prosopis velutina | Prosopis | in |
| 74_1 | dispovq_3 | dispwinterq_3 | altq_2 | Cercidium microphyllum | Cercidium | in |
| 74_2 | dispovq_3 | dispwinterq_3 | altq_2 | Cercidium microphyllum | Cercidium | in |
| 84_1 | dispovq_1 | dispwinterq_1 | altq_1 | Prosopis glandulosa | Prosopis | in |

| | | | | | | |
|-------|-----------|---------------|--------|------------------------|-----------|-----|
| 84_2 | dispovq_1 | dispwinterq_1 | altq_1 | Prosopis glandulosa | Prosopis | in |
| 88_1 | dispovq_3 | dispwinterq_3 | altq_2 | Cercidium microphyllum | Cercidium | in |
| 93_1 | dispovq_2 | dispwinterq_1 | altq_2 | Acacia greggii | Acacia | in |
| 93_2 | dispovq_2 | dispwinterq_1 | altq_2 | Acacia greggii | Acacia | in |
| 97_1 | dispovq_2 | dispwinterq_3 | altq_2 | Prosopis velutina | Prosopis | in |
| 97_2 | dispovq_2 | dispwinterq_3 | altq_2 | Prosopis velutina | Prosopis | in |
| L1 | dispovq_1 | dispwinterq_1 | altq_1 | Cercidium praecox | Cercidium | in |
| L10 | dispovq_3 | dispwinterq_2 | altq_1 | Cercidium floridum | Cercidium | in |
| L11 | dispovq_2 | dispwinterq_2 | altq_1 | Acacia greggii | Acacia | in |
| L12 | dispovq_3 | dispwinterq_3 | altq_1 | Olneya tesota | Olneya | in |
| L13 | dispovq_1 | dispwinterq_2 | altq_1 | Larrea tridentada | Larrea | in |
| L14 | dispovq_2 | dispwinterq_2 | altq_1 | Olneya tesota | Olneya | in |
| L15 | dispovq_2 | dispwinterq_2 | altq_2 | Olneya tesota | Olneya | in |
| L16 | dispovq_2 | dispwinterq_2 | altq_1 | Prosopis velutina | Prosopis | in |
| L17 | dispovq_2 | dispwinterq_2 | altq_2 | Prosopis velutina | Prosopis | in |
| L18 | dispovq_2 | dispwinterq_2 | altq_1 | Prosopis velutina | Prosopis | in |
| L19 | dispovq_2 | dispwinterq_2 | altq_1 | Olneya tesota | Olneya | in |
| L2 | dispovq_2 | dispwinterq_2 | altq_1 | Olneya tesota | Olneya | in |
| L20 | dispovq_2 | dispwinterq_2 | altq_1 | Acacia greggii | Acacia | in |
| L21 | dispovq_2 | dispwinterq_2 | altq_1 | Cercidium microphyllum | Cercidium | in |
| L22 | dispovq_2 | dispwinterq_2 | altq_1 | Acacia greggii | Acacia | in |
| L3 | dispovq_2 | dispwinterq_2 | altq_1 | Cercidium floridum | Cercidium | in |
| L4 | dispovq_2 | dispwinterq_2 | altq_1 | Prosopis glandulosa | Prosopis | in |
| L5 | dispovq_2 | dispwinterq_2 | altq_1 | Olneya tesota | Olneya | in |
| L6 | dispovq_3 | dispwinterq_3 | altq_3 | Prosopis velutina | Prosopis | in |
| L7 | dispovq_2 | dispwinterq_2 | altq_1 | Acacia greggii | Acacia | in |
| L8 | dispovq_2 | dispwinterq_2 | altq_1 | Prosopis velutina | Prosopis | in |
| L9 | dispovq_2 | dispwinterq_2 | altq_1 | Acacia greggii | Acacia | in |
| pser1 | out | out | out | out | out | out |
| pser2 | out | out | out | out | out | out |
| pser3 | out | out | out | out | out | out |
| pser4 | out | out | out | out | out | out |

Appendix 4.2. Methods to obtain the layers on the historical, ecological, and geographic conditions used for population partitioning in the Bayesian coalescent analysis.

Historical vicariant events—Following Riddle *et al.* (2000) and Garrick *et al.* (2009) we draw lines and polygons in ArcMap 10 that correspond to the marine transgression forming the Gulf of California and the trans-peninsular seaway forming the Isthmus of La Paz (line running southwest-northeast at approximately long -110.483° , lat 23.923°) and the mid-peninsular seaway break in central Vizcaino region (long -113.082° , lat 27.370°) across the Baja California Peninsula. The areas separated by these breaks were used to annotate the geographic correspondence of the sampled individuals in the categories described in Table 1.

Vegetation and ecoregional regionalization—We followed Shreve (1951) original regionalization of the Sonoran Desert vegetation and its modified regionalization only for Baja California Peninsula following González-Abraham *et al.* (2010). We modified the contour of the WWF ecoregions (Olson *et al.* 2001) to match the contour of the areas depicted by Shreve and we added the polygons already available by González-Abraham *et al.* (2010). Our second alternative of regionalization was following the WWF ecoregions based on the shapefile available online (<http://worldwildlife.org/publications/terrestrial-ecoregions-of-the-world>). The areas resulting in each regionalization are in Table 1.

Elevation—We reclassified in quartiles the elevation layer at 1 km spatial resolution available from WoldClim (<http://www.worldclim.org>) and assigned values 1-4 to sampled individuals depending on the quartile they fell given their spatial location.

Longitude and latitude—The coordinates of the sampled individuals were divided in quartiles for latitude and longitude and were assigned a value of 1-4 accordingly.

Distance to geographic range center—This distance is a measure of centrality with respect to the overall geographic range of the species. We obtained the geographic centroid of the polygon defining the geographic range of the species, and from this point we calculated the Euclidean distance to every other point in the geography. These distances were reclassified from 1-4 according to their corresponding quartile, and these values were then assigned to the sampled individuals depending on their geographic position. More details on how to calculate this distance can be found in Lira-Noriega & Manthey (2014).

Distance to ecological niche centroid—This distance is a measure of environmental centrality for the species using climatic variables. To obtain the centroid, we extracted values of the 19 bioclimatic variables at 2.5' from WorldClim (<http://www.worldclim.org>) on the thresholded climatic niche of the species using Maxent (see main document for details) and estimated vector of means for each variable. Then, from the vector of means, we calculated Euclidean distances to every other point in the area of study for the same 19 variables. These values were classified in four according to their quartile and projected on geographic space, and each sampled individual was assigned the value that corresponds to their location. More details on how to calculate this distance can be found in Lira-Noriega & Manthey (2014).

Host species and genera—We retrieved the host species for each of the sampled individuals using the specimens and notes collected during fieldwork, and from the information in the label in the case of loan specimens.

Year-round and wintertime dispersers suitability—We overlaid the thresholded suitability models of bird species known to be either specialists or generalists according to their year-round or wintertime distributions from Lira-Noriega & Peterson (accepted), and the resulting richness values in the area of study were divided in quartiles and each sampled individual was assigned a value 1-4 according to their geographic location.

Appendix 4.3 Packrat midden localities from western North America with hosts and mistletoe macrofossil information.

| Region | Locality | Longitude | Latitude | Macrofossils species (years ago) | Reference |
|-------------------------------|-------------------------|--------------------------|----------|---|---|
| Sonoran Desert | Eagle Eye Mountain | -113.177691 | 33.88868 | Acacia greggii (10440-4040), Acacia constricta (3300), Cercidium floridum (6400), Cercidium microphyllum (4500), Larrea tridentata (6400), Prosopis velutina (4500), Phoradendron californicum (6400) | McAuliffe&Van Devender (1998) Palaeogeography, Palaeoclimatology, Palaeoecology 141:253-275 |
| Sonoran Desert | Waterman Mts. | -111.477063 | 32.3595 | Acacia greggii (13000-5000), Cercidium floridum (8000-6500), Cercidium microphyllum (4000), Larrea tridentata (6000), Prosopis velutina (13000) | McAuliffe&Van Devender (1998) Palaeogeography, Palaeoclimatology, Palaeoecology 141:253-275 |
| Sonoran Desert | Puerto Blanco Mts. | -112.857987 | 32.00451 | Acacia greggii (11000-5000), Cercidium floridum (10000-5000), Cercidium microphyllum (6500), Larrea tridentata (8000), Prosopis velutina (11000-5000), Phoradendron californicum (6400) | McAuliffe&Van Devender (1998) Palaeogeography, Palaeoclimatology, Palaeoecology 141:253-275 |
| Sonoran Desert | Hornaday Mts. | -113.6 | 31.98333 | | |
| Sonoran Desert | Tinajas Altas Mts. | -114.075 | 32.3 | Acacia greggii (43000, 11000-), Olneya tesota (9700?, 4000-), Cercidium floridum (8900-8500, 4000), Cercidium microphyllum (2000-) | Van Devender 1990 chp 8 in Betancourt et al. eds (1990) |
| Sonoran Desert | Picacho Peak, CA | -114.641667 | 32.95 | Acacia greggii (11000-8000), Olneya tesota (500-) | Van Devender 1990 chp 8 in Betancourt et al. eds (1990) |
| Sonoran Desert | Whipple Mts. | -114.391667 | 34.24167 | Acacia greggii (12500-), Cercidium floridum (4300, present) | Van Devender 1990 chp 8 in Betancourt et al. eds (1990) |
| Chihuahuan Desert | Maravillas Canyon Cave | -102.833333 | 29.55 | Acacia greggii (9000-), Prosopis glandulosa (10000-) | Van Devender 1990 chp 7 in Betancourt et al. eds (1990) |
| Chihuahuan Desert | Rio Grande Village area | -102.966667, -103.016667 | 29.225 | Acacia greggii (5500-), Prosopis glandulosa (11400-) | Van Devender 1990 chp 7 in Betancourt et al. eds (1990) |
| Chihuahuan Desert | Hueco Mountains | -105.983333, -106.15 | 31.8 | Prosopis glandulosa (11000-) | Van Devender 1990 chp 7 in Betancourt et al. eds (1990) |
| Big Bend, Texas (LGM refugia) | Big Bend (wide region) | -103.1 | 29.53333 | Larrea tridentata (from the Chihuahuan desert and its expansion towards the Sonoran) | Van Devender 1990 chp 7 in Betancourt et al. eds (1990) |

Appendix 4.4 Model evaluation.

| Model | Area 0 | Area 1 | Prob. presence | Trials | Successes | P value |
|----------------------------------|--------|--------|----------------|--------|-----------|-------------|
| <i>Acacia greggii</i> | 51610 | 87723 | 0.629592415 | 100 | 91 | $P < 0.001$ |
| <i>Cercidium floridum</i> | 47971 | 17015 | 0.261825624 | 99 | 78 | $P < 0.001$ |
| <i>Cercidium microphyllum</i> | 22738 | 17744 | 0.438318265 | 100 | 91 | $P < 0.001$ |
| <i>Prosopis glandulosa</i> | 169737 | 122583 | 0.419345238 | 99 | 79 | $P < 0.001$ |
| <i>Prosopis velutina</i> | 121153 | 17068 | 0.123483407 | 100 | 65 | $P < 0.001$ |
| <i>Phoradendron californicum</i> | 52979 | 24782 | 0.318694461 | 100 | 60 | $P < 0.001$ |
| <i>Phainopepla nitens</i> | 206097 | 84569 | 0.290949062 | 100 | 94 | $P < 0.001$ |

Table S4.1 Results from delimitation of lineages using the ML GMYC method. Both single- and multiple-threshold favored the delimitation of more than one group ($P < 0.05$). However, single threshold was favored due to likely artificial overpartitioned of groups in the multiple-threshold criterion (see text).

| | Single | Multiple |
|-----------------------------------|-------------------------|-------------------------|
| Likelihood of null model | 1358.265 | 1358.265 |
| Maximum likelihood of GMYC model | 1362.186 | 1366.448 |
| Likelihood ratio | 7.842902 ($P < 0.05$) | 16.36765 ($P < 0.05$) |
| Number of detected clusters | 5 | 33 |
| Confidence interval | 2-23 | 29-37 |
| Number of ML significant clusters | 5 | 53 |
| Confidence interval | 2-32 | 39-60 |

Table S4.2 Marginal likelihood and Bayes factor of the hypotheses used to test the phylogenetic relationships of the gene tree without population 225 (see Table 4.1).

Hypotheses are listed in order of importance according to the marginal likelihood. Bayes factor is estimated with respect to the hypothesis with largest likelihood.

| Hypothesis | Marginal likelihood | 2ln Bayes factor |
|---|---------------------|------------------|
| Historic 4 (subdivision based on major breaks resulting from geologic vicariant events) | -3939.293 | |
| Historic 2 (trans-peninsular seaway forming the Isthmus of La Paz; 3 mya) | -3949.728 | 20.869 |
| Historic 1 (northward transgression forming the Gulf of California; 3-5 mya) | -3958.404 | 38.222 |
| Latitude (quartiles) | -3959.339 | 40.093 |
| Vegetation (Shreve 1951) | -3961.661 | 44.735 |
| Mid-peninsular seaway break in the central Vizcaino region | -3964.609 | 50.632 |
| Distance to geographic range center (quartiles) | -3965.529 | 52.472 |
| Ecoregions | -3969.383 | 60.179 |
| Distance to ecological niche centroid (quartiles) | -3971.402 | 64.218 |
| Longitude (quartiles) | -3974.747 | 70.907 |
| Isthmus of La Paz break | -3982.316 | 86.046 |
| Wintertime dispersers suitability (quartiles) | -3988.182 | 97.778 |
| Elevation (quartiles) | -3992.386 | 106.185 |
| Year-round dispersers suitability (quartiles) | -3995.294 | 112.002 |
| Genera | -3999.640 | 120.694 |
| Null hypothesis | -3999.703 | 120.819 |
| Host species | -4005.586 | 132.585 |

Note: Following Kass and Raftery (1995), the Bayes factor scale of strength of evidence in favor of one hypothesis is: 0-2 (not worthy of mention), 2-6 (positive), 6-10 (strong), >10 (very strong).

Table S4.3 Levels of nucleotide variability per sequenced chloroplast region.

| | <i>atpH-atpI</i> | <i>rpl32-trnL</i> | <i>trnQ-rpl16</i> |
|---------------------------------|------------------|-------------------|-------------------|
| Sequence length (bp) | 632 | 465 | 552 |
| Variable positions (bp) | 22 | 23 | 30 |
| Number of indels | 31 | 20 | 61 |
| Individuals sequenced (ingroup) | 119 | 124 | 104 |
| Nucleotide diversity (π) | 0.01824 | 0.01149 | 0.00844 |
| Haplotype diversity (h) | 0.86 | 0.818 | 0.763 |
| Tajima's D^* (ingroup) | -0.93063 (n.s.) | -1.05183 (n.s.) | -0.26308 (n.s.) |
| Fu and Li F^* (Ingroup) | -0.93826 (n.s.) | -1.46048 (n.s.) | -0.28532 (n.s.) |

n.s.: non-statistically significant ($P > 0.05$).

Haplotype diversity (h) and nucleotide variability (π) suggest similar levels of variability among regions; tests of neutrality suggest no deviation from neutral variation across regions. Statistics were calculated using DnaSP v5.10.1 (Librado & Rozas 2009).

Librado P, Rozas J (2009) DnaSP v5: A software for comprehensive analysis of DNA polymorphism data. *Bioinform* **25**, 1451 - 1452.

Figure S4.1 *Phoradendron californicum* haplotype network and potential distribution for mistletoe (inset) and hosts distributions during the LGM (21 kya) according to the CCSM climate scenario.

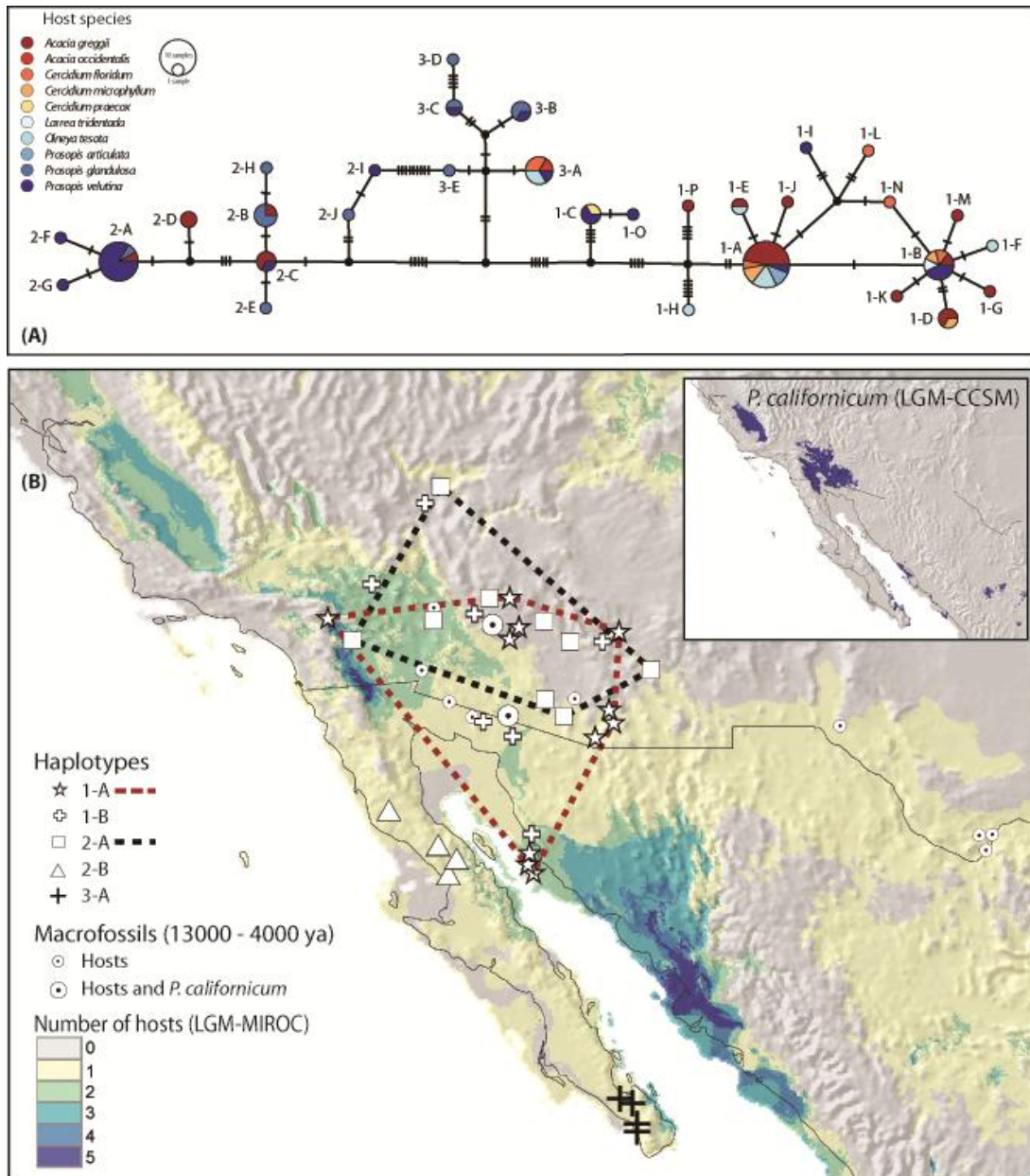


Figure S4.1 (A) *Phoradendron californicum* haplotype network for the three cpDNA concatenated regions colored by host species, excluding haplotypes from clade 4. (B) Potential distribution for mistletoe (inset) and hosts distributions during the LGM (21 kya) according to the CCSM climate scenario, showing geographic locations of most frequent haplotypes and macrofossil localities with mistletoe or hosts. (Supporting Information)

Figure S4.2 Haplotype network configuration on concatenated data sets including two cpDNA regions.

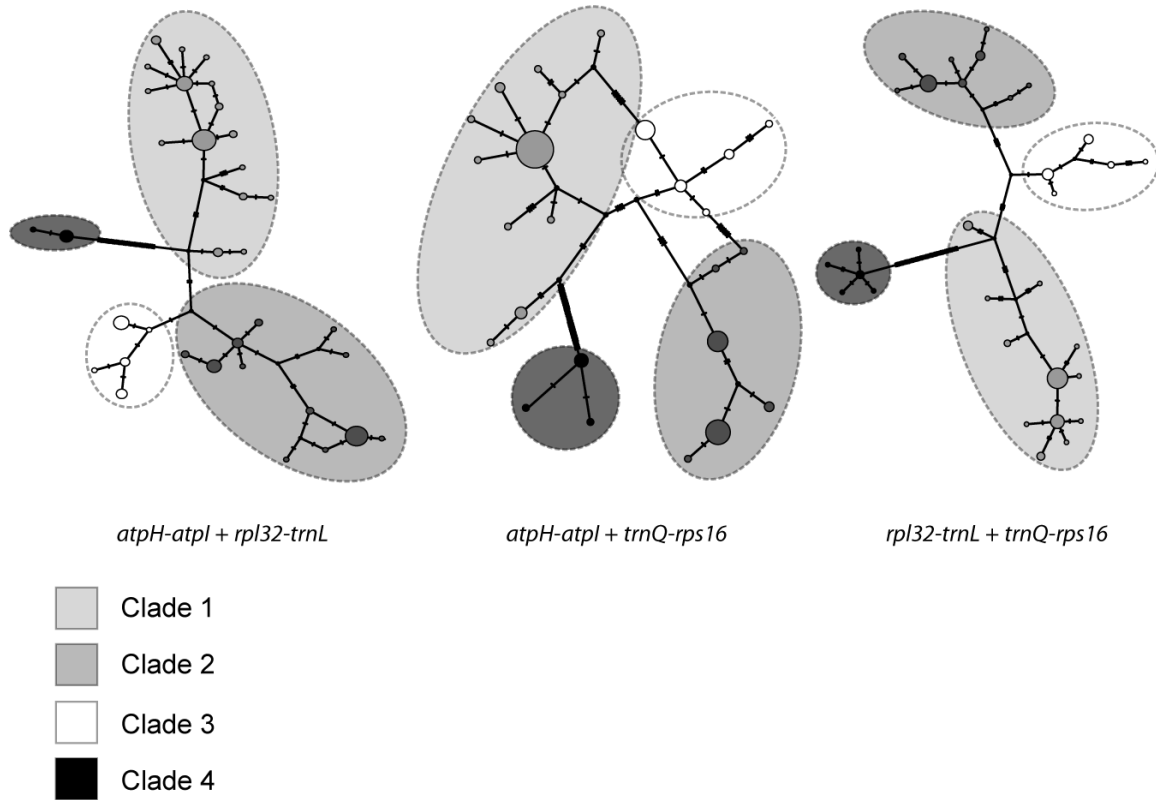


Figure S4.2 Haplotype configuration based on concatenated data sets including two cpDNA regions (*atpH-atpI + rpl32-trnL*, *atpH-atpI + trnQ-rps16*, *rpl32-trnL + trnQ-rps16*). Colors depict the membership established in gene tree reconstruction and GMYC analysis.